

UC Berkeley

Hydraulic Engineering Laboratory Reports

Title

Recent Sediments of the Monterey Deep-Sea Fan

Permalink

<https://escholarship.org/uc/item/5f440431>

Author

Wilde, Pat

Publication Date

1965-05-01

Peer reviewed

RECENT SEDIMENTS OF THE MONTEREY DEEP-SEA FAN

A thesis presented

by

Pat Wilde

to

The Department of Geological Sciences

in partial fulfillment of the requirements

for the degree of

Doctor of Philosophy

in the subject of

Geology

Harvard University

Cambridge, Massachusetts

May 1965

Copyright reserved by the author

HEL 2-13

RECENT SEDIMENTS
OF THE
MONTEREY DEEP-SEA FAN

by
PAT WILDE



HYDRAULIC ENGINEERING LABORATORY
WAVE RESEARCH PROJECTS

UNIVERSITY OF CALIFORNIA
BERKELEY

University of California
Hydraulic Engineering Laboratory

Submitted under Contract DA-49-055-CIV-ENG-63-4 with the
Coastal Engineering Research Center, U. S. Army

Technical Report No. HEL-2-13

RECENT SEDIMENTS OF THE MONTEREY DEEP-SEA FAN

by

Pat Wilde

Berkeley, California

May, 1965

View of the Farallon Islands



from

R/V Paolina-T

Marezine Expedition

Scripps Institution of Oceanography

June 1961

CONTENTS

	<u>Page</u>
Abstract	1
Introduction	5
Definition	5
Location	5
Regional Setting	8
Subjects of Investigation.	9
Sources of Data	10
Acknowledgements	10
Geomorphology	11
Major Features	11
Fan Slope	11
Undersea Positive Relief.	15
Submarine Canyon-Channel Systems	16
Hydraulic Geometry.	19
Calculations	19
Comparison with other Channel Systems	30
Lithology	32
Sampling Techniques	32
Textures	36
Coarser than .062 mm	36
Mud.	39
Sand to Mud Deposition	45
Mineralogy	47
Procedures	47
Coarser than.062 mm	47
Light Fraction	47
Heavy Fraction	69

	<u>Page</u>
Interpretations	70
Clay Fraction	77
Depositional Origin of Sediments	81
Allogenic Sediments	81
Evidence	81
Agency of Transportation.	83
High Velocity Bottom Currents: Turbidity Currents	84
Low Velocity Bottom Currents	89
Source of Sediment	91
Coarser than .062 mm.	99
Finer than .062 m m.	101
Summary.	102
Age of Monterey Fan	105
Fossil Method	105
Radioactive Methods	105
Sedimentary Method	107
Age of Entire Fan	110
Geologic Significance of Deep-Sea Fans.	113
Possible Deep-Sea Fans in the Geologic Record	115
References	121
Appendix A - Lithologic Core Descriptions	131
Cusp	132
Fanfare Smith	134
Fanfare Baird	138
Mendocino	143
Marezine	147
Leapfrog Stranger	149

ILLUSTRATIONS

	<u>Page</u>
Figure 1. Index Map	6
2. Prevailing Current Direction Off Central California	7
3. Location Map of Radial Profiles from the Monterey Fan	12
4. Monterey Fan Profiles	13
5. Index Map for Geographical Names.	14
6. Width Versus Discharge Monterey Channels. .	23
7. Mean Depth Versus Discharge Monterey Channels	24
8. Mean Velocity Versus Discharge Monterey Channels.	25
9. Percentage Discrete Sand 0-50 Centimeters. .	41
10. Percentage Discrete Sand 50-100 Centimeters .	42
11. Percentage Discrete Sand 0-100 Centimeters .	43
12. Percentage Discrete Sand 100-150 Centimeters.	44
13. Grain Size Analyses for Layered Sands and Floating Sand Bodies	48
14. Heavy Mineral Distribution Butano Formation .	94
15. Heavy Mineral Distribution Montara Quartz Diorite.	95
16. Heavy Mineral Distribution Alluvium Western Slope of Montara Mountain	96
17. Heavy Mineral Distribution Pacific Beaches Half Moon Bay to Pacific Grove	97
18. Heavy Mineral Distribution Monterey Fan Sands	98
19. Sediment Distribution Diagram.	103
20. Schematic Comparison of Geologic Structure Between Recent of Central California and Cambro-Ordovician of Western Maine to Eastern New York.	117

TABLES

	<u>Page</u>
Table 1. Monterey Fan Channels Data I	26
2. Monterey Fan Channels Data II	27
3. Relationship between Downslope Distance and Mean Velocity	28
4. Comparison of Hydraulic Functions	29
5. General Core Information	34
6. Percentage Discrete Sand and Sand-Shale Ratios	37
7. Light Mineralogy	49
8. Major Minerals of Light Fraction Average Percent	56
9. Major Minerals of Light Fraction Weighted Average Percent	57
10. X-Ray Data for Alterite	58
11. Heavy Mineralogy	60
12. Heavy Minerals of Layered Sands	67
13. Heavy Minerals of Irregular Sand Bodies	68
14. Comparison of Graywackes with Deep-Sea Sands	73
15. X-Ray Data for Clays - Unheated	75
16. X-Ray Data for Clays - Heated to 450°C	76
17. Drainage Data	92
18. Comparison of Mineral Analysts - Light Fraction	93
19. San Francisco Bay and Bar Sedimentation	100
20. Potassium-Argon Ages for Basement Rocks	106
21. Age of Upper Five Meters	108
22. Age of Monterey Fan	111

ABSTRACT

The Monterey deep-sea fan is an arcuate wedge of sediment that occupies 100,000 square kilometers of the floor of the Pacific Ocean at the base of the continental shelf off the coast of central California. The slope of the fan surface gently decreases radially from an average of 28' at the apex of the fan, at a depth of 3000 meters, to an average of 07' at the outer edge of the fan, at depths about 4500 meters. Two parallel submarine channels (Ascension and Monterey east), which flow respectively out of the mouths of the Ascension and Monterey canyons, cut into the smooth surface of the fan and extend approximately 300 kilometers to the outer edge of the fan. Hydraulic functions (Leopold and Maddock, 1953) calculated for these channels are: (1) $W = 17.3 Q^{0.38}$, (2) $D = 0.39 Q^{0.34}$, and (3) $V = 0.19 Q^{0.26}$. The hydraulic functions indicate that the energy of the current, which forms the channel, is concentrated at the base of the current. Bank-full mean velocities calculated from a modified Chezy-Manning equation (Hurley, 1964) decrease downstream from about 8.5 meters per second, near the apex of the fan, to 1.0 meters per second at the outer margin of the fan.

Turbidity currents, which flow down the submarine canyons and out the submarine channels, seem to be the major agency for transporting material to, and distributing material on the fan. The hydraulic functions suggest that thin-dense currents (Stoneley, 1957) carve the channels. Thick, relatively less dense currents (Plapp and Mitchell, 1960) that are subject to lateral spreading may distribute sediment to regions away from the submarine channels. Repeated migrations of the submarine channels, analogous to the migrations of stream

channels on alluvial fans, resulting in the shift of the areas of maximum deposition probably produce the half-cone shape of the Monterey fan. Low velocity bottom currents of undetermined origin probably play a minor role in redistributing sediments and modifying the shape and surface of the fan.

Forty-six gravity cores and three piston cores of sediments from the upper surface of the Monterey fan and adjacent regions are the primary sources of data for lithologic and mineralogic studies of the fan. The sediments from the surface of the fan are chiefly green-gray mud (silt and finer material) occasionally interbedded with thin (approximately one to two centimeters) dark very fine sand layers, which have a muddy matrix. Cores taken near the submarine channels generally have sediment that is coarser and contains a higher percentage of sand than sediment taken at a distance from the channels. BP 10, a core from the Monterey east channel 274 kilometers from the head of the Monterey canyon, has a 1.8 meter thick unit of a poorly sorted mixture of pebbles, granules, sand and mud, with pebbles up to 50 millimeters long.

The light mineral suite of the sand fraction is characterized by a low quartz-feldspar ratio, and high mica and altered rock fragment content. The heavy mineral suite of the sand fraction consists chiefly of green and brown hornblende, "cockscomb" pyroxene, chlorite, and manganese coated rock fragments. The composition and immature aspect of the sand fraction and the high content of mud matrix in the sand layers indicate that most of the sands on the Monterey deep-sea fan are the modern equivalents of graywackes.

The principal source of the sand-sized material on the Monterey fan are the quartz diorite plutons in the Salinian geologic province near the heads of the Ascension and Monterey canyons. The similarity between the mineralogy of the sand fraction of the fan and that of the quartz diorite bodies indicate that short fluvial transport and short underwater transport by longshore drift and in turbidity flows does not obscure the provenance. The sand layers show a gradual downslope decrease in diagnostic hydraulically heavy grains, such as hornblende and pyroxene, with an increase in hydraulically lighter grains, such as the micas, until the sands on the outer margin of the fan contain over 90 per cent mica flakes. Thus the provenance of turbidite sands deposited from flows that have traveled long distances (more than 300 kilometers for the case of the Monterey fan) would be difficult to determine as most of the mineral grains characteristic of the source would have been deposited upslope.

The sources of silt and finer material on the fan, or the bulk of the fan sediment, are (1) the Great Valley, which contributes 5×10^5 cubic meters per year, that amount which escapes from San Francisco Bay through the Golden Gate, and (2) Salinia and local Coast Range drainage basins, which contribute 5×10^5 cubic meters per year. The estimated annual supply of sediment to the heads of the submarine canyons that debouche onto the fan is 1×10^6 cubic meters per year. Ages calculated from rates of deposition for the upper five meters of sediment, or the approximate thickness of the interval sampled by the cores, are on the order of 500,000 years and agree with the radiolarian ages of Pleistocene to Recent for sediment in the cores. The maximum age of the oldest fan sediment is about

30 to 40 million years, which means an average rate of deposition on the fan of 1.0 centimeters per thousand years.

Sediment on the fan probably is not withdrawn permanently from continental cycles of erosion because eventual uplift of the fan is implied by (1) the suggested common origin for deep-sea fans and certain eugeosynclinal deposits exposed on land that have similar facies, current structures, and areal extent, and (2) the continental aspect of the crust underlying the Monterey fan as indicated by gravity and seismic evidence (Woolard and Strange, 1962). Thus the study of the Monterey and other deep-sea fans may give valuable clues to the perplexing problems of the relationship between the continents and the ocean basins.

Chapter One

INTRODUCTION

Definition::

The continental rise (Heezen, and others, 1959, p. 20) is the portion of the transitional zone between the continents and the deep ocean basins. Two gently sloping sediment aprons, which spread out from the base of the continental slope and merge into the topographically flat-lying abyssal plains, characterize the continental rise off the coast of central California (see Fig. 1). The pie-wedge outlines and half-cone shapes of these aprons are similar to forms of alluvial fans on land. Menard's term (1955, p. 246), "deep-sea fan", thus appears appropriate for such submarine features.

Dill and others (1954) recognized part of the Monterey fan at the mouth of the Monterey submarine canyon. As they did not have extensive bathymetric information, Dill's group did not realize the true size of the Monterey deep-sea fan. Later Menard (1960) described and briefly discussed the age and origin of the two fans, using arguments chiefly based on bathymetric and some seismic data, and named them the Monterey and Delgada.

Location:

The Monterey deep-sea fan coalesces on the north with the Delgada deep-sea fan. (Fig. 1) Both fans lie in a broad trough that is bounded on the north by the Mendocino escarpment and on the south by the Murray fracture zone. On the east, the Monterey fan abuts against the base of the continental slope off central California. The western edge of the Monterey fan grades into abyssal hills. The boundary between the Monterey and the Delgada fans is indistinct, as the two fans interfinger near a series of low relief rises (Menard, 1960, p. 1271). The Monterey fan is the major large scale submarine

FIGURE 1

INDEX MAP

showing the geological provinces on land
and the geomorphologic provinces of the ocean
bottom off central California

INDEX MAP

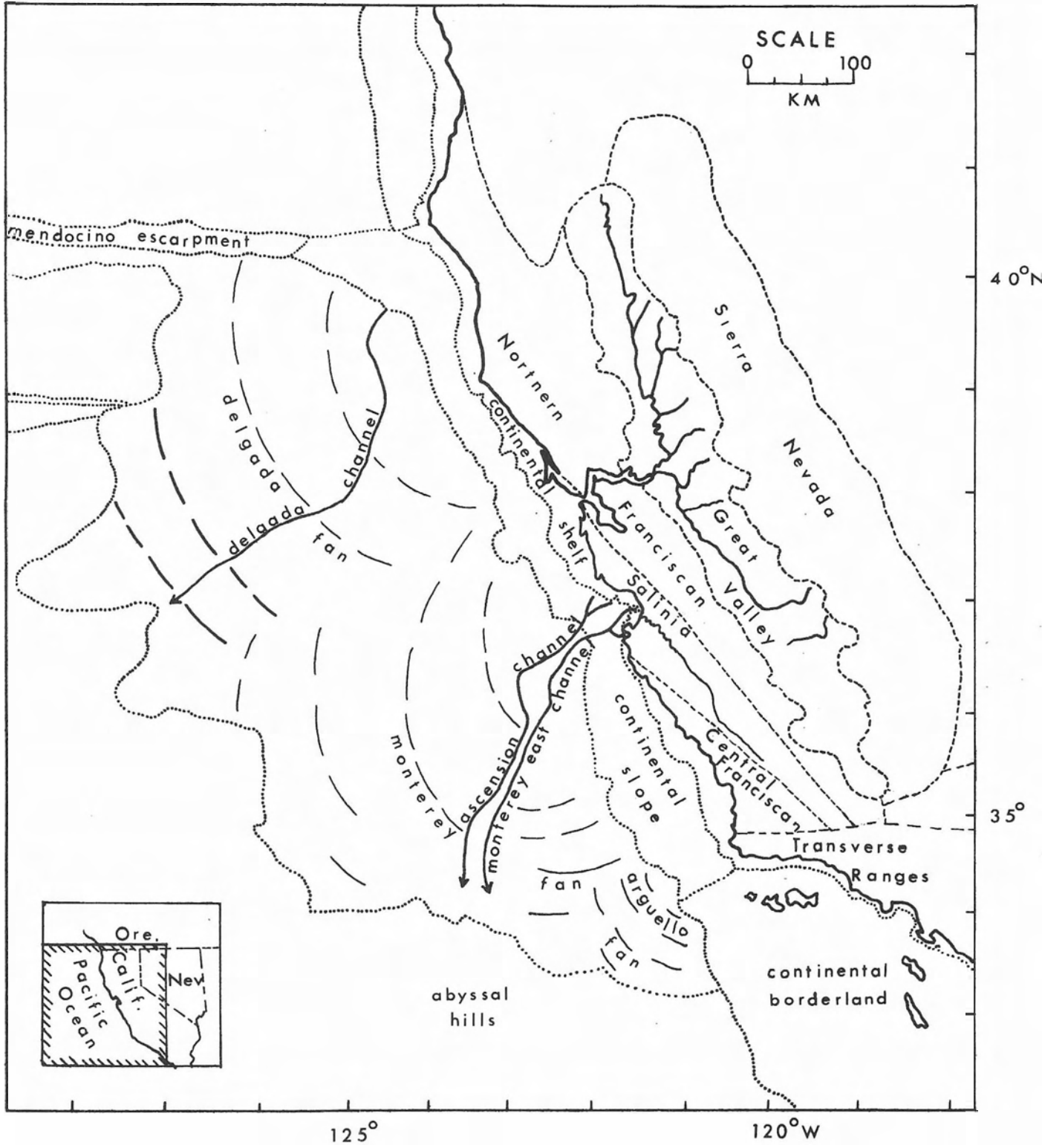
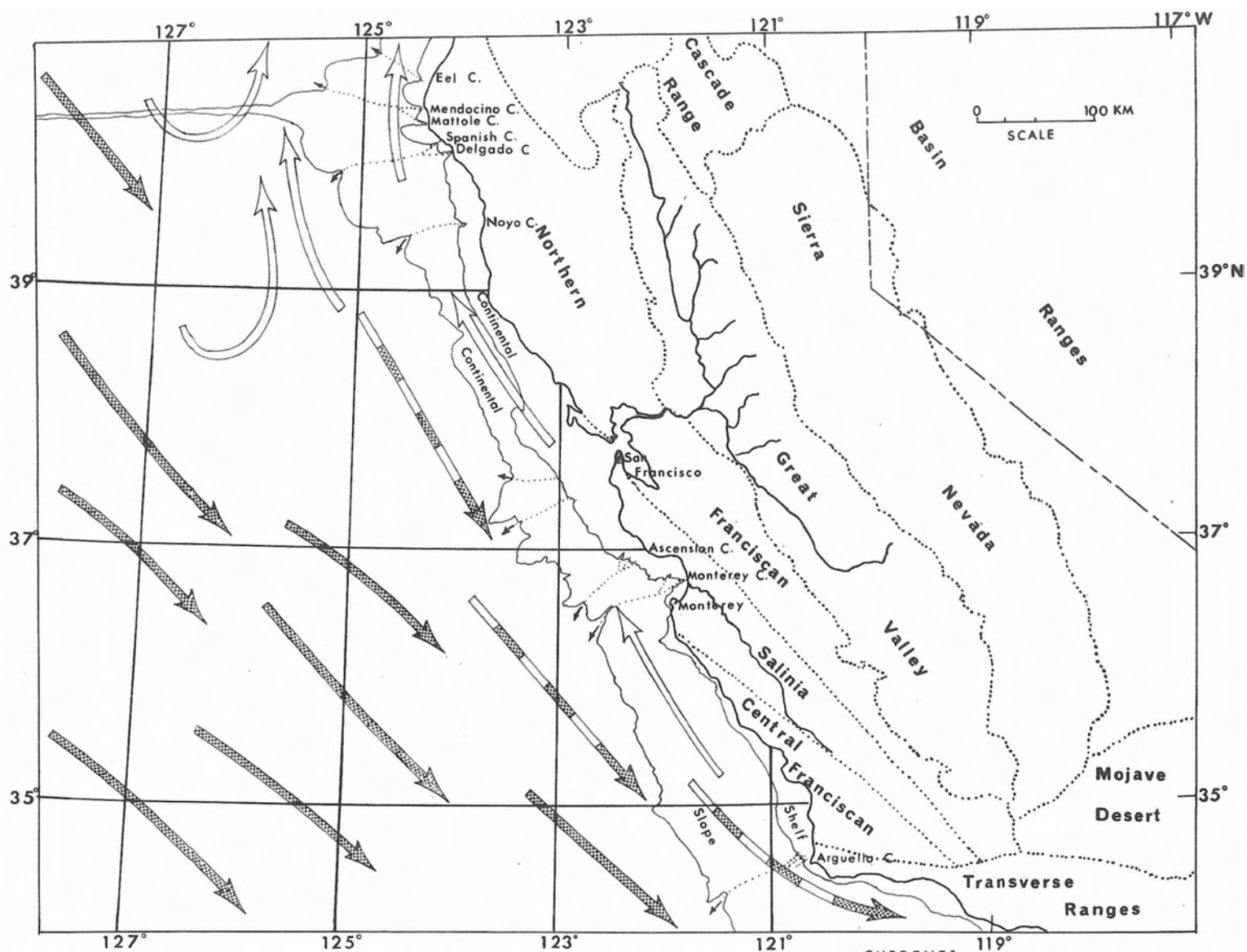


FIGURE 2

**PREVAILING CURRENT DIRECTIONS
OFF CENTRAL CALIFORNIA**

**Source: U. S. Weather Bureau and
U. S. Hydrographic Office, 1961,
Climatological and Oceanographic
Atlas for Mariners**

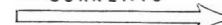


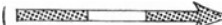
PREVAILING CURRENTS


Velocity Range .05-20 m^2sec

Submarine Canyon

CURRENTS

Davidson  Winter

California  Summer

California  Summer and Winter

feature from 34° to 37° North Latitude and from 122° to 126° West Longitude covering about 100,000 square kilometers of the ocean floor.

Regional Setting:

The bathymetry off the central California coast shows that the apices of the Monterey and Delgada deep-sea fans are at the mouths of the Monterey and Delgada submarine canyons, respectively; and the fans radiate out from the mouths of the canyons. This relationship implies that the bulk of the material on the fans comes down the canyons. If the material is pelagic in origin, the sediment would be expected to be evenly distributed along the edge of the continental slope and the continental rise would be wedge-shaped rather than fan-shaped. Thus, a terrigenous rather than a pelagic source is indicated and the land areas that drain into the heads of the Monterey and Delgada submarine canyons can be inferred as possible sources of sediment now found on these two deep-sea fans.

Sediment could be contributed to the deep-sea fans via the Monterey and Delgada submarine canyon systems from two major drainage basins; (1) the Sacramento-San Joaquin-San Francisco Bay system, which empties through the Golden Gate; and (2) the Salinas-Pajaro system, which empties into the head of the Monterey submarine canyon at Elkhorn Slough. Other contributions may come from numerous small basins that drain the western slopes of the Coast Ranges. The Mendocino and the Mattoje submarine canyons, which extend almost to the shore, probably trap sediment swept southward by longshore currents from areas north of Cape Mendocino (Fig. 2). The southward longshore drift in the vicinity of Point Conception (Trask, 1952) in the summer prevent sediment from areas south of Point Arguello and Point Conception from being retransported onto the Monterey fan. Northward longshore drift during the winter flow of the

Davidson current could transport some material from regions south of Point Conception towards the fan. Most of this material would be carried seaward via the Arguello canyons to the Arguello fan, before it could reach canyons tributary to the Monterey fan. Therefore, only that sediment from rivers that enter the Pacific Ocean from Cape Mendocino south to Point Arguello could be deposited eventually on the Monterey or Delgada deep-sea fans.

Reed (1933, p. 27-31) divided the basement rocks of this central California drainage area into four geologic provinces: (1) northern Franciscan, (2) central Franciscan, (3) Salinia, and (4) Mohavia or the Sierra Nevada. The two Franciscan regions are underlain by metamorphic rocks and ultra-mafic intrusions. The basement rocks of Salinia and the Sierra Nevada consist mainly of felsic igneous rocks, commonly quartz diorite in Salinia. Post-Jurassic sedimentary rocks blanket these four provinces to various degrees. The largest accumulation of post-Jurassic sediments is in the Great Valley of California, which separates the northern Franciscan area from the Sierra Nevada. The Great Valley will be considered as the fifth major geologic province of central California.

Subjects of Investigation:

I have considered mainly the problems associated with the Monterey deep-sea fan in this area off central California because more ~~information~~ information is available on the Monterey fan than on the Delgada fan. Previous workers, Menard (1960) and Dill and others (1954) based their discussions and conclusions about the Monterey fan primarily on interpretations of bathymetric data. Using that work as a starting point, I have reevaluated the bathymetry and supplemented it with previously unavailable data from sediment samples from the surface of the Monterey fan and adjacent areas.

Sources of Data:

Oceanographic information and samples for this study come largely from material gathered by the staff of the Scripps Institution of Oceanography. Where not otherwise noted, the data are from Scripps' sources. For this study of the marine geology of the Monterey fan, primary sources (raw or uninterpreted data) are (1) precision depth records and other sounding information taken during bathymetric surveys, and (2) deep-sea cores and bottom samples collected by me and other members of the Scripps' staff.

Acknowledgements:

This project was undertaken at two centers, Scripps Institution of Oceanography of the University of California and the Department of Geological Sciences of Harvard University. The basic data and most of the technical assistance came from Scripps, whereas academic supervision was from Harvard. Needless to say, many people, both at Scripps and at Harvard, aided this thesis. I particularly wish to thank at Scripps: Prof. H. W. Menard, who originated the project on the fans and supplied the bulk of the financial support, and the G.M.C. Group, S. M. Smith and T. Chase, who offered excellent criticism and friendly encouragement; and at Harvard: Prof. R. Siever, who had the thankless job of seeing that this thesis appeared in my life time.

Financial support for this work was from the Institute of Marine Resources of the University of California, the National Science Foundation Summer Fellowship Program, and the Summer Field Support Program of the Department of Geological Sciences, Harvard University.

Chapter Two

GEOMORPHOLOGY

Major Features:

Three major geomorphic elements of the Monterey fan are (1) the fan slope, (2) undersea positive relief features, and (3) the submarine-canyon-channel systems.

Fan Slope

A significant portion of the fan is a gently sloping surface modified by a series of terraces. The average slope of a series of profiles taken at 15° intervals from the mouth of the Monterey canyon, or at the apex of the fan, is $14'$ corrected for undersea mountains. Near the apex of the fan the average slope is $28'$. Along the outer margin of the fan the slope is only $07'$ (Figs. 3 and 4). These slopes compare with those of the continental rise off the northeast coast of North America, which range from $25'$ to $05'$ (Heezen, and others, 1959, p. 20). No alluvial fans are found on land that have an area comparable to that of the Monterey fan (100,000 square kilometers). However, Bull (1964, p. 92-99) noted that for the Panoche Creek fan (670 square kilometers), the largest of 20 alluvial fans studied in western Fresno County, California; "the slope ranges from $0^{\circ} 17' 24''$ on the uppermost fan segment to $0^{\circ} 8' 14''$ on the lowermost fan segment", which is comparable to the slopes on the Monterey fan. The smaller fans in Bull's study, are at least an order of magnitude smaller than the Panoche Creek fan, and have slopes on the lowermost fan segment as high as $55'$.

Krumbein (1937, p. 588-590) observed that alluvial profiles from fans in southern California plot as negative exponential functions.

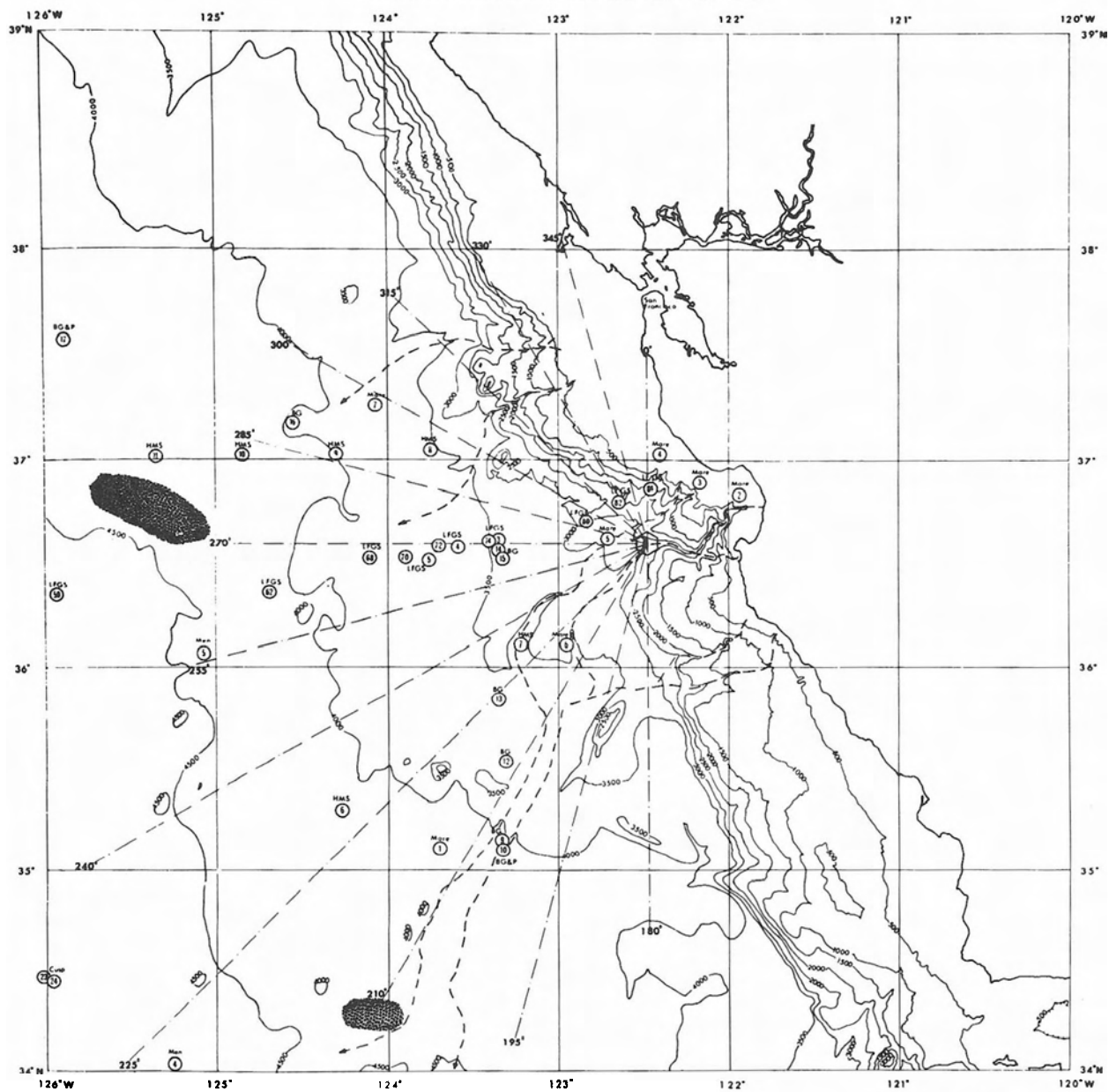
FIGURE 3

**LOCATION MAP FOR RADIAL PROFILES
FROM THE MONTEREY FAN**

FIGURE 4

MONTEREY FAN PROFILES

BATHYMETRIC CHART OF THE MONTEREY DEEP SEA FAN



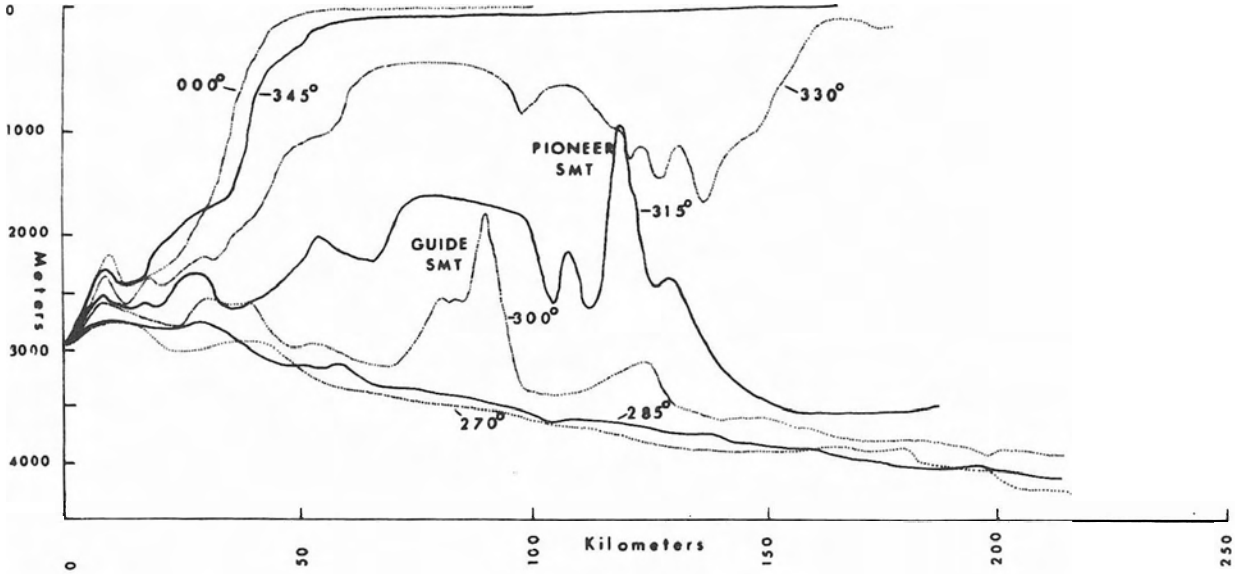
LOCATION OF MONTEREY FAN PROFILES

EXPLANATION

- ① Core Location
- ② Azimuth of Monterey Fan Profile
- 90° Positive Relief Feature
- Canyon Channel System

Contour Interval
500 Meters

MONTEREY FAN PROFILES



Profiles designated by
 azimuth from starting
 point
 36° 35.5' N
 122° 29' W
 near apex of the fan
 Vertical Exaggeration: 25X

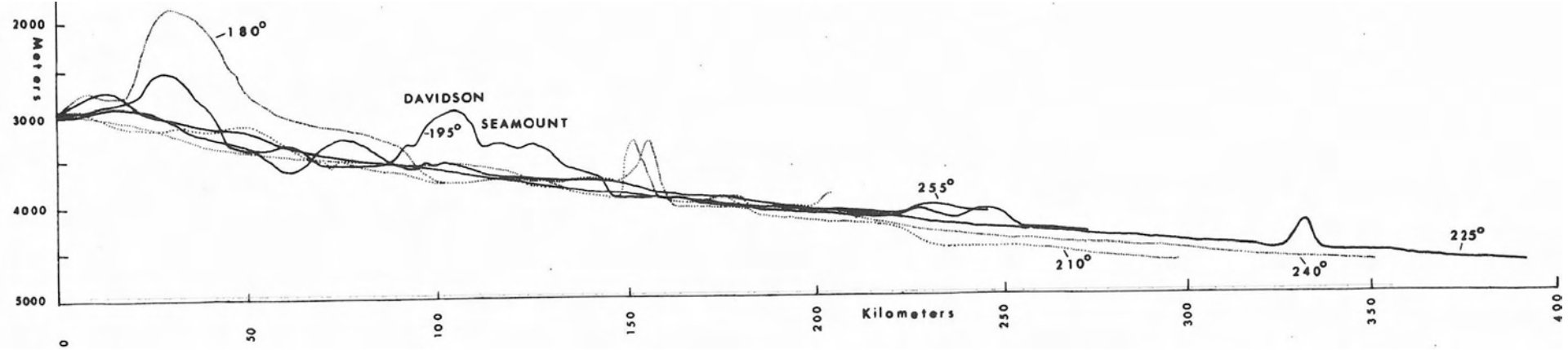
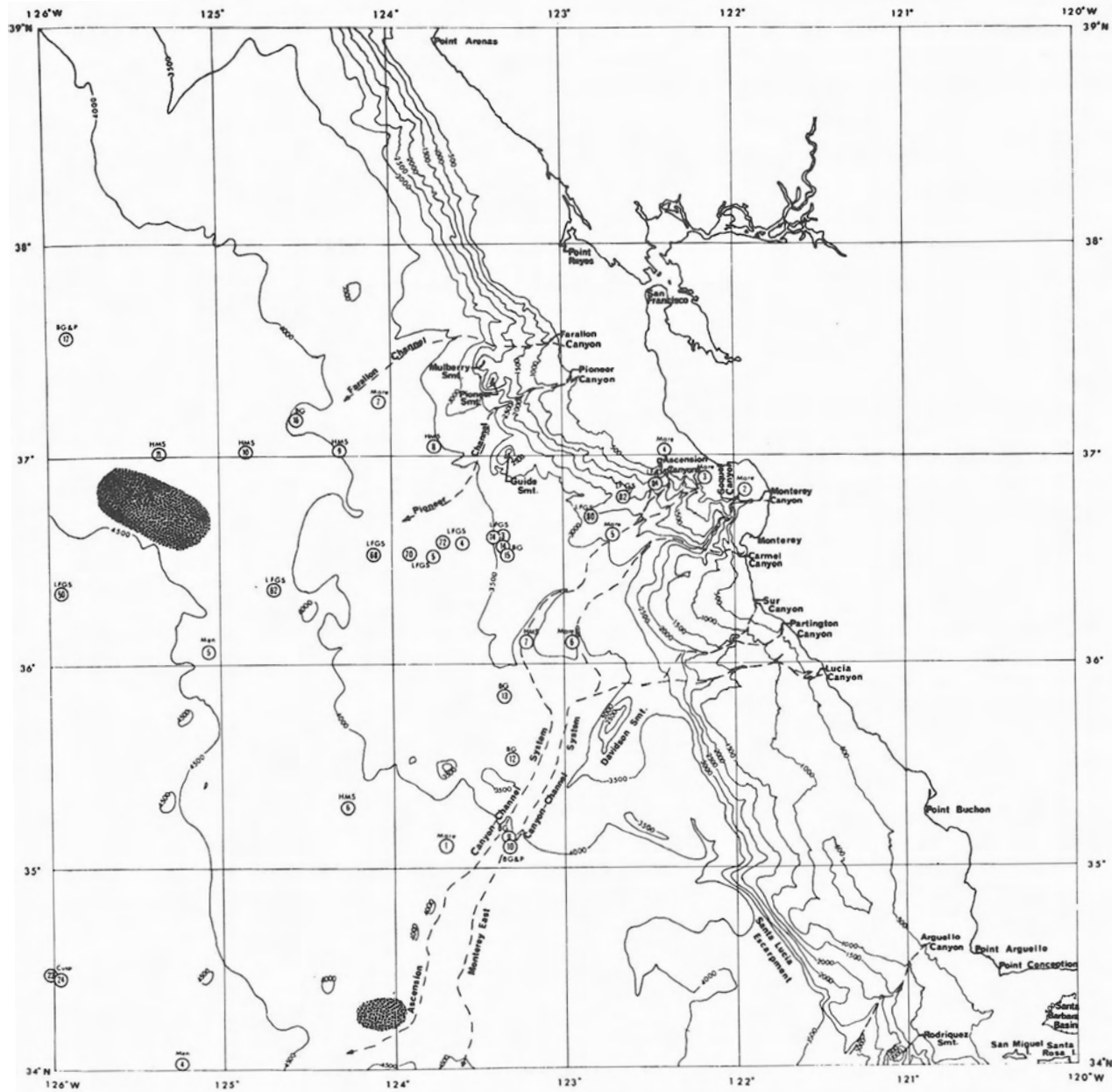


FIGURE 5

INDEX MAP FOR GEOGRAPHICAL NAMES

BATHYMETRIC CHART OF THE MONTEREY DEEP SEA FAN



--- GEOGRAPHICAL INDEX MAP

EXPLANATION

① Core Location

● Positive Relief Feature

- - - Canyon Channel System

Contour Interval
500 Meters

Bull (1964, p. 94-97) showed that the exponential nature of these alluvial profiles can be produced by the smoothing effect of a large contour interval, and that profiles based on maps with small contour intervals are composed of linear segments. The profiles of the Monterey fan surface are derived from the contour map (Plate 3, in the pocket), which has a contour interval of 100 meters, and are essentially negative exponential functions if corrected for seamounts and azimuths not perpendicular to the bathymetric contours. Whether the profiles from the Monterey fan actually are negative exponential functions (concave upward) can not be determined until bathymetric charts of this region are made with the accuracy and contour interval comparable to high quality topographic maps (a contour interval of at least 10 meters).

Undersea Positive Relief

Projecting through the uniform surface of the fan are protuberances of various elevations. Several of these features are aligned in an undersea mountain chain. Menard (1960, p. 1273) noted one such chain that he thought was a ridge partially buried by sediments of the fan. This lineation trends northwest from Rodriguez seamount along the Santa Lucia escarpment (Shepard and Emery, 1941) to just south of Davidson seamount, where the Monterey channels cross the feature (Fig. 5 and Plate 3, in the pocket). Northwest of the Monterey channels, isolated seamounts outline the feature. The topographic lineation is not apparent beyond the northern edge of the fan, where the Monterey fan merges with the Delgada fan. Mason and Raff (1961, p. 1260) however, show a possible off-set of the regional north-south trending magnetic anomalies along the northern extension of the lineation as far to the northwest as the Pioneer ridge. This lineation does not appear to have any connection with any fault

on the southern California mainland.

Four seamounts, Davidson (relief 1900m.), Guide (relief 1400m.), Pioneer (relief 1150m.), and Mulberry (relief 500m.) rise from the sea-floor at the base of the continental slope (Fig. 5 and Plate 3 in the pocket). Davidson seamount rises from a small triangular platform which extends southwest from the continental slope. Other isolated seamounts dot the fan, but these seamounts do not appear to be related to any observed trend. The seamounts on the fan do not have the high relief that characterizes the seamounts at the base of the continental slope and appear to be the tops of low relief hills partially buried by the sediments of the fan. Basalt has been dredged from Guide, Pioneer, and Mulberry seamounts (Chesterman, 1952), evidence that these and probably the seamounts on the fan are volcanic.

Submarine Canyon-Channel Systems

Numerous submarine canyons debouche at the base of the continental slope and continue onto the Monterey fan as submarine channels. Only two systems, the Ascension (Monterey west) and the Monterey east extend for any distance cut onto the fan (400 and 380 km. respectively). The rest of the canyon-channel systems are either tributary to the two long channels or, like the Pioneer and Farallon systems, quickly lose the channel shape and merge into the uniform slope of the fan.

Woodford (1951) tried to relate the profile of the Monterey canyon with the Salinas river valley. He concluded that the Monterey canyon did not have the usual logarithmic profile of subaerial streams as indicated by the Salinas river, but that a straight line was a better fit. Plate 4 (in the pocket) shows the thalweg profiles of the Ascension and the Monterey east systems constructed from bathymetric information

not available to Woodford. The profile of the Ascension system is smoother than the profile of the Monterey east system, in the steeper canyon sections. This is strange as the two systems are essentially parallel throughout their extent and only a few kilometers apart. At equal distances downstream, especially in the upper canyon reaches, the Ascension system is deeper than the Monterey east, indicating deeper erosion in the Ascension system. More erosion could be caused by (1) softer rocks in the walls of the Ascension canyons, (2) larger discharge, or (3) greater age of the Ascension system.

Shepard and Emery (1941, p. 77) and Martin (1964) believe that the knickpoint near the head of the Monterey canyon is formed where the canyon crosses a granite ridge. These workers dredged fresh "granite" (quartz diorite) from this area. To my knowledge no dredge hauls have been made in the Ascension canyon. The nearest shore rocks to the head of the Ascension canyons are Cenozoic sediments. Canyons tributary to the Monterey east system, actually head in igneous rocks (Carmel) and metamorphic rocks (Sur, Partington, and Lucia). The upper section of the Monterey east system, then, appears to be cut into hard igneous and metamorphic rocks, whereas the Ascension canyon may be cut in softer Cenozoic sedimentary rocks, which accounts for its smoother profile.

Whether or not the Ascension system has or had a greater discharge than the Monterey east system is a problem primarily related to the origin of the canyons, a subject not investigated here. Shepard (1963, p. 335-348) gives an excellent summary and critique of the various theories of the origin of submarine canyons. The Ascension system has canyons nearest the Golden Gate in the direction of the southward longshore drift. The mouth of the Sacramento-San Joaquin rivers during the Pleistocene ice maxima may have been

near the head of the Ascension system. The fact that the Sacramento-San Joaquin delivers much more water into the Pacific and much more sediment, most of which is now trapped behind the Golden Gate in San Francisco Bay, than the Salinas river, which is the nearest major source of sediment for the Monterey east; suggests a higher discharge and sediment load for the Ascension system during the Pleistocene low stages of sea level.

The relative ages of the Ascension and the Monterey east systems can not be determined on the basis of current information.

Both the lower reaches of the Monterey east and Ascension channels are smooth and approach a negative exponential curve, except for several breaks in slope. These breaks in slope are correlative between both channels at about the same distance from shore and probably are terraces. As noted above, Menard (1960) thought that one such break in slope was at the crossing of the channels and a northwest trending ridge.

Two-canyon-channel systems, the Pioneer and Farallon (plate 4, in the pocket) do not extend much more than 100 kilometers out onto the fan. The Farallon profile is slightly smoother than the Pioneer profile, which has a small concave down hump about 40 kilometers from the head of the Pioneer canyon. Uchupi and Emery (1963, p. 423) reported Miocene sediments from the upper portions of both the Pioneer and Farallon canyons. Thus the difference in the shape of the profile, in at least the upper sections does not seem to be related to differences in lithology. Uchupi and Emery (1963, p. 423) propose a fault along the Farallon submarine canyon, which may explain its smoother gradient.

Another type of channel exists on the fan, which has no apparent connection to the land through submarine canyons. One such channel heads on the south side of the range of seamounts, 65 kilometers northwest of where the Ascension channel crosses Menard's (1960) proposed ridge. The trend of the channel is southwest, essentially parallel to the direction of the Ascension and Monterey east channels in this area and down the regional slope of the fan. This channel may be the discharge path for slumps associated with volcanic activity on the seamounts in this area.

Hydraulic Geometry:

Calculations

Conventional representations of the geomorphology of channels, such as profiles, gradients, etc. can be augmented by a more mathematical approach. Leopold and Maddock (1953) initiated hydraulic functions as a device to study land streams in a quantitative manner. Their technique was to relate the shape and velocity changes to discharge by the defining continuity equation:

(1)..... $Q = W \cdot D \cdot V$, where $Q =$ discharge,
 $W =$ width,
 $D =$ hydraulic or mean depth, and
 $V =$ mean velocity. From the de-

fining equation (1) it follows that the parameters W , D , and V can be plotted against discharge Q , so that the equations:

(2)..... $W = aQ^b$ where $a \cdot c \cdot k = 1.00$
(3)..... $D = cQ^f$ and $b + f + m = 1.00$,
(4)..... $V = kQ^m$ obtain.

Adapting the hydraulic functions of Leopold and Maddock (1953, p. 8) to data from submarine channels is difficult because, (1) the width and depth values must be read from fathograms, which must be corrected for the side echo effect caused by the wide angle of the sound cone (Krause, 1962), and (2) the velocity (assuming some kind of current flow) has never been measured directly. Thus the parameters for the hydraulic functions must be derived secondarily. By far the most tenuous calculation is that of the velocity term. Theoretically, the combined Chezy-Manning equation gives a good estimation of the mean velocity:

$$(5) \dots\dots\dots V = c^* \left(\frac{\rho_1 - \rho_2}{\rho_1} \right)^{1/2} s^{1/2} \quad (\text{ms})$$

$$c^* = \frac{1.49 m^{1/6}}{n} \text{ for English units,}$$

where

V = mean velocity, in feet per second

c* = Chezy function; in (feet per second)^{1/2}

m = hydraulic radius = $\frac{\text{cross sectional area, in feet}}{\text{wetted perimeter}}$

n = roughness factor, in (feet)^{1/6}

ρ_1 = density of the current flow

ρ_2 = density of the overlying water

s = tangent of the slope of the upper surface of the flow.

The values for the densities of the current flow and the overlying water, and the roughness of the channel have little or no experimental verification, so that these values must be guessed. Hurley (1964) estimated the velocity and discharge for cross sections of the Cascadia submarine channels by using the Chezy-Manning equation as modified by Kullenberg (1954). Wilde (1964) extended the quantification of data from deep-sea

from deep-sea channels by calculating hydraulic functions for the deep-sea channels of the Cocos Ridge, which lies between Costa Rica and the Galapagos Islands. Wilde used depth and width values read from corrected fathograms, and calculated the velocity from Hurley's (1964) Chezy-Manning equation:

$$(6) \dots\dots\dots V = \frac{1.49}{n} \left(\frac{\rho_1 - \rho_2}{\rho_1} \right)^{1/2} (m)^{2/3} (s)^{1/2}$$

The hydraulic functions for the Ascension-Monterey east channels are calculated using equation (6) and the following values and assumptions:

A. roughness factor $n = 0.025$ that of earth (Rouse, 1960, p. 219),

B. $\left(\frac{\rho_1 - \rho_2}{\rho_1} \right)^{1/2} = 0.218$ (Hurley, 1964) based on a $\Delta\sigma$ of 0.05, (Gould, 1951 from observed turbidity currents in Lake Mead),

C. hydraulic radius $m = \frac{\text{cross sectional area}}{\text{wetted perimeter}}$

where the wetted perimeter is twice the maximum width as (1) both the water-flow and the bottom and side-flow boundaries must be considered (Hurley, 1964), and (2) as the width of the channels is much greater than the depth, the sine of the sideslope angle is about equal to the tangent of the sideslope angle, so that the maximum width is approximately equal to the upper perimeter.

D. for channels with triangular cross sections;
 the cross sectional area = $1/2$ maximum depth
 times maximum width
 so $D = 1/2$ maximum depth,
 $W =$ maximum width,
 $m = \frac{1/2 (\text{maximum depth}) (\text{maximum width})}{2(\text{maximum width})}$,
 or $m = \frac{\text{maximum depth}}{4}$

E. for channels with trapezoidal cross sections;
 the cross sectional area = $1/2$ (maximum depth) times
 (upper width + lower width),
 so $D = 1/2$ maximum depth,
 $W =$ (upper width + lower width),
 and $m = \frac{1/2 (\text{maximum depth}) (\text{upper width} + \text{lower width})}{2 (\text{upper width})}$

F. only crossing of the Ascension and Monterey east channels
 on the Monterey fan are used in the calculations, to
 eliminate the possible effects of bedrock canyon walls on
 the flow characteristics.

The hydraulic functions for the Ascension-Monterey east
 channels calculated at bankfull discharge and fitted by a least squares
 analysis are:

(7)..... $W = 17.3Q^{0.38}$,

(8)..... $D = 0.39Q^{0.34}$,

(9)..... $V = 0.19Q^{0.26}$.

FIGURE 6

HYDRAULIC FUNCTIONS -

Width versus Discharge

FIGURE 7

HYDRAULIC FUNCTIONS -

Mean Depth versus Discharge

FIGURE 8

HYDRAULIC FUNCTIONS -

Mean Velocity versus Discharge

Geometric and hydraulic data in
Tables 1 and 2

FIGURE 6

HYDRAULIC FUNCTIONS -

Width versus Discharge

FIGURE 7

HYDRAULIC FUNCTIONS -

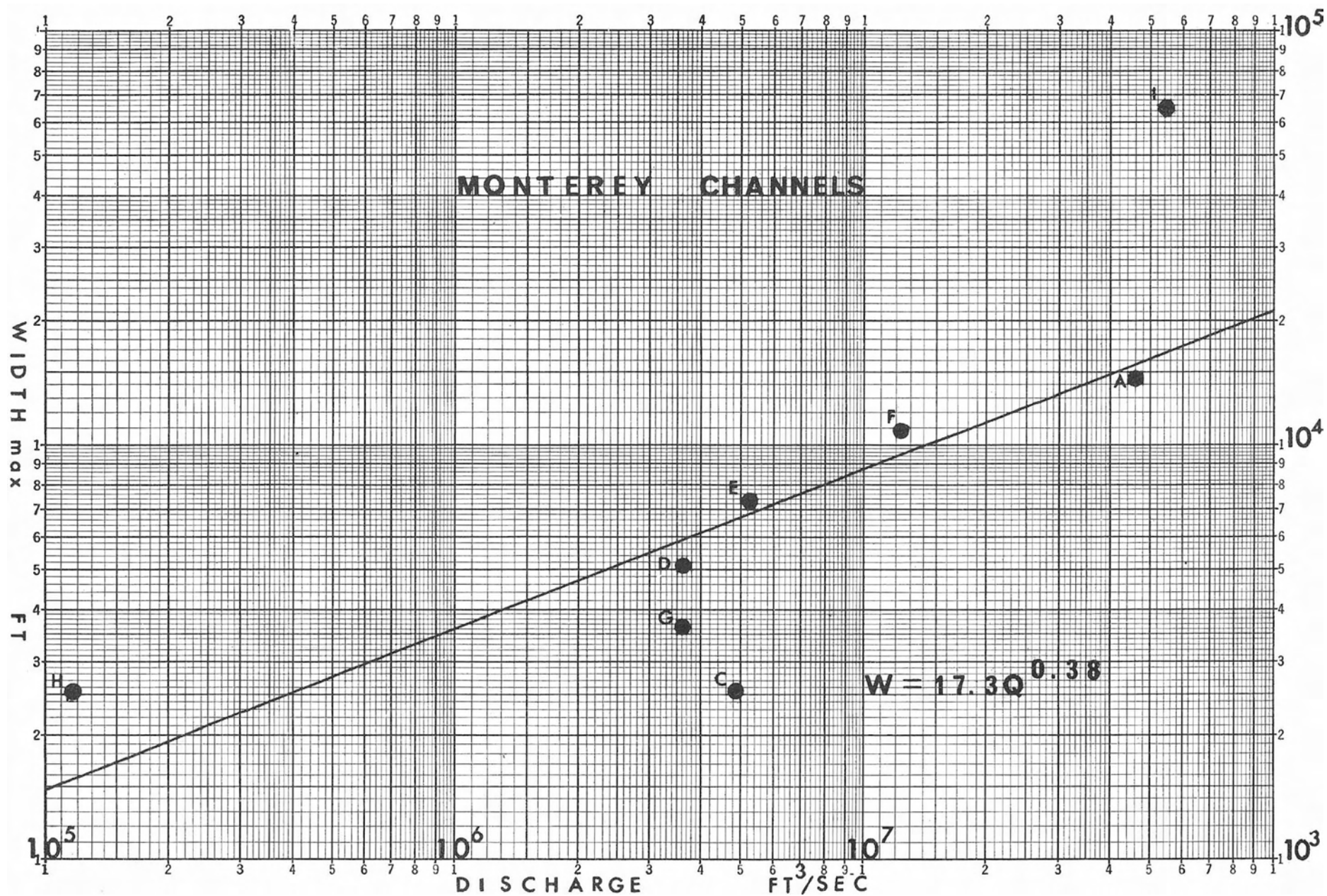
Mean Depth versus Discharge

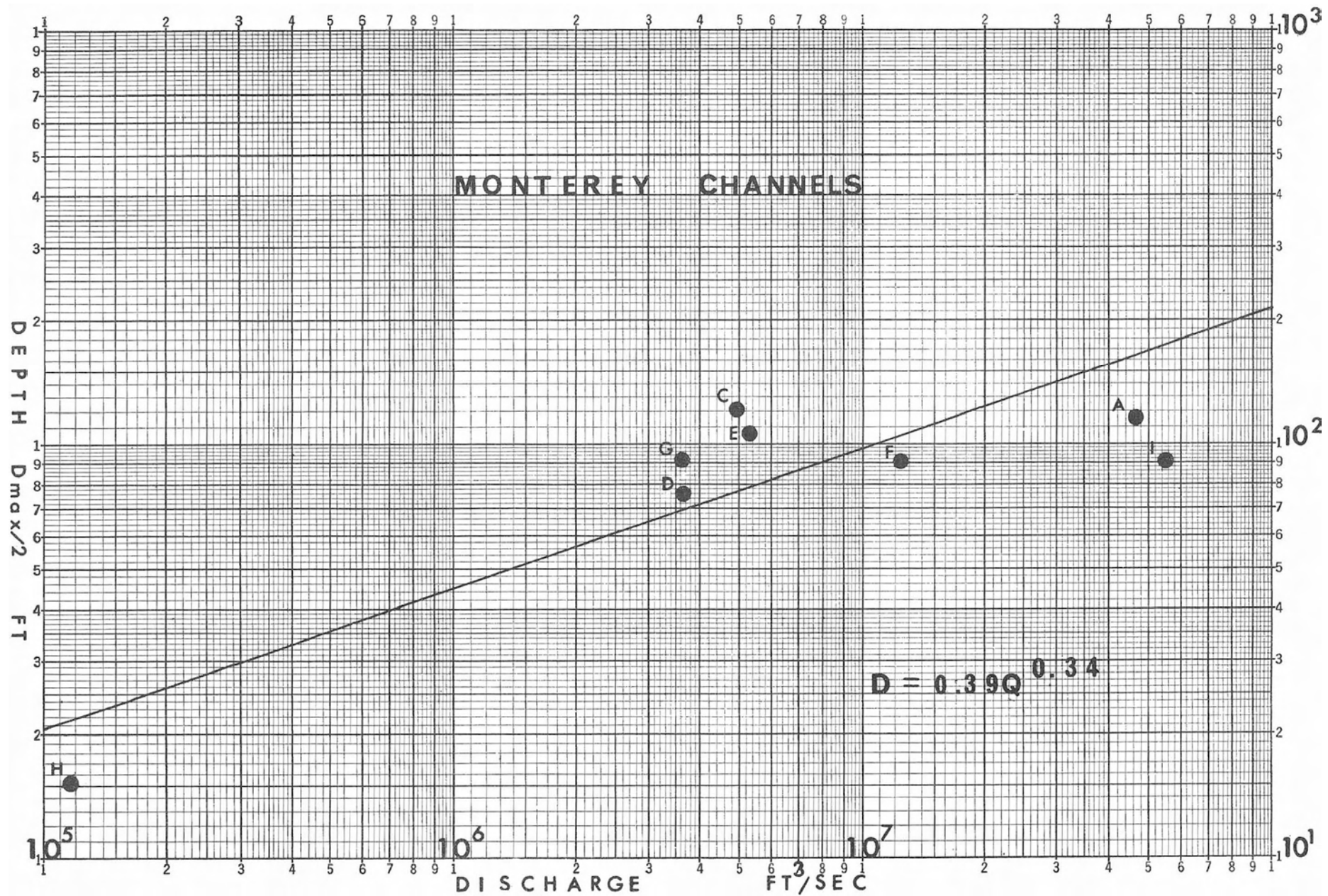
FIGURE 8

HYDRAULIC FUNCTIONS -

Mean Velocity versus Discharge

Geometric and hydraulic data in
Tables 1 and 2





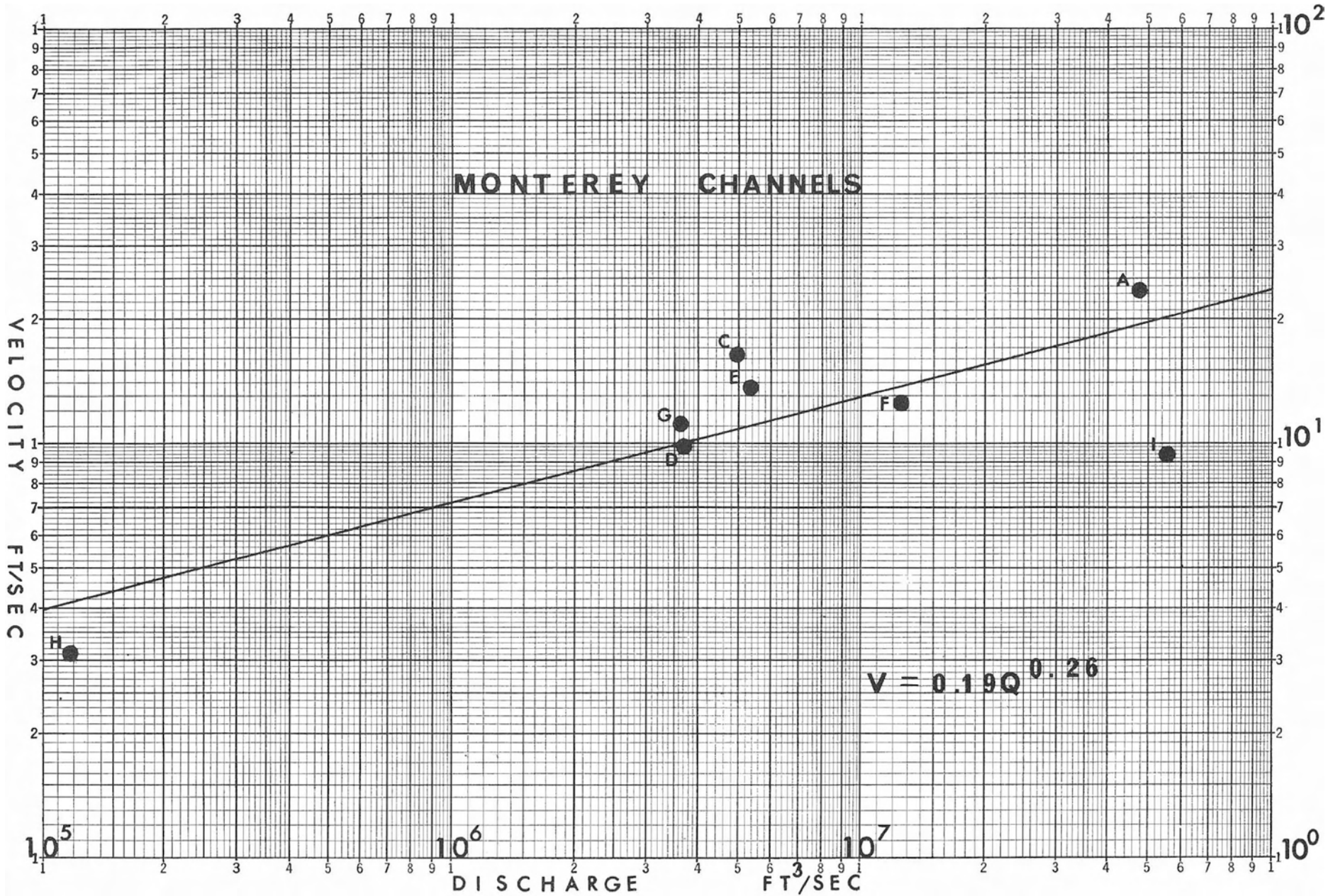


TABLE 1

MONTEREY FAN CHANNELS DATA I

Channel	Latitude	Longitude	Depth of water* meters	Upper Width feet	Lower Width feet	Channel Depth feet
A Monterey E.	36° 09'N	122° 55'W	3480	10,108	4,256	228
B Ascension	36°20'N	123° 03'W	3600	13,832	---	708
C Ascension	36° 07'N	123° 15'W	3680	2,523	---	240
D Monterey E.	35°,08'N	123° 18'W	4090	5,038#	---	150
E Ascension	35° 06'N	123" 27'W	4120	7,387	---	210
F Ascension	35° 01'N	123° 31'W	4190	7,296	3,648	180
G Monterey E.	34° 57'N	123° 25'W	4210	3,648	---	180
H Ascension	34° 47'N	123" 44'W	4260	2,533	---	30
I Monterey E.	34° 44'N	123" 33'W	4310	44,585	21,279	180
J Unnamed	36° 08'N	123° 24'W	3550	42,559	36,479	150
K Pioneer	36° 51'N	123" 35'W	3620	16,233	9,018	78
L Unnamed	35° 16'N	124° 00'W	4110	5,472	---	108

* Measured at bottom of channel

Corrected for non-perpendicular crossing of the channel

TABLE 2

MONTEREY FAN CHANNELS DATA II

Channel	cross Sectional Area: square feet	Slope	Mean Velocity: feet per second	Discharge: cubic feet per second
A Monterey E.	1,637,496	.0197	28.5	46,668,636
B Ascension	4,896,351	.0067	26.8	131,222,207
C Ascension	302,772	.0067	16.3	4,935,184
D Monterey E.	377,850	.0046	9.7	3,665,145
E Ascension	383,030	.0056	13.8	5,285,814
F Ascension	984,960	.0056	12.4	12,213,504
G Monterey E.	328,311	.0047	11.1	3,644,252
H Ascension	37,995	.0039	3.1	117,785
I Monterey E.	5,927,760	.0033	9.3	55,128,168
J Unnamed	5,927,850	.0132	16.4	97,226,740
K Pioneer	984,789	.0061	7.3	7,188,960
L Unnamed	295,477	.0030	6.1	1,802,410

TABLE 3
 RELATIONSHIP BETWEEN DOWNSLOPE DISTANCE
 AND MEAN VELOCITY

<u>Channel Crossing</u>	<u>Downslope Distance:*</u> <u>kilometers</u>	<u>Mean Velocity;</u> <u>feet per second</u>	<u>kilometers</u> <u>per hour</u>
Ascension			
B	104	26.8	29
C	137	16.3	18
E	263	13.8	15
F	274	12.4	14
H	305	3.1	3
Monterey East			
A	145	28.5	31
D	274	9.7	11
G	298	11.1	12
I	326	9.3	10

*Distances to Ascension crossings measured from head of North Ascension Canyon;

Distances to Monterey East crossings measured from head of Monterey Canyon at Moss Landing.

TABLE 4
COMPARISON OF HYDRAULIC FUNCTIONS

Ascension- Monterey East Channels*	Cascadia Channel*	Cocos Ridge Channels*	Average U.S. #	Tidal Estuary*
$W = 17.3 Q^{0.38}$	$118.6Q^{0.26}$	$11.7Q^{0.40}$	$aQ^{0.5}$	$aQ^{0.71}$
$D = 0.39 Q^{0.34}$	$0.07Q^{0.45}$	$0.45Q^{0.33}$	$cQ^{0.4}$	$cQ^{0.24}$
$V = 0.19 Q^{0.26}$	$0.10Q^{0.27}$	$0.19Q^{0.27}$	$kQ^{0.1}$	$kQ^{0.05}$

* Calculated at bankfull stage

Calculated at mean annual discharge

Sources:

Ascension-Monterey East and Cascadia - this report

Cocos Ridge - Wilde (1964)

Average U. S. stream - Leopold and Maddock (1953, p. 16)

Tidal Estuary - Langbein in Myrick and Leopold (1963, p. 17)

The plotted points for these functions are given in Figures 6, 7, and 8. Values for channel crossings other than for the Ascension and the Monterey east systems are not included in the calculations of the above hydraulic functions, equations (7), (8), and (9), as these channels may have a different flow regime than the two parallel Monterey channels. Tables 1 and 2 give the hydraulic and geometric data for all the channel crossings on the Monterey fan that could be analysed.

The discharge of the Monterey submarine channels, unlike the discharge of most subaerial streams, decreases downstream or downslope (Table 3). Changes in the characteristics of the channels are considered in the direction of flow, that is (A) in the direction of decreasing discharge for submarine channels, and (B) in the direction of increasing discharge for subaerial streams. For the Ascension-Monterey east channels, the width function decreases at a higher rate than does the depth function. This difference can be interpreted to mean either that in a downstream direction the sides of the channel are more resistant to scour than the bottom, or possibly that the energy of the flow is concentrated at the bottom. As crude approximations are used in the calculations of the hydraulic functions, slight variation of the slopes of the width and depth functions may have no significance. Thus a conservative evaluation of the meaning of the hydraulic functions is that the width and depth vary at about the same rate because the slopes of these functions vary by only four percent.

Comparison with Other Channel Systems

Hydraulic functions for the Cocos Ridge and Cascadia submarine channels, tidal channels, and the average for United States streams are listed in Table 4. The flow regime for the Cascadia and Ascension-Monterey east channels should be the same, as both systems connect to

land drainage via submarine canyons. Nevertheless, the hydraulic functions for each system are significantly different. The functions for the Cascadia channels were calculated by me from Hurley's (1964) data. These profiles probably included crossing with at least partial bedrock walls. The data from such crossings would give the cross sectional area of a valley rather than the area of a channel which adjusts the geometry of its banks to a maximum flow. Thus the Cascadia functions probably describe the composite effect of rock in the walls of the Gascadia canyons and sediment in the banks of the Cascadia channels.

The values for the Cocos Ridge channels and the Ascension-Monterey-east system show a close correlation. The channels on the Monterey fan are connected to land drainage, whereas the channels on the Cocos Ridge are isolated from land drainage (Wilde, 1964). The similarity of the hydraulic functions indicates that for the measured reaches of the two systems, the flow regime was similar and that this regime is independent of the source of material in the flow. Therefore, the values of the hydraulic functions for the Ascension-Monterey east and the Cocos Ridge channels probably give a quantitative approximation of the variations of channel shape and velocity produced by an undersea current that flows over a soft bottom at a low gradient of less than one degree.

Chapter Three

LITHOLOGY

Sampling Techniques:

Gravity and piston cores are the primary sources of lithologic information on the sediments of the Monterey fan. The advantages of gravity cores are (1) the core apparatus is cheap, so that the expense of replacing the core device is not a factor in picking sampling locations; (2) the coring operation is simple, as it depends only on the impact of the core with the bottom; and (3) removal of the sample from the core barrel is easy. The disadvantages of gravity cores are (1) the length of the sample is short, only up to three meters, and (2) the sample obtained is shorter than the depth penetrated by the core tube. Emery and Dietz (1941, p. 1686) noted, that for gravity cores, "the core length was commonly only 40 to 70 per cent of the distance of penetration of the core-tube." Pratje (1935, p. 25) found that the average ratio of core-length to penetration for cores in red clay was 59.4 per cent. Experiments on shortening of the core sample by Piggot (1941) and Emery and Dietz (1941, p. 1713-1714) show that (a) the gravity core tube takes nearly equal increments per unit of penetration, and (b) the shortening is not caused by compaction or dewatering of the sediment, "but that only part of each layer of sediment is added to the core while the remainder of the layer is pushed aside." The length of a gravity core varies with the type of bottom and the weight of the instrument; the maximum obtainable length is about three meters. The inside diameter of the plastic liner, which contains the sample for the gravity cores examined here, is 4.5 centimeters.

The advantages of piston cores are that (1) they can sample a deeper portion of the bottom than can gravity cores, and (2) they give a relatively undisturbed and complete sample of the interval penetrated. The disadvantages of piston cores are (1) the core apparatus is expensive, especially if the core barrels are stainless steel; (2) the coring procedures are complex; and (3) the core apparatus is unwieldy on shipboard, except in very calm weather. The great advantage of long undisturbed samples makes the piston core a more useful oceanographic tool than the gravity core.

Piston coring uses the force of gravity to drive the core tube into the bottom and hydrostatic pressure to permit easy entry of the bottom material into the core tube. A piston, that is attached to the main wire by a length of wire equal to the length of the core barrel plus the length of the trigger mechanism and the weights above the core barrel, is placed in the lower end of the core barrel in the core nose. As the core barrel goes into the bottom, driven by the weight of the coring apparatus, and the main wire to the ship is stopped; the piston, ideally, remains stationary at the level of the sea floor. A pressure differential is created between the space in the core tube below the piston and the sea water outside the tube, as the core barrel falls passed the immobilized piston. This partial vacuum acts counter to the retarding force of side wall friction and enables the sediment to move into the core tube more freely than if just forced into the core tube by the weight of the apparatus. The sediment in the core tube represents a relatively undisturbed sample of the material penetrated by the core barrel if the piston remains stationary. Kullenberg (1956, p. 42-76) gave a detailed analysis of the mechanics and mathematics of piston coring.

TABLE 5

GENERAL CORE INFORMATION

<u>CORE</u>	<u>LATITUDE</u>	<u>LONGITUDE</u>	<u>DEPTH</u> in <u>Meters</u>	<u>LENGTH</u> in <u>Centimeters</u>
<u>CUSP 1954</u>				
CUSP 4G	39°30'N	125°52'W	3805	120
CUSP 23G	34°29'N	126°02'N	4770	148
CUSP 24G	34°28.5'N	125°59'W	ca. 4750	145
<u>FANFARE 1959</u>				
HMS 6G	35°18'N	124°16'W	4170	104.5
HMS 7G	36°06'N	123°14'W	3530	128
HMS 8G	37°03'N	123°46'W	3550	131
HMS 9G	37°01'N	124°18'W	3980	126
HMS 10G	37°01'N	124°50'W	4240	109.5
HMS 11G	37°01'N	125°21'W	4350	148.5
HMS 12G	38°03'N	126°24'W	4430	143
HMS 13G	39°44'N	125°22'W	3210	13
HMS 17G	39°51'N	129°39'W	4550	120
HMS 18G	39°26'N	129°13'W	4320	178
BG 9G	35°08'N	123°19'W	4025	42
BP 10P	35°06'N	123°19'W	4100	273
BG 12G	35°31'N	123°19'W	4300	77.5
BG 13G	35°51'N	123°21'W	3660	42
BG 14G	36°33'N	123°21'W	3470	54
BG 15G	36°32'N	123°20'W	3470	171
BG 16G	37°11'N	124°34'W	3850	126
BG 17G	37°34'N	125°53'W	4350	133.5
BP 17P	37°34'N	125°53'W	4350	713
BG 18G	39°14'N	125°03'W	3200	127
BP 18P	39°14'N	125°03'W	3200	610
BG 27G	40°08'N	128°12'W	ca. 4510	121
BG 29G	38°32'N	127°56'W	4660	29
<u>MENDOCINO 1960</u>				
MEN 4G	34°02'N	125°15'W	4640	157
MEN 5G	36°04'N	125°04'W	4460	163
MEN 6G	38°25'N	126°09'W	4280	176
MEN 13G	40°07'N	128°10'W	4510	134

Table 5 - continued

<u>CORE</u>	<u>LATITUDE</u>	<u>LONGITUDE</u>	<u>DEPTH</u> <u>in</u> <u>Meters</u>	<u>LENGTH</u> <u>in</u> <u>Centimeters</u>
<u>MAREZINE 1961</u>				
MARE 1G	35°06'N	123°42'W	4100	73
MARE 2G	36°51'N	121°55'W	68	87.5
MARE 3G	36°55'N	122°11'W	88	18
MARE 4G	37°02'N	122°24'W	113	15
MARE 5G	36°37'N	122°43'W	2860	132
MARE 6G	36°06.5'N	122°57'W	3440	135
MARE 7G	37°15'N	124°05'W	4000	5*
<u>LEAPFROG 1961</u>				
LFGS 3G	36°36.5'N	123°22'W	3500	144.5
LFGS 4G	36°35'N	123°35.5'W	3620	12*
LFGS 5G	36°31'N	123°46'W	3750	18.5*
LFGS 50G	36°23'N	125°56'W	4610	161
LFGS 62G	36°22'N	124°41'W	4180	66
LFGS 68G	36°32'N	124°06'W	3920	153
LFGS 70G	36°32'N	123°54'W	3845	150
LFGS 72G	36°35'N	123°42'W	3710	112
LFGS 74G	36°37'N	123°27'W	3500	149
LFGS 80G	36°42'N	122°51'W	2630	117
LFGS 82G	36°48'N	122°51'W	2165	125
LFGS 84G	36°52'N	122°28'W	1520	109

*Sample from core catcher only.

G = Gravity Core

P = Piston Core

With the side wall friction effectively reduced by the use of a piston, the depth of penetration is increased to a maximum of about 20 meters.

The location of the 49 cores examined is found in Table 5.

Table 5 also lists the depth of water at the core station, length of the core, and type of core. Lithologic descriptions of each core listed in Table 5 are in Appendix A.

Textures:

Coarser than ,062 mm

Twenty-nine of the 49 cores examined have discrete sand units. The shape of the sand bodies varies from irregularly shaped blebs and globules "floating" in a mud matrix to well defined horizontal sand layers. The color of the sands is a dark shade of gray, almost black. The only exceptions of the rule of dark color for the sands are (1) the brown sands in Men 4, and (2) the light yellow sand in BP 10. The size of the sands is fine to very fine grained (. 250 to 062 mm., Krumbein and Pettijohn, 1938, p. 80), except for one medium sand (. 50 to .25 mm.) in BP 10, smeared along the sides of the core from 73 to 126 centimeters. Coarser fragments, mostly granules (4 to 2 mm.) associated with a few pebbles (64 to 4 mm.), are not in discrete sand layers, but are mixed with sand and mud in a poorly sorted mud in BP 10. No core except BP 10 has particles coarser than fine sand.

Four brown sands in Men 4, at 23-26, 53-56, 87-91, and 107. 5-112. 5 centimeters are graded upward from fine sand to very fine sand to silt. These units have a distinct sharp basal contact and a gradational top. Above each of the brown sand layers is an exactly repeated sequence of mud and gray sand layers terminating upward in a brown mud, which was presumably oxidized at the sea water-sediment interface. It is unlikely that the same oxidation-reduction conditions,

With the side wall friction effectively reduced by the use of a piston, the depth of penetration is increased to a maximum of about 20 meters.

The location of the 49 cores examined is found in Table 5.

Table 5 also lists the depth of water at the core station, length of the core, and type of core. Lithologic descriptions of each core listed in Table 5 are in Appendix A.

Textures:

Coarser than ,062 mm

Twenty-nine of the 49 cores examined have discrete sand units. The shape of the sand bodies varies from irregularly shaped blebs and globules "floating" in a mud matrix to well defined horizontal sand layers. The color of the sands is a dark shade of gray, almost black. The only exceptions of the rule of dark color for the sands are (1) the brown sands in Men 4, and (2) the light yellow sand in BP 10. The size of the sands is fine to very fine grained (. 250 to 062 mm., Krumbein and Pettijohn, 1938, p. 80), except for one medium sand (. 50 to .25 mm.) in BP 10, smeared along the sides of the core from 73 to 126 centimeters. Coarser fragments, mostly granules (4 to 2 mm.) associated with a few pebbles (64 to 4 mm.), are not in discrete sand layers, but are mixed with sand and mud in a poorly sorted mud in BP 10. No core except BP 10 has particles coarser than fine sand.

Four brown sands in Men 4, at 23-26, 53-56, 87-91, and 107. 5-112. 5 centimeters are graded upward from fine sand to very fine sand to silt. These units have a distinct sharp basal contact and a gradational top. Above each of the brown sand layers is an exactly repeated sequence of mud and gray sand layers terminating upward in a brown mud, which was presumably oxidized at the sea water-sediment interface. It is unlikely that the same oxidation-reduction conditions,

TABLE 6

<u>CORE</u>	<u>PERCENTAGE DISCRETE SAND AND SAND-SHALE RATIOS</u>				<u>Total</u>	<u>Sad-Shale Ratio</u>
	<u>0-50</u>	<u>Length in 50-100</u>	<u>Centimeters 0-100</u>	<u>100-150</u>		
CUSP4	0.2%	2.8%	1.5%	---	1.2%	1:41
CUSP 23	0.0	0.0	0.0	---	0.0	----
CUSP 24	0.0	0.0	0.0	---	0.0	----
HMS 6	8.0	7.5	7.75	---	7.4	1:6
HMS a	1.0	0.0	0.5	---	1.6	1:31
HMS 8	0.0	0.0	0.0	---	1.1	1:45
HMS 9	0.0	0.0	0.0	---	0.2	1:250
HMS 10	0.0	6.0	3.0	---	2.7	1:18
HMS 11	0.0	21.4	10.7	16.0	12.3	1:4
HMS 12	0.0	0.0	0.0	---	0.3	1:166
HMS 13	---	---	---	---	0.0	----
HMS 17	0.0	0.5	0.25	---	0.2	1:250
HMS 18	0.0	0.0	0.0	0.0	0.0	----
BG 9	---	---	---	---	0.0	----
BP 10	0.0	8.0	4.0	5.9	2.9	1:17
BG 12	2.5	---	---	---	6.8	1:8
BG 13	---	---	---	---	3.5	1:14
BG 14	0.0	---	---	---	0.0	----
BG 15	0.0	0.0	0.0	3.0	2.3	1:21
BG 16	0.0	0.0	0.0	---	0.0	----
BG 17	1.0	0.0	0.5	---	0.4	1:125
BP 17	10.0	0.0	5.0	0.0	3.4	1:14
BG 18	0.0	1.5	0.75	---	0.6	1:83
BP 18	0.0	0.0	0.0	0.0	0.0	----
BG 27	0.0	0.0	0.0	---	0.0	----
BG 29	---	---	---	---	0.0	----
MEN 4	Contains sand, but as core bounced, no estimates of percentage sand can be made.					
MEN 5	0.0	0.0	0.0	0.0	0.0	----
MEN 6	0.0	0.0	0.0	0.0	0.0	----
MEN 7	5.0	---	---	---	10.2	1:4
MEN13	0.0	10.0	5.0	---	3.7	1:13
MARE 1	6.0	---	---	---	4.1	1:12
MARE2	0.0	---	---	---	0.0	----
MARE 3	---	---	---	---	0.0	----
MARE 4	---	---	---	---	0.0	----
MARE5	0.0	0.0	0.0	---	0.0	----
MARE 6	2.5	10.0	6.3	---	7.1	1:6

Table 6 • continued

<u>CORE</u>	<u>0-50</u>	<u>50-100</u>	<u>0-100</u>	<u>100-150</u>	<u>Total</u>	<u>Sand-Shale Ratio</u>
LFGS 3	0.0	0.0	0.0	---	1.4	1:36
LFGS 4	---	---	---	---	0.0	----
LFGS 5	---	---	---	---	0.0	---
LFGS 50	0.0	0.0	0.0	0.0	0.0	----
LFGS 62	1.0	---	---	---	0.8	1:65
LFGS 68	0.0	22.0	11.0	2.0	7.8	1:6
LFGS 70	0.0	5.0	2.5	4.0	3.0	1:16
LFGS 72	0.0	3.0	1.5	---	1.3	1:37
LFGS 74	0.0	8.0	4.0	2.0	3.3	1:14
LFGS 80	0.0	0.0	0.0	---	0.0	----
LFGS 82	0.0	0.0	0.0	---	0.0	----

which control the color of the mud, would be duplicated exactly four times or that a cyclic process could deposit four exact sequences of layers of sand, silt, and mud in the same order and thickness. A reasonable explanation is that the repetition is caused by a bouncing core barrel ricocheting off some hard layer in the bottom. The four brown sands in Men 4 are interpreted as being from one layer that was penetrated four times by a bouncing core tube.

Numerous other sands in the cores have sharp basal contacts, but do not show size grading that is apparent under 14 power magnification. The upper contacts of these sand units are either sharp or gradational. No sand body has a gradational lower contact.

The fine material (less than .062 mm.), or matrix, of the sand bodies varies in amount, especially in the sands that grade into mud. The minimum amount of matrix is in the basal portions of the sand layers and is about 25 to 50 per cent by volume. All the sands analyzed had at least 25 per cent 'matrix finer than sand size, except for the medium sized sand from 73 to 126 centimeters in BP 10 which is well sorted. In general the fine sands are not clean like beach sands and on the basis of color, gray-black and sometimes brown, and high matrix content, the sands would be called "dirty".

Mud

Table 6 and the core descriptions show that about 90 per cent or more of each core is material finer than .062 mm. Samples of this fine material from the cores were too small to be sized by standard settling velocity methods. However, this material was wet sieved in .062 and .044 mm. sieves. Over 95 per cent of the material by weight and volume passed through the .044 mm. sieve. Thus the fine material is silt size and finer. This fine material is a mud, according to

Revelle's (1944, p. 16) classification of deep-sea sediments. Accurate determinations of the weight of the mud, both associated with the sands and in individual mud layers, for the purpose of size analysis can be done only by drying the sample. Petelin and Aleksina (1961) reported that the size distribution determined on a dried sample is a function of the sieve initially used. Splits from the same sample could give varying results when washed through different mesh sieves. So for this study, the samples were kept moist in sea water and no complete size analysis of the silt and finer fractions was attempted.

Three types of mud, brown, green, and gray, are distinguished. Various shades of brown, that is, chocolate, dark, light yellow, sometimes mottled with combinations of shades, indicates oxidation of the iron in the clays to the ferric state (Edward Goldberg, oral communication). Usually the brown muds are at the tops of the cores and along the core walls, where chemical changes undoubtedly take place caused by diffusion of oxygen from the air through the plastic core liner. Gorsline and Emery (1959, p. 288) believed the green muds of the San Pedro and Santa Monica basins, just south of the Monterey fan, to be pelagic in origin. It is not unlikely that the olive drab muds of the Monterey fan also may be pelagic. The third type of mud, which is the most abundant, is colored various shades of gray. Green gray, almost green, and light gray are the commonest shades, although blue gray and wet cement gray muds are noted.

The brown muds show gradational contacts compatible with their interpretation as oxidation products. The olive drab green muds generally have sharp distinct upper and lower contacts (see Cusp 24, 100-101 centimeters, Appendix A). The numerous gray muds show sharp contacts occasionally. The most characteristic feature of the

FIGURE 9

PERCENTAGE DISCRETE **SAND**

0 - 50 Centimeters

FIGURE 10

PERCENTAGE DISCRETE SAND

50 - 100 Centimeters

FIGURE 11

PERCENTAGE DISCRETE **SAND**

0 - 100 Centimeters

FIGURE 12

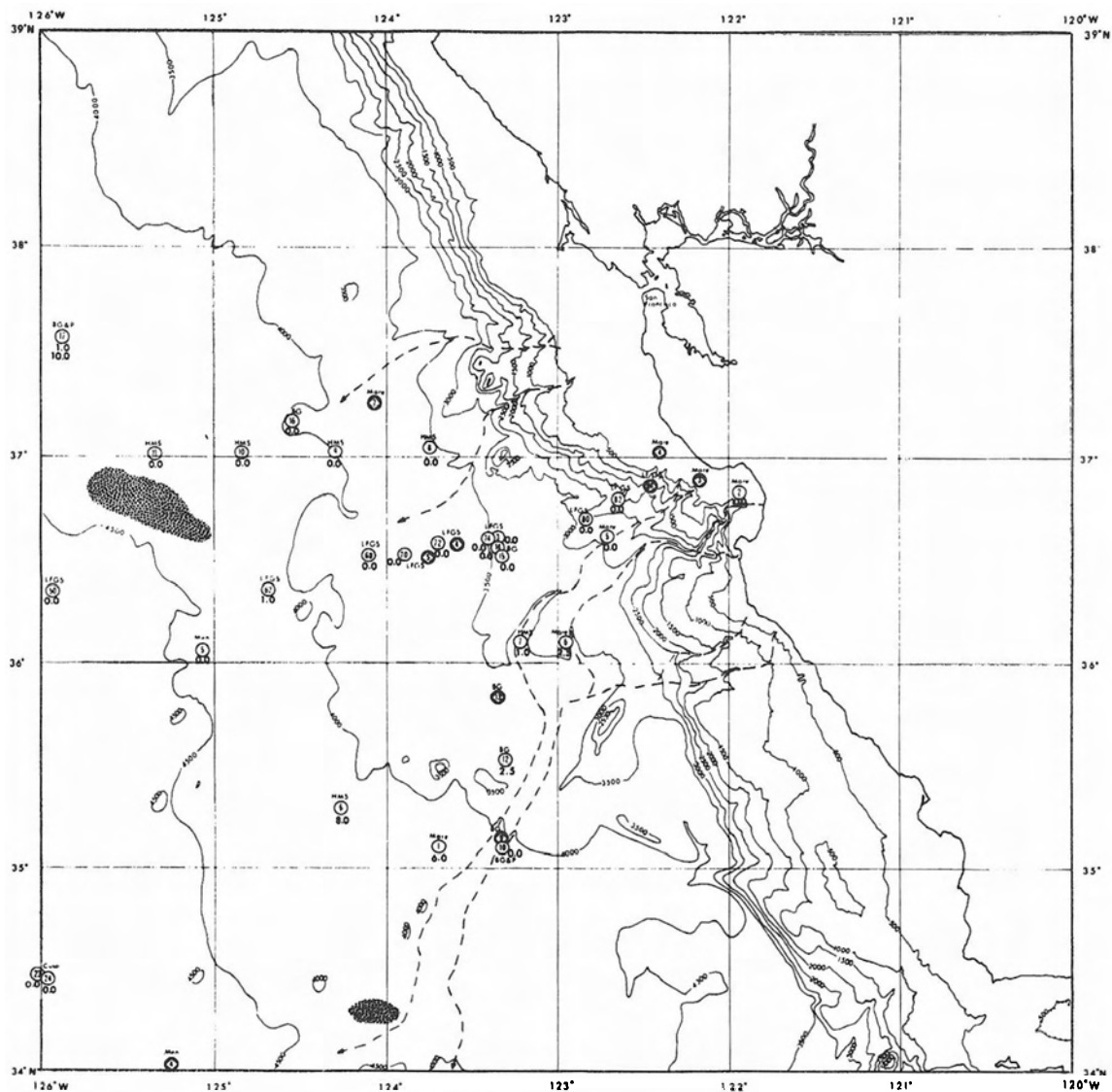
PERCENTAGE DISCRETE **SAND**

100 - 150 Centimeters

Data from Table 6

41-42-43-44

BATHYMETRIC CHART OF THE MONTEREY DEEP SEA FAN



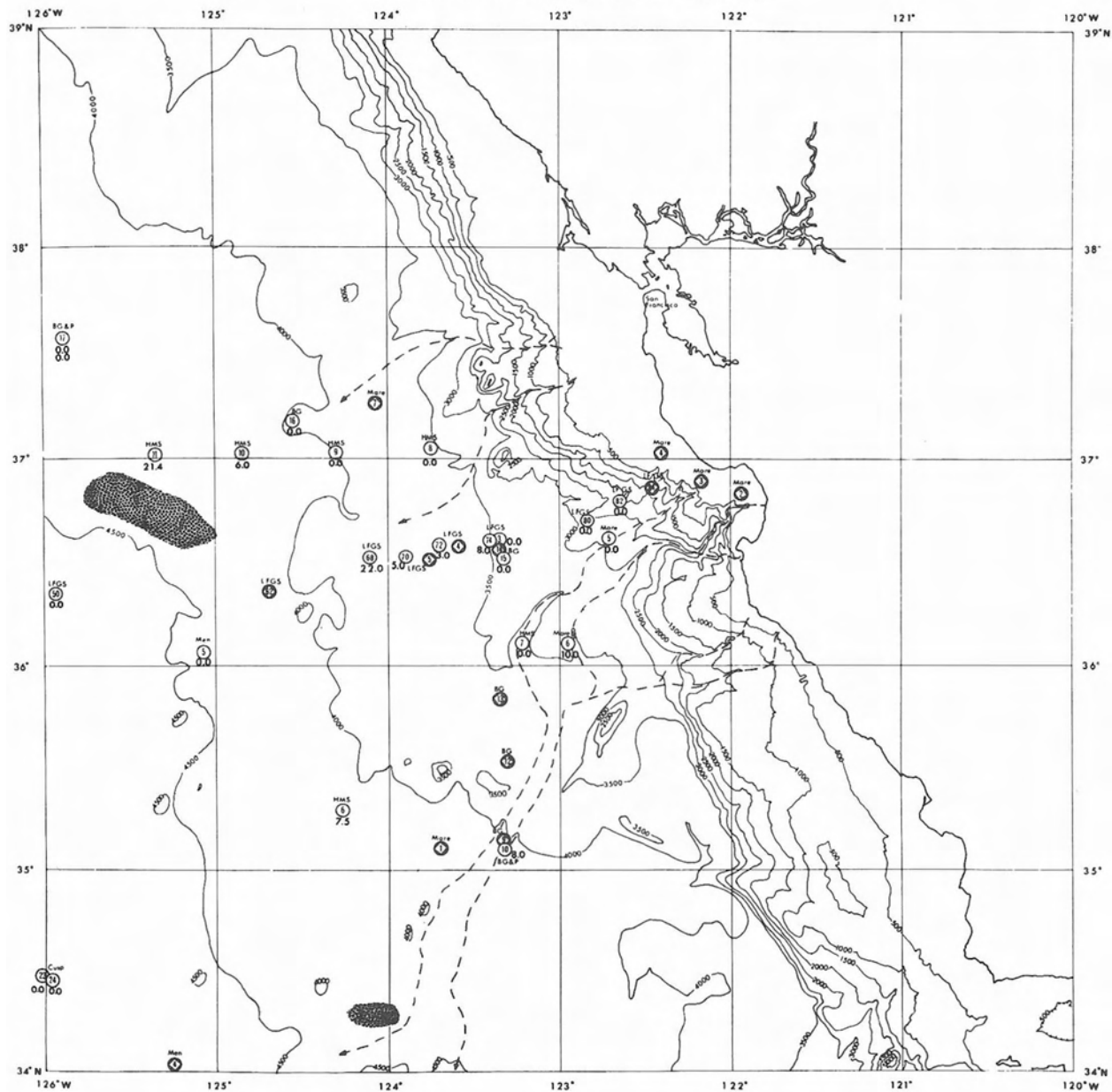
PERCENTAGE DISCRETE SAND
0-58 CM

EXPLANATION

- Core Location
- Percentage Discrete Sand
- Positive Relief Feature
- Canyon Channel System
- Core Did Not Penetrate Interval

Contour Interval
500

BATHYMETRIC CHART OF THE MONTEREY DEEP SEA FAN



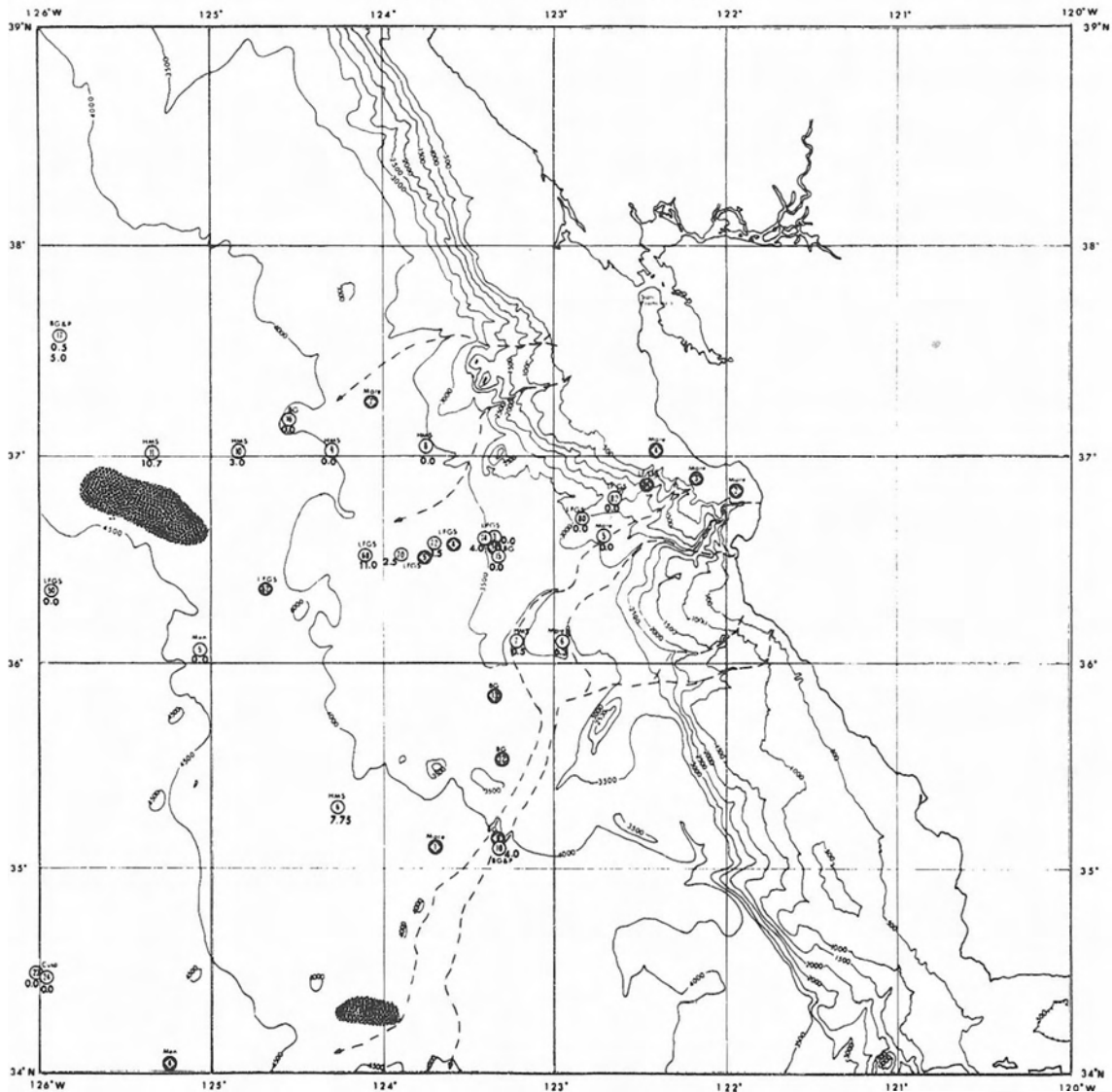
PERCENTAGE DISCRETE SAND
50-100 CM

EXPLANATION

- ⑩ Core Location
- ⑧⑩ Core Did Not Penetrate Interval
- 8.0 Percentage Discrete Sand
- Positive Relief Feature
- Canyon Channel System

Contour Interval
500 Meters

BATHYMETRIC CHART OF THE MONTEREY DEEP SEA FAN



PERCENTAGE DISCRETE SAND
0-100 CM

EXPLANATION

- ① Core Location
- ⊖ Core Did Not Penetrate Interval
- 40 Percentage Discrete Sand
- ⊕ Positive Relief Feature
- Canyon Channel System

Contour Interval
500 Meters

contacts of the gray muds is the gradual transition from green gray at the base to light gray or blue gray at the top of the layer (see **LFGS** 50, 87.5-92.5 centimeters). Sometimes the contacts are churned and indistinct, probably the result of the actions of boring organisms living in the sediment.

Sand to mud deposition

An estimation of the percentage of sand in discrete lenses or layers gives an approximation of the relative amount of sand deposition. Continuous sampling of Scripps' cores along the entire length of the core is not permitted to insure an ample supply of material for various types of investigations on deep-sea sediment. This restriction prevented an estimation of the sand-mud ratio for each core, based on laboratory size analysis of the samples. In this study, what is not considered discrete sand is considered mud. This appears to be a valid assumption for all cores except BP 10, which was taken in the Monterey east channel. As noted above, BP 10 has considerable coarse material bound in a poorly sorted sandy mud; thus the sand-mud ratio listed for this core is too low.

The percentage value is obtained by estimation of the thickness of the sand layer. This procedure is difficult because most sand layers are not linear bands, but have irregular shapes. For example, if the the thickness of all discrete sand lenses in a core is 7.5 centimeters, and the core is 100 centimeters long, the percentage discrete sand is 7.5. The percentage of discrete sand is calculated for the total core, and intervals from, 0-50, 50-100, 0-100, and 100-150 centimeters (Table 6, and Figures 9, 10, 11, and 12).

Sand-shale ratios are calculated for the sandy cores by using the percentage discrete sand values and applying Gorsline and Emery's (1959, p. 283) assumption that mud is compacted to one-half its original thickness upon the conversion of mud to shale (Table 6). The lithification of the material sampled by the cores from the Monterey deep-sea fan would produce a shale with numerous sandy partings and thin sand lenses.

Chapter Four

MINERALOGY

Procedures:

The samples analysed are from cores from the Monterey fan and adjacent submarine areas. The raw samples were wet sieved with sea water^{1/}. Sand samples were washed through .250, .125, .077, and .062 mm. mesh sieves. The wash water, which contained material finer than the smallest sieve opening, was collected in a glass tube with a plastic vial taped to its base. After the silt and clay had settled into the plastic vial, the overlying clear wash water was siphoned off and the vial removed from the bottom of the tube. The contents of each sieve were washed with distilled water to remove salt. Each size was separated into a light and heavy fraction in tetrabromoethane (specific gravity 2.89 at 25^o C.). Each fraction was weighed and a grain mount for microscope work was made for each fraction that had sufficient material. Figures 13a and 13b show the grain size distribution in weight per cent for the sand fraction. One hundred grains per slide were counted and identified, unless so designated.

Coarser than .062 mm. :

Light Fraction (specific gravity less than 2.89)

Table 7 shows the mineralogy determined for the light fraction. Tables 8 and 9 give a synopsis of the data in Table 7 for the major

^{1/} Sea water from Narragansett Bay and Long Island Sound with a salinity approximately 29 to 30^o/oo.

FIGURE 13

GRAIN SIZE ANALYSES

Layered Sands

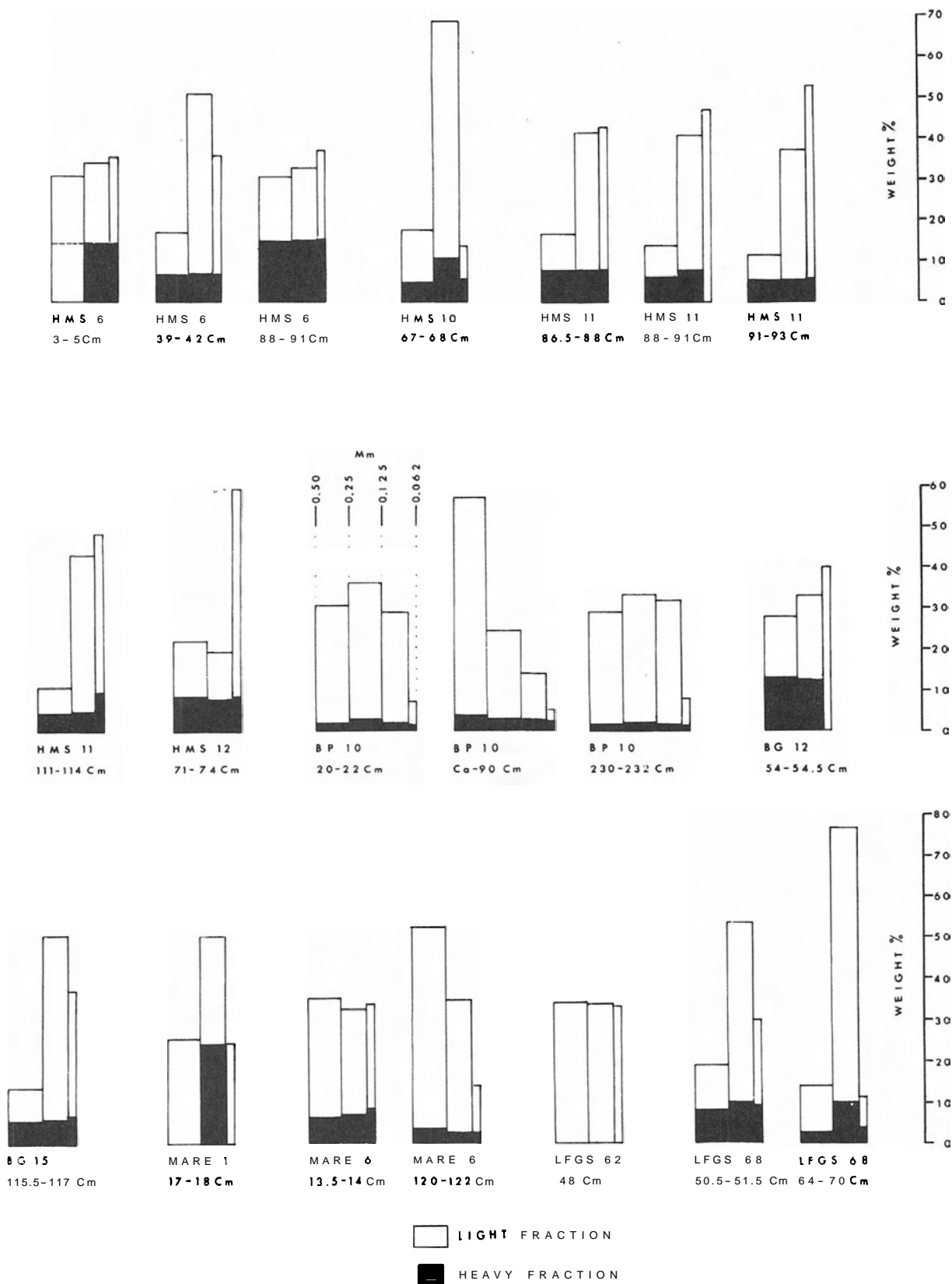
Floating Sand Bodies

Data from Tables 7 and 11

GRAIN SIZE ANALYSES

Sand Fraction Computed To 100 Percent

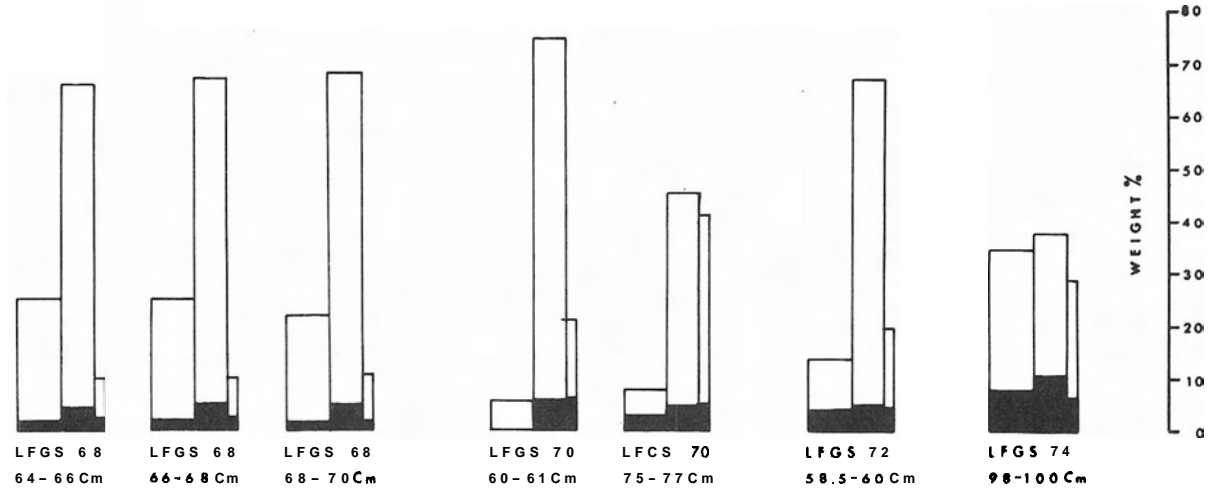
Layered Sands



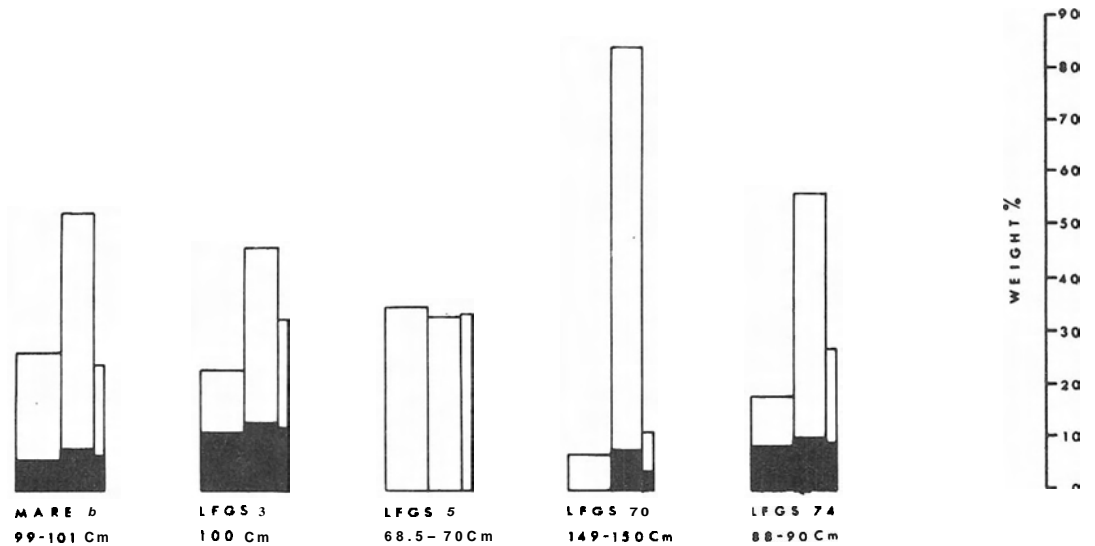
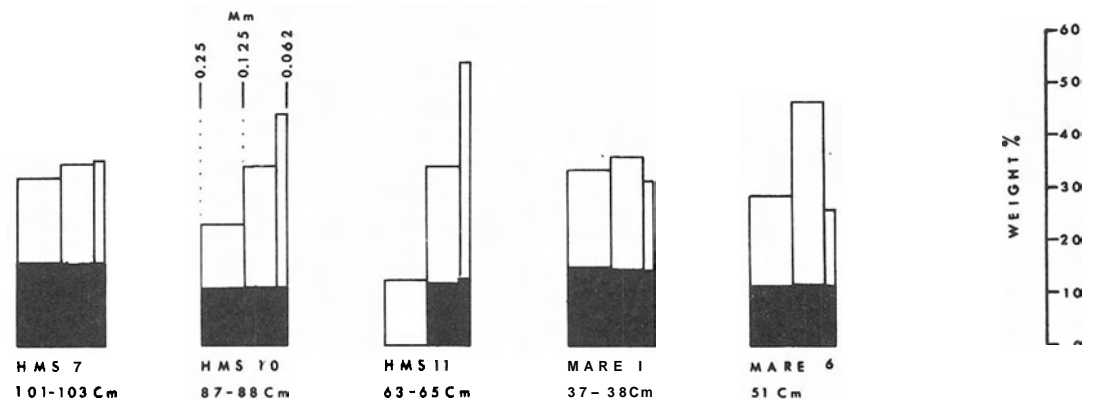
GRAIN SIZE ANALYSES

Sand Fraction Computed To 100 Percent

Layered Sands



Floating Sand Bodies



LIGHT FRACTION
 HEAVY FRACTION

TABLE 7
LIGHT MINERALOGY
 Percent by Count

FANFARE H. M. Smith

Sample	% weight	Quartz	Chert	Glass	Ortho- class	Plagio- class	Alter- ite	Chlor- ite	Biotite	Opaque	Calcite
HMS-6 3-5 cm											
0.125mm	16.59	x	x	x	x	x	x	x	x	x	x
0.125-0.074mm	19.69	11	x	x	10	13	39	16	6	4	1
0.074-0.062mm	20.81	12	1	x	10	34	23	15	5	x	x
HMS-6 39-42cm											
0.125mm	10.38	10	x	x	3	9	19	37	15	7	x
0.125-0.074mm	43.80	18	2	1	5	22	17	31	2	2	x
0.074-0.062mm	25.84	16	x	x	5	33	38	15	2	1	x
HMS-6 88-91cm											
0.125mm*	15.74	12	x	4	2	2	26	36	14	2	2
0.125-0.074mm	17.91	10	x	x	x	10	5	60	9	6	x
0.074-0.062mm	21.73	13	x	x	9	21	13	36	6	x	2
HMS-7 101-103 cm											
0.125mm	15.77	1	x	x	1	3	8	67	13	7	x
0.125-0.074mm	18.41	6	x	x	4	17	7	53	10	3	x
0.074-0.062mm	19.56 ^a	18	x	x	10	36	20	13	2	1	x
HMS-10 67-68cm											
0.125mm	12.90	15	1	x	5	29	42	6	1	1	x
0.125-0.074mm	58.00	25	1	x	4	39	25	6	x	x	x
0.074-0.062mm	7.92	23	1	x	7	42	20	7	x	x	x

Table 7 - continued

FANFARE H. M. Smith

Sample	% weight	Quartz	Chest	Glass	Ortho- clase	Plagio- clase	Alter- ite	Chlor- ite	Biotite	Opaque	Calcite
HMS-11 63-65cm											
0.125mm*	12.29	x	x	x	2	2	10	74	12	x	x
0.125-0.074mm	22.25	13	1	3	a	9	14	50	2	1	x
0.074-0.062mm	41.30	19	1	4	5	24	32	12	2	1	x
HMS-11 86.5-88cm											
0.125mm	8.92	1	x	x	2	4	12	64	15	2	x
0.125-0.074mm	33.94	9	2	x	10	20	27	26	3	2	1
0.074-0.062mm	34.66	23	x	x	7	33	22	14	1	x	x
HMS-11 88-91cm											
0.125mm	7.45	7	1	x	1	2	15	62	9	3	x
0.125-0.074mm	32.36	23	x	x	10	27	17	19	4	x	x
0.074-0.062mm	46.57	21	1	x	7	36	21	13	1	x	x
HMS-11 91-93cm											
0.125mm	6.23	5	1	1	1	5	6	67	13	1	x
0.125-0.074mm	31.32	17	x	x	10	30	11	27	5	x	x
0.074-0.062mm	46.94	24	x	x	7	40	8	20	1	x	x
HMS-11 111-114cm											
0.125mm	6.07	2	x	x	1	2	37	48	8	1	1
0.125-0.074mm	37.78	12	2	x	4	28	26	24	4	x	x
0.074-0.062mm	38.04	11	3	x	2	36	29	17	2	x	x
HMS-12 71-74cm											
0.125mm†	11.90	x	x	x	1	4	6	77	4	8	x
0.125-0.074mm	13.68	16	1	x	5	13	57	6	1	x	x
0.074-0.062mm	50.67	20	1	x	4	33	47	5	x	x	1

*not enough grains to count 100

@opaque filled forams

†many woody-fibrous flakes

Table 7 - continued

Fanfare

S. F. BAIRD

Sample	% weight	Quartz	Chert	Glass	Ortho- class	Plagio- class	Alter- ite	Chlor- ite	Biotite	Opaque	Calcite
BP-10 20-22cm											
0.250mm	28.79	x	x	x	x	x	x	x	x	x	x
0.250-0.125mm*	32.96	20	x	x	10	30	14	18	6	x	2
0.125-0.074mm	26.90	25	x	x	6	20	25	22	2	x	x
0.074-0.062mm	5.74	26	x	x	20	31	10	12	1	x	x
BP-10 STREAK											
Ca90cm											
0.250mm	53.47	x	x	x	x	x	x	x	x	x	x
0.250-0.125mm	21.72	30	1	x	10	27	20	7	1	3	1
0.125-0.074mm	11.31	16	1	x	11	33	21	15	1	2	x
0.074-0.062mm	2.93	19	x	x	11	32	20	11	2	5	x
BP-10 230-cm											
232cm											
0.250mm	27.08	14	x	x	7	32	19	15	10	2	1
0.250-0.125mm	31.19	30	x	x	9	30	15	11	4	1	x
0.125-0.074mm	29.38	18	x	x	11	30	16	15	8	1	1
0.074-0.062mm	6.77	22	x	x	15	31	13	16	3	x	x
BG-12 54-54.5cm											
0.125mm	14.66 [#]	x	x	x	x	x	x	x	x	x	x
0.125-0.074mm	20.15	15	x	x	11	34	11	23	4	2	x
0.074-0.062mm	26.48	23	1	x	6	29	23	14	3	x	x
BG-15/115.5-117cm											
0.125mm@	8.07	14	x	x	6	19	37	20	1	3	x
0.125-0.074mm	43.95	26	1	x	8	41	18	6	x	x	x
0.074-0.062mm	29.65	23	x	x	11	36	19	8	1	2	x

*Not enough grains to count 100 grains

@Opaque filled forams #100% clay balls

Table 7 - continued

Marezine

Sample	% weight	Quartz	Chert	Glass	Ortho- clase	Plagio- clase	Alter- ite	Chlor- ite	Biotite	Opaque	Calcite
MARE 1 17-18cm											
0.125mm	25.68 [#]	x	x	x	x	x	x	x	x	x	x
0.125-0.074mm	25.72	8	x	x	1	16	65	10	x	x	x
0.074-0.062mm	24.39	10	1	x	7	15	50	9	4	4	x
MARE 1-37-38cm											
0.125mm	18.51	x	x	x	x	x	7	82	7	4	x
0.125-0.074mm	21.42	x	x	x	x	1	2	68	22	7	x
0.074-0.062mm	16.87	x	x	x	x	x	x	85	12	3	x
MARE-6 51cm											
0.125mm	17.28	19	x	x	11	26	34	8	2	x	x
0.125-0.074mm	34.47	16	2	x	8	29	21	17	6	1	x
0.074-0.062mm	14.33	20	x	1	5	30	30	21	1	x	1
MARE-6 13.5-14cm											
0.125mm	28.75	10	1	1	6	43	30	8	1	x	x
0.25-0.074mm	25.76	23	1	1	10	32	23	10	x	x	x
0.074-0.062mm	24.50	13	1	x	8	38	31	9	x	x	x
MARE-6 99-101cm											
0.125mm	20.18	11	1	x	3	8	38	28	9	2	x
0.125-0.074mm	44.07	13	x	x	7	45	14	18	x	2	1
0.074-0.062mm	17.30	20	x	x	6	39	20	9	1	3	2
MARE-6 120-122cm@											
0.125mm	48.22	17	1	x	14	32	23	9	4	x	x
0.125-0.074mm	31.86	x	x	x	x	x	x	x	x	x	x
0.074-0.062mm	11.45	17	2	x	3	33	24	13	6	1	1

@opaque filled forams

100% clay balls

Table 7 - continued

Leap Frog Stranger

Sample	% weight	Quartz	Chert	Glass	Ortho- class	Plagio- class	After- ite	Chlor- ite	Biotite	Opaque	Calcite
LFGS 3 100cm											
0.125mm	11.84	14	1	x	3	27	45	3	3	4	x
0.125-0.074mm	32.52	19	x	1	6	44	15	12	2	1	x
0.074-0.062mm	20.24	19	1	x	12	25	26	15	x	2	x
LFGS 50 68.5-70cm											
0.125mm	34.30 [#]	x	x	x	x	x	x	x	x	x	x
0.125-0.074mm	32.62	12	1	x	4	13	41	19	3	7	x
0.074-0.062mm	33.08	4	x	1	4	9	29	44	7	2	x
LFGS 62 48cm											
0.125mm*	33.78	4	x	x	12	24	48	8	x	4	x
0.125-0.074m ²	33.30	11	x	1	3	15	33	25	6	6	x
0.074-0.062mm [@]	32.92	13	1	x	7	27	25	16	3	8	x
LFGS 68 50.5-51.5cm											
0.125mm	10.79	11	x	x	2	17	32	22	8	8	x
0.125-0.074mm	43.04	19	2	x	8	35	11	20	5	x	x
0.074-0.062mm	20.24	22	2	x	13	34	16	11	2	x	x
LFGS-68-64-66cm											
0.125mm	23.09	15	x	1	3	32	33	15	1	x	x
0.125-0.074mm	61.38	17	5	x	6	41	26	6	x	x	x
0.074-0.062mm	7.60	17	2	x	4	40	26	11	x	x	x
LFGS-68 66-68cm											
0.125mm	22.66	21	x	1	7	24	25	17	4	1	x
0.125-0.074mm	61.87	16	1	x	5	37	31	8	x	2	x
0.074-0.062mm	7.15	20	x	x	9	35	31	4	x	1	x

*not enough grains to count 100 grains

@opaque filled forams
8100% clay balls²much skeletal material

Table 7 - continued

Leap Frog Stranger - continued

Sample	% weight	Quartz	Chert	Glass	Ortho- class	Plagio- class	Alter- ite	Chlor- ite	Biotite	Opaque	Calcite
LFGS 68 68-70 cm											
0.125mm	20.19	10	1	1	8	32	20	24	4	x	x
0.125-0.074mm	62.93	21	1	x	11	39	17	7	3	1	x
0.074-0.062mm	8.65	15	1	x	18	30	21	13	1	1	x
LFGS 68 SMEAR											
64-60cm											
0.125mm	11.31	16	x	x	12	26	27	15	4	x	x
0.125-0.074mm	66.11	20	1	x	12	47	13	6	x	1	x
0.074-0.062mm	7.17	13	1	x	8	39	24	14	1	x	x
LFGS 70 60-61cm											
0.125mm	5.24	x	x	x	x	x	x	x	x	x	x
0.125-0.074mm	68.35	20	1	1	6	42	20	10	x	x	x
0.074-0.062mm	14.76	14	2	x	5	49	14	15	1	x	x
LFGS 70 75-77cm											
0.125mm	4.24	18	x	x	6	16	47	10	2	1	x
0.125-0.074mm	47.26	17	1	x	8	42	20	11	x	1	x
0.074-0.062mm	36.20	21	1	x	6	40	21	9	1	1	x
LFGS 70 149-150cm											
0.125mm	3.33	16	x	x	2	15	21	46	x	x	x
0.125-0.074mm	75.94	23	2	x	10	29	18	14	2	2	x
0.074-0.062mm	7.69	23	1	x	8	36	24	8	x	x	x
LFGS 72											
58.5-60cm											
0.125mm	10.05	11	1	1	2	23	37	24	x	x	1
0.125-0.074mm	62.23	21	2	x	13	26	22	14	1	1	x
0.074-0.062mm	14.99	19	x	x	10	44	19	7	1	x	x

Table 7 - continued

Leap Frog Stranger - continued

Sample	% weight	Quartz	Chert	Glass	Ortho- clase	Plagio- clase	Alter- ite	Chlor- ite	Biotite	Opaque	Calcite
LFGS 74 88-90cm											
0.125mm	9.89	22	x	x	11	34	17	12	4	x	x
0.125-0.074mm	45.61	17	1	x	8	35	25	13	1	x	x
0.074-0.062mm	18.60	18	x	1	7	40	18	14	2	x	x
LFGS 74 98-100cm											
0.125mm	26.53	21	x	x	2	35	27	11	1	3	x
0.125-0.074mm	27.04	14	x	x	7	29	15	25	8	2	x
0.074-0.062mm	21.86	13	x	x	9	44	15	13	4	2	x

TABLE 8**MAJOR MINERALS OF THE LIGHT FRACTION**

	Average Percent		
<u>Mineral</u>	.250 - .125 mm.	.125 - .075 mm.	.075 - .062 mm.
Quartz	12.0	16.1	17.2
K-Feldspar	4.9	7.0	8.0
Plagioclase	18.3	27.8	32.2
Alterite	23.8	22.1	22.4
Chlorite	<u>31.4</u>	<u>20.9</u>	<u>15.9</u>
TOTAL	90.4	93.9	95.7

TABLE 9

MAJOR MINERALS OF THE LIGHT FRACTION

Weighted Average Percent*

Mineral	.250 -.125 mm.	.125 -.075 mm.	.075 -.062 mm.	TOTAL
Quartz	2.3	6.5	3.8	12.6
K-Feldspar	1.1	2.8	1.6	5.5
Plagioclase	3.7	11.7	6.9	22.3
Alterite	4.3	8.1	5.3	17.7
Chlorite	<u>4.2</u>	<u>6.5</u>	<u>3.6</u>	<u>14.3</u>
TOTAL	15.6	35.6	21.2	72.4

*Weighted average percent = \sum weight percent of total sample times percent of mineral in that interval divided by number of samples.

TABLE 10

X RAY DATA FOR ALTERITE
AND
COATED ALTERITE

<u>Alterite</u>		<u>Coated Alterite</u>	
BP 10		BP 17	
<u>Cu/Ni</u>		<u>Fe/Mn</u>	
<u>d</u>	<u>A</u>	<u>d</u>	<u>A</u>
3.339	Mus., Qtz., Or.	10.015	Mus.
3.187	Or., Plag.	7.092	Clay
2.840	Or.	4.458	Mus.
2.6217	Mus.	4.242	Qtz.
2.442	Mus.	4.032	Plag.
1.989	Mus., Or., Plag. ?	3.342	Mus., Qtz., Or.
1.817	Qtz., Or.	3.127	Plag., Or.
1.669	Mus., Plag. ?	2.575	Mus.
1.537	Or.	2.449	Mus.
1.379	Or., Plag.	2.391	Or., Plag. ?
		2.275	?????
		2.130	Or., Plag. ?
		1.982	?????
		1.815	Qtz.
		1.668	Mus., Plag. ?
		1.539	?????
		1.499	Mus., Plag. ?
		1.374	Or., Plag. ?

Mus. - Muscovite
Qtz. - Quartz
Or. - Orthoclase
Plag. - Plagioclase, low calcium
????? - spacing not common to above minerals or mineral groups

constituents of the light fraction.

Alterite, plagioclase, and chlorite are the most abundant minerals of the light fraction both by number and by weight. Alterite is used here in the sense of Van Andel (1958) as a grain that can not be positively identified under the microscope presumably because the optical properties of the grain are obscured by alteration. X-ray diffraction analysis of a random sample of the alterite grains show them to be a mixture of quartz, muscovite, orthoclase, and high sodium plagioclase (Table 10). The general aspect of the alterite is that of a clear to cloudy low index feldspar intergrown with translucent to opaque micaceous and/or clay minerals. It is apparent under the microscope that these grains are not mono-mineralic.

Potassium feldspar counts include both microcline and orthoclase. Most of the grains listed as K-spar in Table 7 are orthoclase.

The micas, chlorite and biotite, are abundant, chlorite being the most common mica. The range of specific gravities of these micas spans that of the heavy liquid (2.89); so that they appear both in the light and heavy fractions.

The quartz grains are relatively clear and unstrained; although some grains are rutilated. No secondary overgrowths were observed. Some chert was found occasionally, but never in great abundance.

Opagues and glass fragments were generally less than five per cent of the light fraction.

Organic remains, such as tests of foraminifera, radiolarian and diatom skeletons, and woody fibrous material account for less than five per cent by number of the samples and are not included in

TABLE 11

HEAVY MINERALOGY

Percent by count

Fanfare H. M. Smith

Sample	% weight	Calcite Apatite	Chlorite	Rutile	Zircon	Tourmaline	Mozonite	Garnet	Biotite	Apatite	Epidote	Green Hornblende	Oxy-Hornblende	Actinolite Tremolite	Glaucophane Andalusite	Topaz	Sphene	Clinozoisite Zoisite	Augite	Xenophane	Quartz	
HMS 6 3-5 cm																						
0.125 mm@	14.23		Slide Missing																			
0.125-0.074mm@	14.38	16	41	x	x	1	x	1	31	x	x	7	x	x	x	x	x	x	2	x	1	
0.074-0.062mm#	14.30	27	11	1	x	1	1	4	13	x	x	10	7	x	1 ^A	5	x	x	3	7	9	
HMS 6 39-42cm																						
0.125 mm	6.60	2	66	x	x	x	x	x	28	x	x	2	x	x	x	x	x	x	x	x	2	
0.125-0.074mm	6.84	20	3	x	x	1	1	1	5	1	8	26	7	x	x	1	4	1 ^C	5	6	9	
0.074-0.062mm+	6.54	13	24	x	x	x	1	2	24	x	3	13	2	2 ^T	x	1	x	x	2	5	8	
HMS 6 88-91cm																						
0.125 mm	14.73	x	58	x	x	x	x	x	40	x	x	1	x	x	x	x	x	x	1	x	x	
0.125-0.074mm	14.90	1	65	x	x	x	x	1	27	x	x	2	x	x	x	x	x	x	x	x	4	
0.074-0.062mm#	14.99	6	57	x	x	x	x	x	35	x	x	x	x	x	x	x	x	x	x	x	2	
HMS 7 101-103cm																						
0.125 mm*	15.41	x	56	x	x	x	x	x	34	x	x	x	x	x	x	x	x	x	2	x	8	
0.125-0.074mm	15.45	4	13	x	x	x	x	x	77	x	x	3	x	x	x	x	x	x	x	x	3	
0.074-0.062mm	15.40	5	34	x	x	x	x	2	41	x	x	7	x	x	x	1	x	x	x	3	7	
HMS 10 67-68cm																						
0.125 mm	4.87	54	2	x	x	x	x	x	3	x	2	17	1	1 ^T	x	x	1	x	4	4	11	
0.125-0.074mm	10.64	22	x	x	x	3	1	1	x	1	5	24	x	6 ^T	5 ^G	6	4	1 ^C	7	2	12	
0.074-0.062mm	5.67	14	1	x	1	x	7	1	1	x	6	26	3	x	x	1	1	2 ^Z	4	10	22	
HMS 10 87-88cm																						
0.125 mm	10.82	2	54	x	x	x	x	1	30	x	x	6	x	1 ^T	x	1	x	x	2	x	3	
0.125-0.074mm	10.86	13	46	x	x	x	x	x	25	x	x	6	1	x	x	2	x	1 ^C	1	2	4	
0.074-0.062mm	10.85	15	29	x	x	x	x	x	26	x	x	14	1	x	x	x	x	1 ^Z	3	3	8	

Table 11 - continued

Fanfare H. M. Smith

Sample	% weight	Coated Alterite	Chlorite	Rutile	Zircon	Tourmaline	Monazite	Garnet	Biotite	Apatite	Epidote	Green Hornblende	Oxy-Hornblende	Actinolite Tremolite	Glaucophane Andalusite	Topaz	Sphene	Clinozoisite Zoisite	Augite	Hypersthene	Opaque	
HMS 11 63-65cm																						
0.125mm	TRACE	9	73	x	x	x	x	x	13	x	x	x	x	x	x	x	x	x	x	x	5	
0.125-0.074mm	11.92	1	53	x	x	x	x	x	36	x	x	4	x	x	x	x	x	x	1	2	2	
0.074-0.062mm@	12.24	42	21	x	x	x	x	1	9	x	x	17	x	x	x	3	x	x	1	2	4	
HMS 11 86.5-88cm																						
0.125mm	7.36	2	79	x	x	x	x	x	17	x	x	1	x	x	x	x	x	x	x	1	x	
0.125-0.074mm	7.45	31	25	x	x	x	x	1	11	x	1	18	1	2 ^T	x	1	x	1 ^Z	1	4	3	
0.074-0.062mm@	7.67	36	8	x	x	x	2	x	4	x	x	2	6	x	6 ^G	2	x	3	6	3	3	
HMS 11 88-91cm																						
0.125mm*	5.95	4	70	x	x	x	x	2	18	x	x	2	x	x	x	x	x	x	x	x	4	
0.125-0.074mm	7.66	x	x	x	x	x	x	x	x	x	x	x	x	x	x	x	x	x	x	x	x	
0.074-0.062mm	TRACE	x	x	x	x	x	x	x	x	x	x	x	x	x	x	x	x	x	x	x	x	
HMS 11 91-93cm																						
0.125mm*	5.06	35	47	x	x	x	x	1	12	x	x	2	x	x	x	x	x	x	x	x	3	
0.125-0.074mm*	5.09	33	35	x	x	x	x	x	16	x	1	6	1	x	x	2	x	x	2	1	3	
0.074-0.062mm†	5.35	19	9	x	x	1	x	1	1	x	x	32	8	1 ^T	4 ^G	5	x	x	6	7	6 ²	
HMS 11 111-114cm																						
0.125mm*	4.25	6	56	x	x	x	x	x	34	x	x	2	x	x	x	x	x	x	x	x	2	
0.125-0.074mm#	4.35	19	14	x	x	x	x	x	13	x	x	33	4	x	2 ^G	x	x	5 ^Z	3	4	3	
0.074-0.062mm	9.60	23	x	1	3	4	x	3	8	1	x	2	0	6	3 ^T	1 ^G	7	3	x	4	8	6
HMS 12 71-74cm																						
0.125mm@	8.11	94	x	x	x	x	x	x	1	x	x	x	x	x	x	x	x	2	x	x	3	
0.125-0.074mm*	7.74	4	56	x	x	x	x	x	30	x	x	x	x	x	x	x	x	x	x	x	10	
0.074-0.062mm*	8.41	60	1	x	x	x	x	3	3	x	1	7	4	x	2 ^G	2	1	1 ^{C3Z}	2	x	10	

Table 11 - continued

		Fanfare S. F. Baird																			
Sample	% weight	Coated Albite	Chlorite	Rutile	Zircon	Tourmaline	Monazite	Garnet	Biotite	Apatite	Epidote	Green Hornblende	Oxy-Hornblende	Actinolite Tremolite	Glaucophane Andalusite	Topaz	Sphene	Clinozoisite Zoisite	Augite	Hypersthene	Opaque
BP 10 20-22cm																					
0.250mm*	1.21	16	x	x	x	x	x	x	4	x	8	4	8	x	x	4	x	x	4	8	44
0.250-0.125mm	2.27	14	x	x	x	x	x	4	4	x	11	20	1	x ^T	x	1	2	x	5	5	33
0.125-0.074mm	1.26	16	8	x	x	x	3	9	14	x	2	22	2	1 ^T	3 ^G	2	1	x	4	8	5
0.074-0.062mm	0.87	6	x	1	1	2	3	18	x	1	1	27	2	4 ^T	x	2	2	1 ^c	11	8	14
BP 10 STREAK ca																					
90cm																					
0.25mm	3.31	46	x	x	x	x	x	4	x	x	9	x	3	x	x	2	x	1 ^Z	1	1	3
0.250-0.125mm	2.91	17	x	x	x	x	1	1	1	x	14	11	7	x ^T	2 ^G	2	1	x	4	12	27
0.125-0.074mm	2.35	11	x	x	x	x	2	1	2	x	4	12	5	1 ^T	1 ^G	9	x	x	6	7	29
0.074-0.062mm	2.00	17	6	x	x	x	1	1	2	1	3	18	5	x	x	x	1	1 ^Z	6	5	15
BP 10 230-232cm																					
0.250mm	1.38	24	1	x	x	x	x	3	3	x	8	13	7	x ^T	x	2	x	x	3	9	27
0.250-0.125mm	1.55	22	1	x	x	x	1	11	x	x	11	14	12	1 ^T	x	3	x	x	1	9	14
0.125-0.074mm	1.44	11	5	x	x	x	3	5	5	x	3	28	15	1 ^T	x	2	x	1 ^Z	7	6	8
0.074-0.062mm	1.21	4	1	x	x	x	3	10	2	x	2	33	8	x	x	2	1	1 ^Z	9	4	20
BG 12 54-54.5cm																					
0.125mm	12.87	20	25	x	x	x	3	x	22	x	3	8	5	x	x	x	x	x	1	2	11
0.125-0.074mm	12.69	3	32	x	x	x	1	x	59	x	x	1	2	x	x	x	x	x	x	x	2
0.074-0.062mm	13.15	x	x	x	x	x	x	x	x	x	x	x	x	x	x	x	x	x	x	x	x
BG 15 115.5-117cm																					
0.125mm	5.60	14	30	x	x	x	x	x	20	x	2	14	4	x	x	x	2	x	2	2	10
0.125-0.074mm	5.87	37	x	x	x	x	x	1	x	x	x	23	11	1 ^T	1 ^G	1	1	1 ^Z	7	7	9
0.074-0.062mm	6.86	15	3	x	x	2	1	3	1	x	3	27	13	x	1 ^G	1	x	3 ^Z	7	9	11

Table 11 - continued

Leap Frog Stranger

Sample	Weight %	Coated Ankerite	Chlorite	Rutile	Zircon	Tourmaline	Monazite	Garnet	Biotite	Apatite	Epidote	Green Hornblende	Oxy-Hornblende	Actinolite Tremolite	Glaucophane Andalusite	Topaz	Sphene	Clinozoisite Zoisite	Augite	Hypersthene	Opaque	
LFGS 3 100cm																						
0.125mm	10.88	33	28	x	x	x	x	1	15	x	x	6	1	x	x	x	x	x	3	3	10	
0.125-0.074mm	12.64	6	2	x	1	2	4	x	x	x	2	30	8	3 ^T	1 ^G	x	x	1	10	10	20	
0.074-0.062mm	11.88	11	3	x	1	x	3	1	x	1	1	3	2	x	1 ^G	1	2	x	2	15	23	
LFGS 50 68.5-70cm																						
0.125mm	TRACE	x	x	x	x	x	x	x	x	x	x	x	x	x	x	x	x	x	x	x	x	x
0.125-0.074mm	TRACE	x	x	x	x	x	x	x	x	x	x	x	x	x	x	x	x	x	x	x	x	x
0.074-0.062mm	TRACE	x	x	x	x	x	x	x	x	x	x	x	x	x	x	x	x	x	x	x	x	x
LFGS 62 48cm																						
0.125mm	TRACE	x	x	x	x	x	x	x	x	x	x	x	x	x	x	x	x	x	x	x	x	x
0.125-0.074mm	TRACE	x	x	x	x	x	x	x	x	x	x	x	x	x	x	x	x	x	x	x	x	x
0.074-0.062mm	TRACE	x	x	x	x	x	x	x	x	x	x	x	x	x	x	x	x	x	x	x	x	x
LFGS 68 50.5-51.5cm																						
0.125mm#	7.66	17	4	x	x	x	x	2	13	x	5	1	2	3	x	2	x	x	3	7	32	
0.125-0.074mm*	9.38	45	x	x	x	x	1	3	6	x	6	10	11	2 ^T	x	4	x	2 ^Z	2	x	8	
0.074-0.062mm	8.90	5	1	x	x	x	4	8	4	x	x	34	25	x	x	2	x	1 ^Z	9	3	4	
LFGS 68 64-66cm																						
0.125mm#	1.62	38	x	x	x	x	x	x	1	x	10	25	2	x	x	2	x	x	13	1	8	
0.125-0.074mm	4.03	26	x	x	x	x	1	x	1	x	4	41	x	1 ^T	1 ^G	2	x	1 ^C ; 1 ^Z	6	10	5	
0.074-0.062mm	2.28	20	3	x	x	x	5	5	x	x	3	33	3	1 ^T	1 ^G	x	x	4 ^Z	4	9	9	

Table 11 - continued

Leap Frog Stranger

Sample	% weig t	Coated Alterite	Chlorite	Rutile	Zircon	Tourmaline	Monazite	Garnet	Biotite	Apatite	Epidote	Green Hornblende	Oy -Hornblende	Actinolite Tremolite	Glaucophan Andalusite	T az	Sphene	Clinozoisite Zoisite	Albite	Hypersthene	Opaque
LFGS 68 66-68cm																					
0.125mm*#	1.46	24	4	1	x	2	1	x	x	x	4	32	3	x	1 ^G	x	2	1 ^C ;2 ^Z	12	4	7
0.125-0.074mm	4.73	13	7	x	x	x	x	2	x	x	3	45	7	x	x	5	x	x	x	9	5
0.075-0.062mm	2.13	10	2	x	x	x	x	1	x	x	5	47	5	2 ^T	1 ^G	5	x	x	9	7	6
LFGS 68 68-70cm																					
0.125mm#	1.56	20	3	x	x	x	1	x	2	x	3	34	4	x	x	2	2	1 ^C	13	4	15
0.125-0.074mm	4.95	33	3	x	x	x	x	1	2	x	6	26	5	1 ^T	1 ^G	1	x	x	2	6	13
0.074-0.062mm	1.72	14	x	x	1	x	3	1	x	x	1	38	6	3 ^T	1 ^G	6	1	1 ^Z	9	5	10
LFGS SMEAR 68 64-70cm																					
0.125mm#	2.32	41	3	x	x	x	x	x	2	x	7	22	2	1 ^T	x	x	x	4 ^Z	2	7	9
0.125-0.074mm*#	9.89	37	1	x	x	1	2	x	1	x	4	26	7	1 ^T	2 ^G :1 ^A	x	x	1 ^Z	5	3	8
0.074-0.062mm	3.19	8	x	x	x	x	4	1	1	x	4	40	11	2 ^T	1	x	x	2 ^Z	7	9	10
LFGS 70 60-61cm																					
0.125mm	5.24	x	x	x	x	x	x	x	x	x	x	x	x	x	x	x	x	x	x	x	x
0.125-0.074mm	5.67	28	1	x	x	x	2	x	x	x	3	24	x	1 ^T	3 ^A	1	3	1 ^C ;2 ^Z	14	10	7
0.074-0.062mm	5.99	13	x	x	x	x	2	x	1	x	5	39	6	x	x	2	x	3 ^C ;6 ^Z	8	5	10
LFGS 70 75-77cm																					
0.125mm	2.84	27	26	x	x	1	x	1	18	x	3	9	1	x	x	2	x	x	x	4	8
0.125-0.074mm	4.61	25	2	x	x	x	x	x	2	x	4	44	5	x	x	x	x	1 ^C ;1 ^Z	6	5	5
0.074-0.062mm	4.84	9	2	x	x	x	5	1	2	x	3	45	10	2 ^T	3 ^G	1	x	1 ^C ;2 ^Z	4	1	9

Table 11 • continued

Leap Frog Stranger

Sample	% weight	Crated Alterite	Ubrile	Rutile	Zircon	Tourmaline	Monazite	Garnet	Biotite	Apatite	Epidote	Green Hornblende	Xy-Hornblende	Clintonite remolite	Caucophane Albite	Quartz	Shene	Unzoi-site site	Ugite	Ypersthene	Opaque
LFGS 70 149-150cm																					
0.125mm	2.91	2	57	x	x	x	x	2	14	x	3	6	1	1 ^F	x	1	x	x	1	4	8
0.125-0.074mm	7.06	25	1	x	x	1	1	x	1	x	5	29	2	4 ^F	5 ^G	1	x	2 ^C ; 2 ^Z	8	7	7
0.074-0.062mm	3.07	19	5	x	x	x	4	x	1	x	x	36	6	1 ^F	2 ^G	2	x	1 ^C	5	6	10
LFGS 72 58.5-60cm																					
0.125mm#	3.62	41	2	x	x	x	x	x	1	x	2	21	1	x	x	1	x	1 ^Z	5	5	20
0.125-0.074mm	4.82	20	x	x	x	x	2	x	x	x	4	24	5	x	2 ^G	1	x	1 ^C ; 2 ^Z	12	8	9
0.074-0.062mm	4.29	8	2	x	x	1	1	3	x	x	6	36	4	x	2 ^G	3	x	1 ^C ; 5 ^Z	9	8	11
LFGS 74 88-90cm																					
0.125mm*	7.76	4	58	x	x	x	x	x	10	x	x	14	x	x	2 ^A	x	x	x	6	x	6
0.125-0.074mm	9.62	27	1	x	x	x	1	x	x	x	3	31	9	x	x	1	x	1 ^C ; 1 ^Z	10	6	9
0.074-0.062mm#	8.52	21	3	x	x	2	2		2	x	5	30	3	x	x	1	x	x	1 1 1 5		3
LFGS 74 98-100cm																					
0.125mm#	7.81	43	1	x	x	1	1	1	x	x	17	12	1	x	1 ^G	1	x	1 ^Z	3	9	8
0.125-0.074mm	10.41	10	x	x	x	x	5	1	1 0	x	11	25	2	x	1 ^G ; 1 ^A	1	x	x	8	8	17
0.074-0.062mm	6.34	65	x	x	x	x	1	1	x	x	x	4	2	x	x	1	x	x	4	4 ^C	18 ^C

* Too few grains to count 100

@ Poor Separation

²Some look like pellets

+Rads filled with opaque material

#Forams filled with opaque material

cGrains coated with opaque material

TABLE 12
MAJOR MINERALS OF THE HEAVY FRACTION*
SAM) LAYERS

Mineral	.250 - .125 mm.	.125 - .075 mm.	.075 - .062 mm.
Coated Alterite	24.0	21.6	18.2
Chlorite	23.6	11.9	6.1
Biotite	12.6	9.7	5.1
Green Hornblende	12.8	21.9	5.1
Augite	3.5	5.2	6.1
Hypersthene	3.3	5.4	6.0
Opaque	<u>10.3</u>	<u>7.9</u>	<u>9.5</u>
TOTAL	90.1	83.6	77.2

* Density greater than 2.89

TABLE 13

MAJOR MINERALS OF THE HEAVY FRACTION*
IRREGULAR SAND BODIES

Average Percent

Mineral	.250 - .125 mm.	.125 - .075 mm.	.075 - .062 mm.
Coated Alterite	9.3	8.5	14.3
Chlorite	43.0	22.8	22.1
Biotite	25.6	22.9	12.9
Green Hornblende	5.9	13.9	19.8
Augite	2.9	5.1	2.8
Hypersthene	1.5	3.5	4.4
Opaque	<u>6.6</u>	<u>6.9</u>	<u>9.8</u>
TOTAL	94.8	83.6	86.1

*Density greater than 2.89

the mineral count. Globorotalia and Globigerina are the most common genera of foraminifera (Victoria Kohler, oral communication, 1964).

Heavy fraction (specific gravity greater than 2.89)

Table 11 lists the minerals found in the heavy fraction plotted in order of persistence (Pettijohn, 1957, p. 516). The samples from distinct layers have a different mineral composition than do samples from irregular shaped sand bodies, which float in a mud matrix. Tables 12 and 13 list the summary of data for the most common heavy minerals from each of these two types of samples.

Hornblende and coated alterite, which is a black colored aggregate of minerals, are the commonest heavy particles in the sand layers, with the micas, chlorite and biotite next in abundance. In the irregular individual sand bodies, the micas are the most abundant particles, with hornblende and coated alterite less common.

The green hornblende generally is unaltered. Some hornblende grain edges have been altered to chlorite. Resinous brown oxyhornblende grains are relatively unaltered. Augite is characterized by the "cockscorn" variety; although rounded augite grains are not uncommon. Hypersthene is white to yellow brown in blocky cleavage fragments or prismatic grains.

The coated alterite grains have a black iridescent sheen under low power magnification reminiscent of desert varnish. The mineral phases of the coated alterite, identified from X-ray diffraction patterns, are quartz, muscovite, orthoclase, sodium plagioclase and 7 Å clay (Table 10). This is the same as the composition of the alterite found in the light fraction. Several lines from the X-ray pattern of the coated alterite, which are not found on the alterite pattern of the light fraction, presumably are from the black coating. The X-ray pattern

of the coated alterite is identical with those of some micro-manganese modules from ~~Atlantic deep-sea~~ cores (Jeffrey Hanor, oral communication). Thus the coating is probably a manganese oxide crust; although the exact mineralogy of the coating is not known.

Igneous accessory minerals such as monazite, topaz, and possibly garnet are found in most samples, but are not abundant. Metamorphic minerals found in small amounts in most samples include glaucophane, which is easily identified by its distinctive purple pleochroism, and bottle green epidote. Epidote is locally abundant, especially near the Pioneer channel.

The opaque minerals are in crusts, irregular shapes, and globular forms. Some of the globular forms may be filled tests of foraminifera. Table 11 indicates those samples that have tests of foraminifera and skeletons of radiolaria and diatoms partially filled with a black opaque material, which may be the same as the black coating on the alterite. Grains that obviously were filled organic structures were not counted in the percentage calculations.

The rest of the heavy minerals, such as zircon, tourmaline, actinolite, and zoisite occur sporadically and in small numbers.

The total aspect of the heavy mineral assemblage is immature as indicated by the relative lack of persistent minerals, such as zircon, rutile, and tourmaline, and the abundance of easily altered minerals such as hornblende, augite, and hypersthene.

Interpretations

Grains, such as the micas, that have relatively low settling velocities because of their shape are more abundant in the coarser fractions (Tables 12 and 13). The more spherical grains (those with more than one cleavage), which settle faster than the mica flakes for

particles in the same size interval, are more abundant in the finer fractions. Each equivalent sample is from a particular hydraulic regime so that the larger micas are deposited with the smaller, more spherical grains such as the hornblendes and augites. Part of the size discrepancy is caused by the difference in specific gravities among the micas and the other heavy minerals. The micas are both lighter and have greater surface areas than the heavier, more spherical grains. Differences in heavy mineral sizes were noted by Rittenhouse (1943) and related to hydraulic equivalence, which is the difference in Udden size grades or phi units between the size of quartz and the size of the particular mineral deposited with the quartz. Rittenhouse's data show that the hydraulic equivalence is essentially a direct function of specific gravity. On the other hand, Briggs, and others (1962, p. 653) demonstrated that "differences in shape of heavy minerals can produce about the same differences in size distribution as can the usual differences in specific gravity!" Unfortunately, for this study, neither Rittenhouse or Briggs and his co-workers give any information on the relationship among the micas and other heavy minerals.

Tables 12 and 13 show that the mica is commonly at least one phi unit coarser than green hornblende, which has a hydraulic equivalence of 0.2 (Rittenhouse, 1943). This would give the micas a hydraulic equivalence of about -1.0. The negative sign indicates that the mica flakes are larger than the reference mineral quartz. The significance of precise numerical values for hydraulic equivalence for the micas is questionable because (1) the minerals listed by Rittenhouse (1943) are roughly spherical, whereas the micas are flakes, so that different shapes are being compared, and (2) the sizes of the minerals

used in Rittenhouse's study are in or close to the range where Stokes's law applies, while the sizes of the micas from the Monterey fan (over 0.2 mm.) are in the range where different settling velocity laws such as the impact law obtain (Krumbein and Pettijohn, 1938, p. 95). The use of hydraulic equivalence in a general sense is justified, as this concept fits well with observed frequency distributions of minerals.

The difference between the layered sands and the individual irregular shaped sands is mainly that the layered sands contain major amounts of minerals with a positive hydraulic equivalence such as hornblende and augite; whereas the irregular shaped sand bodies, which float in a lutite matrix, contain mostly mica flakes, which have negative hydraulic equivalence. This means that for the same grain size, the order of settling would be first, the roughly spherical heavy minerals, then quartz, and finally the micas. The difference in the sign of the hydraulic equivalence may indicate that the layers consist of minerals from the bed load and saltation load of the depositing agent and that the floating sand bodies are supplied with minerals from the suspended load.

The sand bodies, whether layered or in irregularly shaped masses, upon lithification would be called graywackes. The sands from the Monterey deep-sea fan have a mineralogical content which falls within the broad variations of mineralogy shown by graywackes listed by Pettijohn (1957, p. 304). Most important is that the deep-sea sands from the Monterey fan have in common with described graywackes, (1) a high silt-clay matrix content, and (2) significant amounts of feldspar, rock fragments (alterite), mica, and quartz (Table 14). The chlorite and sericite (from the alterite) for the Monterey fan

TABLE 14

MINERALOGICAL COMPARISON OF GRAYWACKES WITH
MONTEREY DEEP-SEA SANDS

	A	B	C	D	E	F	G	H	Monterey Sands
Quartz	45.6	46.0	24.6	9.0	tr.	34.7	39	28	12.6
Chert	1.1	7.0	-	-	-	-	-	-	tr.
Feldspar	16.7	20.0	32.1	44.0	29.9	29.7	4	4	27.8
Hornblende	-	-	-	3.0	10.5	-	-	-	
Rock Fragments	6.7	- ^a	23.0	9.0	13.4	-	12	12	17.7
Carbonate	4.6	2.0	-	-	-	5.3	4	4	
Chlorite Sericitic	25.0	22.5	20.0 ^b	24.0	46.2 ^d	23.3	26 ^d	44 ^d	14.3 ^e
TOTALS	99.7	97.5	99.7	90.0 ^c	100.0	96.0	85.0	93.0	72.4

A through F from Pettijohn (1957, p. 304)

A Average of six (3 Archcan, 1 Huronian, 1 Devonian, 1 Late Paleozoic)

B Average high rank graywacke (Krynine, 1948)

C Average of three Tanner graywackes (Helmbold, 1952)

D Average of four Cretaceous graywackes, Papua (Edwards, 1947)

E Average of two Miocene graywackes, Papua (Edwards, 1947)

F Average of two parts average shale and one part average arkose

G Average of three deep-sea graywackes from the Mid-Ocean Canyon
(Hollister and Heezen, 1964)

H Graywacke from Sohm Abyssal Plain (Hollister and Heezen, 1964)

a not separately listed

b includes 2.8% "limonitic substance":

c balance is glauconite, mica, chlorite, iron ores

d matrix

e includes only chlorite in light fraction

graywackes are detrital grains. How much mud matrix would be transformed into chlorite and sericite after diagenesis and low rank metamorphism depends on the amount and kind of matrix that remains with the sand fraction after lithification. The data in Table 14 suggest that even if all the mud were removed from the sands by some post-depositional sorting process, or in this case, removed by sieving; the Monterey deep-sea sands upon lithification and low rank metamorphism still would fulfill Bailey's (1930) definition of a graywacke, which is a rock with a matrix with the composition of a slate. In this case the matrix could be derived from completion of the sericitization of the detrital sand-sized alterite grains. It is unlikely that all the interstitial mud could be removed naturally from the sand bodies of the Monterey fan. Also the sands now found buried on the fan do contain significant amounts of interstitial mud. Thus the matrix minerals of a graywacke made from the Monterey deep-sea sands would be partially detrital, derived from the breakdown of alterite grains, and partially authigenic, produced by the recrystallization of the interstitial mud. The mixed detrital-authigenic origin for the matrix minerals for a graywacke from the Monterey sands supports an intermediate position between Krynine's (1945) contention that the matrix minerals of graywackes are chiefly detrital and Pettijohn's (1957, p. 305) view that the matrix minerals are all authigenic caused by recrystallization of the interstitial mud.

The significant feature of the sands from the Monterey deep-sea fan is that they are one of the few documented examples of modern sediments of the graywacke type. For example, a preliminary analysis of 100 deep-sea cores by the Lamont group (Columbia University) (Hollister and Heezen, 1964) has revealed only four

TABLE 15

X-RAY DIFFRACTION DATA FOR UNTREATED CLAY SAMPLES

<u>Sample</u>	<u>Intensity Order*</u>					
	<u>1</u>	<u>2</u>	<u>3</u>	<u>4</u>	<u>5</u>	<u>6</u>
MARE 1**	14.7#	7.1	10	3.56- 3.53	4.98	
MARE 2	14.7	7.1	=10	3.56	4.98	4.74
MARE 3	14.7s	10	= 7.1	3.56	4.98p	4.71p
MARE 5	14.7	7.1	=10	3.57		
MARE 6	14.7- 14.2	7.18- 7.07	10	3.55	3.31	4.95
MEN 4 upper	14.7	10	7.1	3.53	4.98	4.71p
MEN 4 lower	14.7	7.1	=10	3.56	4.98	4.74
BG 16	15.2- 14.2	10	7.1	3.58- 3.51		

*Intensity of peaks decreases to the right (to higher numbers)

position of peaks in Angstrom units

s reflection strong

p reflection poor

** :poor separation of qtz. and feld.

TABLE 16

X-RAY DIFFRACTION DATA FOR CLAY SAMPLES HEATED TO 450°C

Sample	Intensity Order*						
	<u>1</u>	<u>2</u>	<u>3</u>	<u>4</u>	<u>5</u>	<u>6</u>	<u>7</u>
MARE 1	10#	7.1	3.53	4.71p			
MARE 2	10	12.27	3.32	7.1	3.56	4.98	4.71
MARE 3	10	14.2- 13.1	3.32	7.1	3.56	4.98	4.71
MARE 6	13.3- 12.01	10	7.1	3.32	3.56	4.98	4.71
MEN 4 upper	10	7.1	3.53	4.71	4.98		
MEN 4 lower	14.2- 13.1	10	7.1	3.56	4.71		
BG 16	14.24s	10	7.1	3.56	4.71		

*Intensity of peaks decreases to the right (to higher numbers)

#Position of peaks in Angstrom units

s Reflection strong

p Reflection poor

distinct graywacke sands from only two cores.

Clay Fraction:

A total of eight samples of the less than two micron (.002mm.) fraction from cores from (1) the continental shelf near the heads of the Ascension and Monterey canyons, (2) the head of the Monterey fan, (3) the basal apron of the Monterey fan, and (4) the top of a low relief seamount that rises through the Monterey fan, were examined by X-ray diffraction techniques. Each raw sample was mixed with distilled water and centrifuged until the <math> < 2 </math> micron fraction was separated. This fraction was settled as an oriented aggregate on glass slides. Each slide was X-rayed (CuK radiation = 1.5418 Å nickel filtered) after standing at room temperature and humidity and again after heating to 450^o C. (Tables 15 and 16). The slides were heated for 45 minutes at 450^o C. to eliminate poorly crystalline material, particularly chlorite, as the prominent (001) second order reflection of chlorite and the (001) first order reflection of kaolinite have the same 2θ values. According to Johns, and others (1954, p. 243) heating to 450^o C. will not destroy any kaolinite peaks, so that the absence of any common peaks on the diffraction patterns of the heated samples indicate that the mineral in the sample was chlorite. However, Johns, and others (1954, p. 243) also point out that if these peaks are retained on the pattern of the heated slide, the presence of either kaolinite, or well crystallized chlorite or both is indicated.

No significant difference can be discerned among the mineralogy of the unheated samples. This also was the case in a similar environment of abyssal hills and plain of the Sigsbee Deep, in front of the Mississippi cone in the Gulf of Mexico (Murray and Harrison,

1956). All samples show high proportions of montmorillonite and mixed layer clays, probably a chlorite-vermiculite, as indicated by its swelling properties in ethylene glycol (Weaver, 1956). Illite and chlorite are present in smaller amounts. Grim, and others (1949) found that samples from the Monterey canyon contained chiefly montmorillonite and illite.

The destruction of some of the mixed layer clays by heating showed that these clays were poorly crystalline although still among the most abundant clay minerals. Partial collapse of chlorite-vermiculite mixed layer clays in some heated slides is probably due to dewatering of the vermiculite component. Although data from eight samples from an area of 100 square kilometers is insufficient for valid generalizations, the well crystallized clays left after heating do show mineralogical variations among the samples that warrants analysis.

The material introduced to the heads of the canyons for later transportation onto the Monterey fan is on the continental shelf. Samples from the shelf at the heads of Ascension and Monterey canyon (Mare 2 and Mare 3) show more intense illite reflections (10 \AA (001) and 3.34 \AA (003)) than those of chlorite and mixed layer chlorite-vermiculite. Thus the well crystallized component of the clay source material is a mixture of illite, chlorite, and mixed layer chlorite-vermiculite. These clay minerals are probably detrital land erosion products, as the part of the shelf where the samples were taken is only a few kilometers off shore. The simplest explanation is that the illite is detrital fine grained mica (muscovite), which is consistent with the views of Yoder and Eugster (1955), who think that most illites are in reality fine grained muscovite.

On the outer apron of the fan, the clays in cores near the present channels (Mare 1 and Men 4 upper) also have dominant mica plus chlorite, but no mixed layer clays. The lack of mixed layer clays suggests that these clays have been upgraded into well crystallized mica (illite) and chlorite, as the clays on the outer margin of the fan probably have been in contact with sea water longer than the clays now at the surface on the continental shelf.

BG 16 is from a flat topped sea knoll, so that the clay there may be pelagic. Mixed layer clays predominate over mica and chlorite in BG 16. Samples from Men 4 lower from the fan apron, and Mare 6 near the apex of the fan, also have the same clay mineralogy as BG 16 and thus may be inferred to be pelagic clays. An alternate interpretation is that these clays represent an intermediate diagenetic step between the source clays on the shelf and the clays, as in Mare 1, on the fan apron. In this interpretation the poorly crystallized mixed layer detrital clays are upgraded into well crystallized mixed layer clays, so that after heating the sample the mixed layer component dominates over the mica and chlorite fraction. However, diagenesis has not progressed enough in these intermediate clays to convert the mixed layer chlorite-vermiculite to mica and chlorite.

Dietz (in Grim, 1942, p. 260) suggested that diagenesis may be an important factor in producing clay mineral variations besides source or differential flocculation, as he found illite forming in the marine environment probably from montmorillonite.

The sequence of well crystallized clay mineral suites derived from heated samples from the Monterey fan also suggests diagenetic change with time in contact with sea water. The proposed diagenetic

sequence in the vicinity of the Monterey fan is (1) poorly crystallized degraded terrestrial clays introduced to the continental shelf, to (2) poorly crystallized mixed layer clays formed on the shelf, to (3) well crystallized mixed layer clays on the fan, to (4) well crystallized clays such as mica (illite) and chlorite in the deeper more seaward portions of the fan, which have had the longest exposure to sea water. If this sequence is valid then the 10 Å reflections from the deep-sea clays on the Monterey fan are mixtures of detrital mica and authigenic illite derived from the diagenetic conversion of mixed layer clays and possibly montmorillonite. The chlorite in the clays on the fan also would be partially detrital and partially authigenic.

Chapter Five
DEPOSITIONAL ORIGIN OF THE SEDIMENTS

Allogenic Sediments:

Evidence

Transportation of sediment onto the Monterey fan is indicated by (1) the half-cone shaped outline of the fan; (2) current structures, such as the channels; (3) downslope gradient of minerals; and (4) concentration of coarse particles in and near the channels.

The half-cone shape of the Monterey fan is shown in the profiles of Figure 4 and Plate 3 in the pocket. Gilbert (1877, p. 133-134) described the development of similar shaped bodies on land: "From each mountain gorge the products of its erosion are discharged into the valley. The stream which bears the debris builds up the bed of its channel until it is higher than the adjacent land and then abandons it, and by the repetition of this process accumulates a conical hill of detritus which slopes equally in all directions from the mouth of the mountain gorge." In like manner, except that the process is under the ocean, sediment transport and deposition radiating downslope from essentially a point source is the most reasonable origin of such a feature as the Monterey deep-sea fan.

The various channels on the Monterey fan, chiefly the Ascension and the Monterey east, indicate at least some type of downslope motion; if the channels are not structurally controlled as in fault grabens. Whether the channels are downcutting or aggrading is not known. If the channels are downcutting, they may be

secondary features and not an agent in building up the fan. In either case, erosion or aggradation, the channels would be conduits for redistributing sediment from a higher to a lower elevation on the fan. This would produce a fan shape if the channels wandered much in the manner of the Mississippi River on its delta during the Recent (Fisk, 1944). At least two old extensions of the Ascension channel to the west of the present location of the channel, are suggested by the configuration of the contours on the bathymetric chart (Plate 3 in the pocket). These possible ancient channels fill in the area between the Ascension and the Pioneer channels, so that all points on the fan may have been near a channel at one time or another.

Analysis of the sand-sized sediment in layers show a downslope increase in mica content with the decrease of hydraulically heavier minerals such as hornblende. For example, the sands in Men 4, at the outer edge of the fan, consist almost entirely of micas; although the sands have about the same grain size as the sands upslope.

Cores taken near or in the axes of the channels generally are coarser and contain more sand than cores from the smooth surface of the fan (Figures 9, 10, 11, 12, and 13). Mare 6 and BP 10, both from the Monterey east channel axis, have the only sands analyzed with modal diameters greater than .250 mm., or coarser than fine sand. BP 10 has material up to pebble size (64-4 mm.). These sands are not residual sands with fine material removed as they all have abundant (at least 25 per cent by weight and volume) silt and clay matrix, except for one well sorted sand in BP 10.

Agency of Transportation

Possible means for transporting sediment onto the Monterey fan are (1) wind, (2) ice rafts, (3) subaerial streams, (4) kelp, and (5) bottom currents. I believe that the first four methods are quantitatively unimportant.

The prevailing wind direction in this region is westerly or from the sea landward (U. S. Weather Bureau, Oceanographic Atlas, 1961). The coast line of central California is rugged and mountainous so that even if a dust storm did blow from the east from the Great Valley, most likely the dust would be left on the eastern slopes of the Coast Ranges. Rex and Goldberg (1958) showed that for areas off the west coast of North America, the wind blown quartz contribution was small compared to the amount from stream sources. They demonstrated that in the sections of the Pacific far from the continents, where red clay is being deposited, the wind blown contribution is significant. -

Debris laden ice rafts that were brought south by the Japanese-California current from Canadian and Alaskan ice fields during glacial maxima, which melted in the warmer southern waters off central California, could have supplied sediment to the fan. If this amount were significantly large, the fan should slope north to south, thickening towards the source. Melted ice rafts may contribute some material to the fan which later was redistributed, preserving the present fan shape.

The Monterey fan is not a subaerial feature such as a giant alluvial fan formed at a low stand of sea-level, as the apex of the Monterey fan is about 3000 meters deep, or thirty times lower than the generally accepted estimated low stand of sea-level of -100 meters,

during the glacial maximum (Flint, 1957, p. 270). Also, no alluvial fan on land has the extent of the Monterey fan, which is 100,000 square kilometers.

Emery and Tschudy (1941) showed that kelp could transport rock into deep water, especially of the embayed southern California coast. Rock falling from rotten kelp is not a significant sediment source for the Monterey fan because (1) the fan sediments are overwhelmingly clay and silt and some sand, whereas the rocks carried by kelp are pebble and boulder sized rocks entangled in the kelp's holdfast; and (2) the currents off central California (Figure 2) flow along the coast, which would tend to keep floating kelp close to shore so that rocks entangled in the kelp would drop on the continental shelf or slope rather than on the fan.

The only reasonable possibility left is that the Monterey fan is a submarine feature formed by submarine processes. The primary source of sediments appears to be the adjacent land as (1) the fan radiates out from the mouths of the landward heading Ascension and Monterey canyons, and (2) hydraulically light grains, the micaceous, increase in abundance away from land, which suggest a decrease in the competency of the transporting media seaward and a landward source.

High velocity bottom currents: Turbidity currents

Turbidity currents, flowing down submarine canyons and out submarine channels, are the most probable agency for moving large volumes of material, particularly sand-sized sediments, onto the Monterey fan. If the deep-sea sands are deposited by turbidity currents, then why don't they show graded bedding or more gradational upper contacts? Kuenen (1951, p. 29), reasoning from experimental evidence,

stated that sands deposited by turbidity currents do not necessarily grade into lutites (silts or muds) if (1) the flow reaches a constant velocity for a considerable time so that only one size range of particles will be deposited, (2) overriding turbidity currents may cut off and pick up the lutite upper portion, and (3) on a moderate slope, the dilute tail of the turbidity current may retain sufficient velocity to keep the lutite suspended. The sands that are not graded, but do have sharp basal contacts, except for the mica sands of Men 4, are on the sloping upper portion of the fan near the mouths of the submarine canyons. Here the turbidity current would retain its momentum gained by passage down the steep grade of the canyon floor for some distance out onto the fan proper. Thus all three of Kuenen's criteria for non-grading and lack of transitional tops are applicable to sands near the apex of a submarine fan.

As shown in Table 6 (1) most of the sediment on the fan is finer than very fine sand (.062 mm.); and (2) the sand layers are thin, on the order of two centimeters (Appendix A). To produce even such a small thickness of sand, the depositing turbidity current must be thicker and contain much fine material to maintain the density difference which permits the flow to move downslope. This fine material eventually must be deposited when the flow either breaks up or loses velocity and no longer can carry even a fine sediment load. So a turbidity current which deposits even thin sand layers must deposit a much greater volume of lutite, although not necessarily in the same place as the sand.

Johnson (1962, p. 268-269) felt that the settling tendency in a turbid flow on the continental rise is negligible for particles with a settling velocity less than one tenth the mean current velocity

times the slope. Thus at the upper reaches of the channels of the Monterey fan, where the calculated mean velocity is on the order of 10 meters per second and the tangent of the slopes are about .01 (Table 2); particles finer than 1.0 mm. mean diameter will still be in suspension for a bankfull flow. Of course, coarser material may be carried in the bed load or by saltation. At the low end of the fan, where the calculated mean velocity is about two meters per second and the tangent of the slopes are about .004, only sediment finer than .03 (coarse silt) should still be in suspension. Both of these calculations are based on Rubey's (1933) settling velocity formula for quartz spheres (specific gravity = 2.65). These figures indicate that bankfull flows have the ability to carry coarse silt size quartz particles out to the edge of the fan. If the material in the turbidity current is hydraulically lighter than quartz, as is mica, larger sizes can be carried, as demonstrated by the very fine mica sand in Men 4 from the outer apron of the fan.

All flows, when they reach the break in slope at the apex of the fan, between the steep canyon floor and the gentle gradient of the fan surface, tend to conserve their momentum gained in the passage down the relatively steep canyons. Small scale flows, those whose thickness is less than the depth of the channel walls on the fan, carry less sediment or have less mass than bankfull flows. On the fan, because the slope is much lower than in the canyons, the flow velocity is reduced so that the small scale flows have a lower momentum (mass times velocity) than the bankfull flows. Such flows would dissipate and deposit their sediment load within the channel walls, which are adjusted to the larger bankfull flows. The terraces noted on the thalweg profiles of the Ascension and Monterey east channel

(Plate 4 in the pocket) may be submarine deltas, where small turbidity flows dump their sediment load.

Subsequent erosion of material deposited from flows that did not reach the edge of the fan is suggested by the enrichment of manganese coated alterite grains in the heavy mineral fraction of the sand layers. Either because of some ability to scavenge manganese ions (Goldberg, 1954) or because the alterite is the most abundant sand grain, some alterite particles become coated with manganese oxides. The grains probably are coated on the fan, as no manganese coated grains are reported in the beach sands of the vicinity (Hutton, 1959) or from the continental shelf and slope (Uchupi and Emery, 1963). If all the coated alterite grains are coated in the place where they are found, there should be no difference between the amount of coated alterite in the sand layers and the amount in the irregular sand bodies. However, a comparison of Table 12 with Table 13 shows the sand layers have about twice as much coated alterite as the irregular sand bodies. The grains must remain in one place on the fan long enough to be coated. If the original non manganese coated alterite was deposited by a given small flow, a later and larger flow must erode some of the now coated grains and deposit them with sediment already in the flow in a new sand body downslope. As noted in Chapter Four, the sand layers contain grains chiefly with positive hydraulic equivalents, so that the coated alterites, which are now heavier due to the coating, would tend to concentrate in the sand layers rather than in irregular sand bodies, which are more micaceous. Thus the coated alterites in the sand layers analyzed are mixtures of grains coated upslope and transported to the present site plus grains coated in place after deposition. Most of the coated alterites in the irregular sand bodies probably are coated in place.

Very large turbidity currents, thicker than the height of the walls of the channels, probably supply sediment to areas away from the channels, as rivers in flood deposit mud on their surrounding flood plains. Dill, and others (1954, p. 191) found levees that could be produced by such lateral spreading of the turbidity flow on the upper reaches of the Ascension channel.

The shape of the vertical sediment distribution in a marine turbidity current is unknown. Stoneley (1957) proposed a model in which the current was thin and dense using arguments based on dam break theory. Plapp and Mitchell (1960) described a thick and relatively less dense model. Both models can explain some features of the Monterey fan. Stoneley's thin-dense type flow may carve the submarine channels, as the material in this model is concentrated in the sole and toe of the flow. As noted in Chapter Two the hydraulic functions suggest that the energy of the flow that produced the channels is concentrated in the bottom of the flow. Pebbles from core BP 10, from the axis of the Monterey east channel, also imply Stoneley model for the transporting agent. Plapp-Mitchell type flows are more susceptible to lateral spreading and thus could carry sediment out into areas away from the channels, therefore could produce the smooth surface of the fan.

Numerous small canyons debouche onto the fan between the Pioneer and the Ascension canyons. Turbidity flows from these canyons are likely to be small and they are not confined in channels. These flows probably spread laterally and dissipate rapidly after leaving the constricting mouth of the submarine canyon. This situation, as Johnson (1962, p. 272) noted, also would produce small fan-like surfaces.

Low velocity bottom currents

Heezen and Johnson (1964, p. 70) demonstrated that the Mediterranean Undercurrent, which flows out the Straits of Gibraltar, with a maximum velocity of one meter per second, produces sand waves oriented transverse to the current flow to depths of 1400 meters and 200 kilometers from shore. Thus there is a possibility that surface and near surface currents can influence movement of deep ocean bottom sediments. The California current, which flows south parallel to the coast and across the major axis of the Monterey fan, is the principal current off central California. Jennings and Schwartzlose's (1960) study of parachute drogue behavior for three days in the California currents over the Monterey fan indicated that the current appears to split and intensify on either side of Davidson seamount. This demonstrates that there is some drag on the top of Davidson seamount, which is at a depth of 1300 meters. The velocity of the California current is at least one third less than that of the Mediterranean undercurrent^{1/}, which is felt to a depth of 1400 meters. So the California current's drag on the bottom is not likely to reach 3000 meters, which is the depth at the landward apex of the Monterey fan.

Photographs of ripple marks and scour features at great depths (Heezen, and others, 1959); the presence of cross-beds in deep-sea cores (Heezen and Hollister, 1964); and deep current measurements by Swallow (1957) demonstrate the reality of low

^{1/} Jennings and Schwartzlose (1960, p. 45) give an average current velocity of about .25 meters per second for a three day period in March. The U. S. Weather Bureau's Oceanographic Atlas (1961) lists an annual range from .05 to .20 meters per second.

velocity bottom currents. Such currents probably redistribute material once the sediment gets to the fan surface. Randomly oriented low velocity bottom currents might produce the fan shape by redistributing terrestrial material dumped at the mouths of **the** submarine canyons. Low velocity bottom currents are not suggested as the primary agent in transporting material and shaping the fan because (1) the cause of such currents, their orientation, and their effectiveness as a transporting agent has not been demonstrated, and (2) the channels definitely exist and appear to be the most logical pathway for distributing sediment. Low velocity bottom currents may move sediment downslope in areas away from the channels, possibly originating as a Plapp-Mitchell (1960) type sheet flow turbidity current.

Chapter Six

SOURCE OF SEDIMENT

The initial source of material now on the Monterey fan is landward from the apex of the fan. The Monterey fan forms the continental rise for about 350 kilometers along the coast of California from Point Reyes south to Point Arguello. As mentioned in Chapter One nearshore heading submarine canyons essentially prevent introduction of sediment from areas north of Cape Mendocino and south of Point Arguello. Sediment could be swept south by the southward longshore drift from as far north as Cape Mendocino, but north of Point Reyes, most of the sediment eventually would be swept out onto the Delgada fan to the north of the Monterey fan. So the land drainage basins that empty into the Pacific from Point Reyes to Point Arguello are the most probable source areas for sediment on the Monterey fan.

The continental shelf must be included as a potential source area because the shelf was exposed to erosion during Pleistocene glacial maxima. Menard (1960) showed that the contribution from the shelf by erosion of the various submarine canyons is only about one-tenth of the minimum amount of sediment deposited on the fan. The shelf off central California is relatively narrow so that the amount of debris produced through erosion of relief features on the shelf during low stands of sea level-also should be small. The geology and lithology of the bed rock on the shelf (Uchupi and Emery, 1963) is similar to that of the adjacent land areas so that sediment eroded from the shelf would be difficult to distinguish from material derived from the land. For example, the Farallon Islands on the shelf off San Francisco

TABLE 17

MONTEREY CANYONS DRAINAGE

River	Years of Record*	Annual Discharge:	<u>Acre-feet</u> Year	Drainage Area:	Miles ²
Salinas	31		320,000		4,341
Pajaro	21		117,300		1,249
Carmel	2		----		224
Big Sur	9		69,570		55
San Lorenzo	8&11#		<u>106,200</u>		<u>132</u>
TOTALS			613,070		6,001

SAN FRANCISCO BAY DRAINAGE

Sacramento	12		17,100,000\$		26,322
San Joaquin	32		3,370,000 ^a		19,096
Streams draining into S.F. Bay			<u>500,000^b</u>		<u>3,465</u>
SUB TOTAL			20,970,000		48,883
OCCASIONALLY IN DRAINAGE BASIN					
Tulare Lake Basin					13,635
Goose Lake Basin					<u>412</u>
GRAND TOTAL			20,970,000		62,920

* To 1960 #Combination of two gauge records ; \$ At Sacramento gauge
a at **Vernalis** gauge b estimated

Information from: Hofmann and Phillips (1961)
Homan and Schultz (1963)

TABLE 18

COMPARISON OF MINERAL ANALYSES*

	PERCENT QUARTZ	FELDSPAR
SALINIA: SOUTHWEST OF SAN ANDREAS FAULT		
Dip Creek; Taliaferro , 1944, p. 515	60	32
Asuncion: Taliaferro , 1944, p. 492	60	28
Quartz Diorite : Cheaterman , 1952, p. 361	35-50	40-60
Sur Series paragneiss: Reiche , 1937, p. 119	75	15
Ben Lomond Quartz Diorite: Leo , 1961, p. 119	24	57
NORTHEAST OF SAN ANDREAS FAULT		
Livermore: Huey , 1948, p. 47	30	65
Cierbo: Huey , 1948, p. 41	70	10
Oursan : Huey , 1948, p. 39	40	ca. 20
Domengine: Daviess , 1946, pp. 70-72	40	60
Tesla: Huey , 1948, p. 36	10	--
Martinei: Daviess , 1946, pp. 70-72	44	56
Panoche : Huey , 1948, p. 26	30	65
Panoche-Moreno : Briggs , 1953, p. 426	28	38
Moreno : Daviess , 1946, pp. 70-72	39	61
Franciscan: Taliaferro , 1943, p. 135	43	53
UPPER MONTEREY FAN	24	57 ^a

* Light fraction computed to 100 percent

a Clear feldspar plus alterite

FIGURE 14

HEAVY MINERAL DISTRIBUTION

Butano Formation

Source: Beveridge, 1958

BUTANO FORMATION

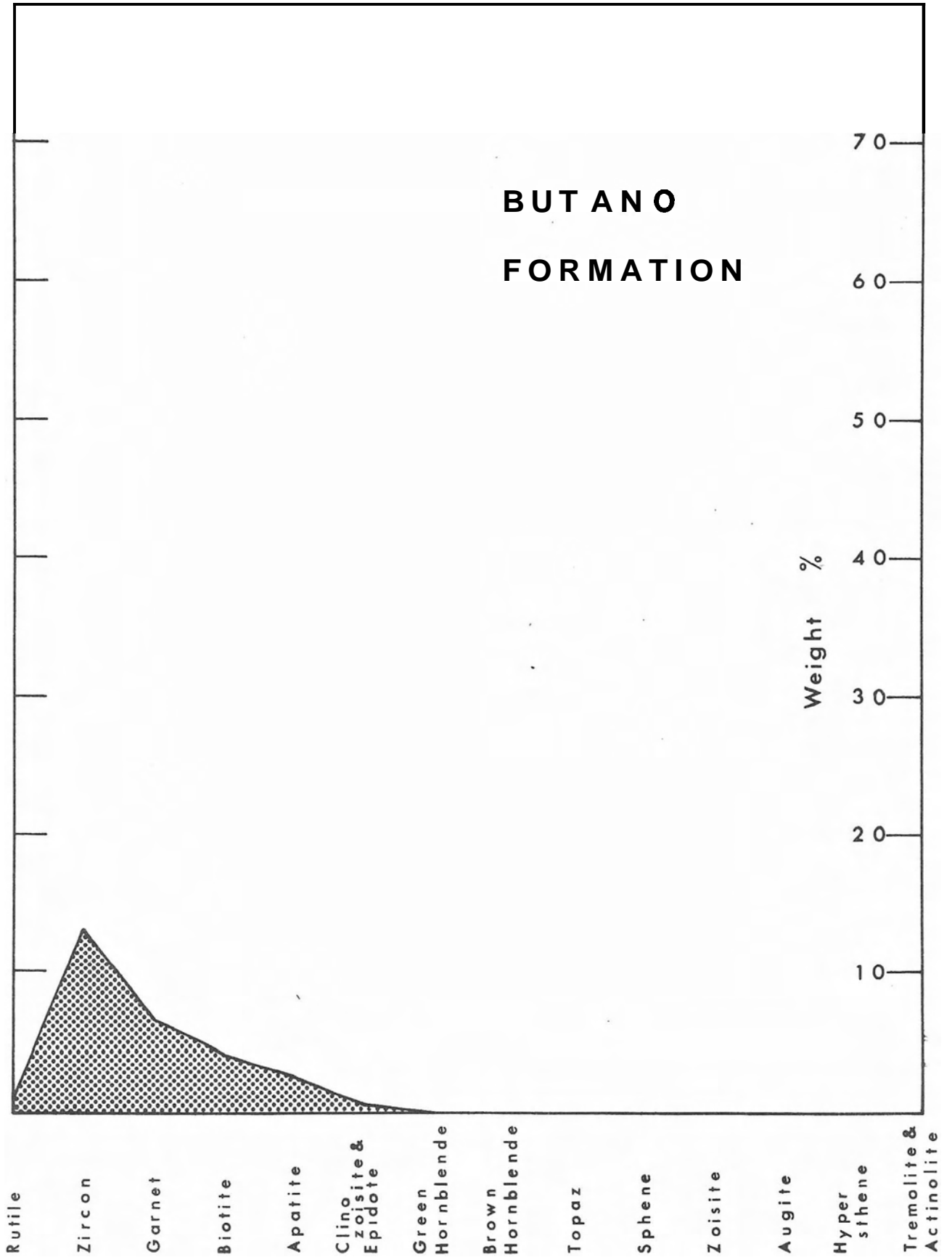


FIGURE 15

HEAVY MINERAL DISTRIBUTION

Montara Quartz Diorite

Source: Spotts, 1958

**MONTARA
QUARTZ
DIORITE**

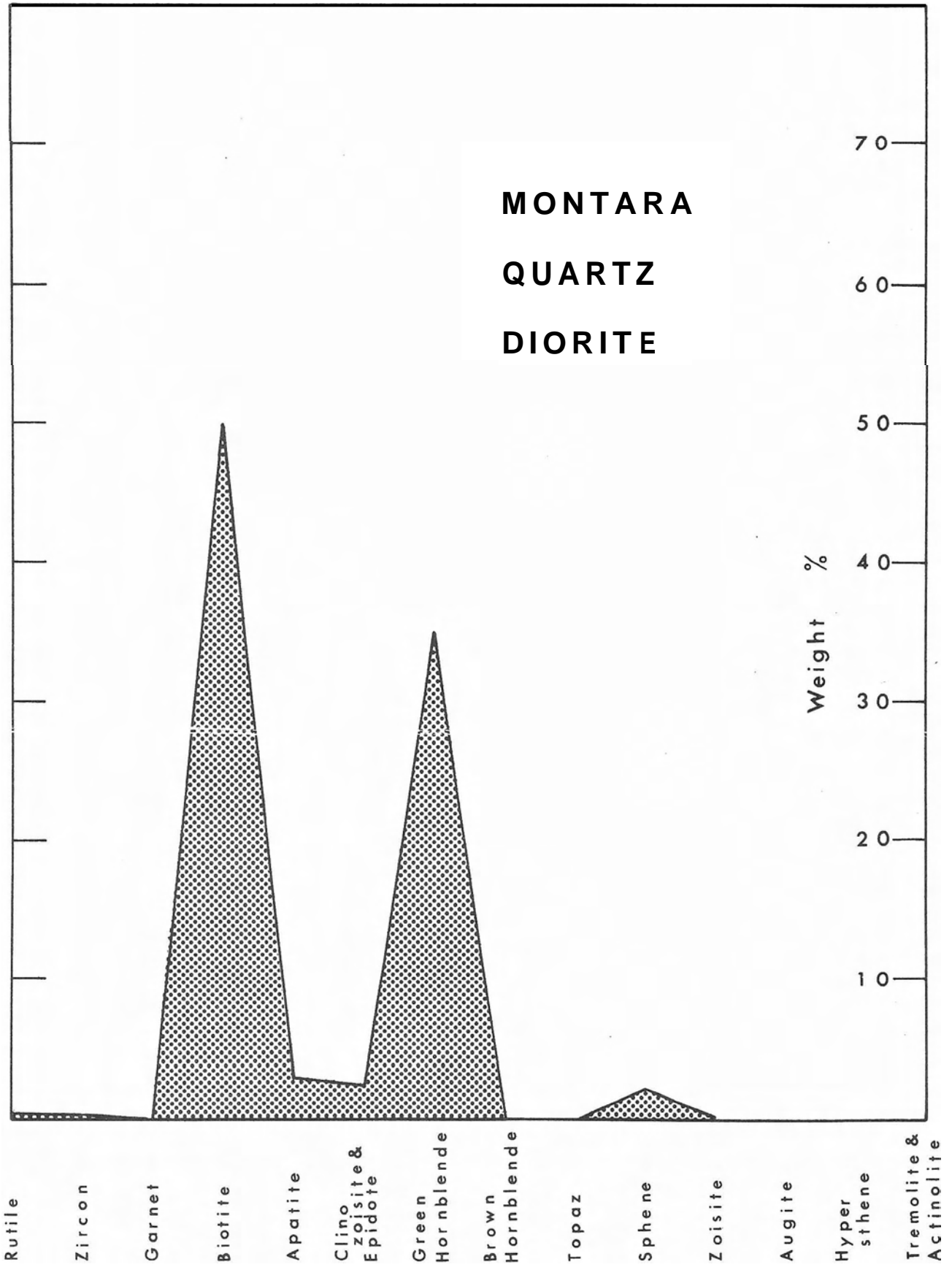


FIGURE 16

HEAVY MINERAL DISTRIBUTION

**Alluvium - Western slope
of Montara Mountain**

Source: Richmond, and others, 1959

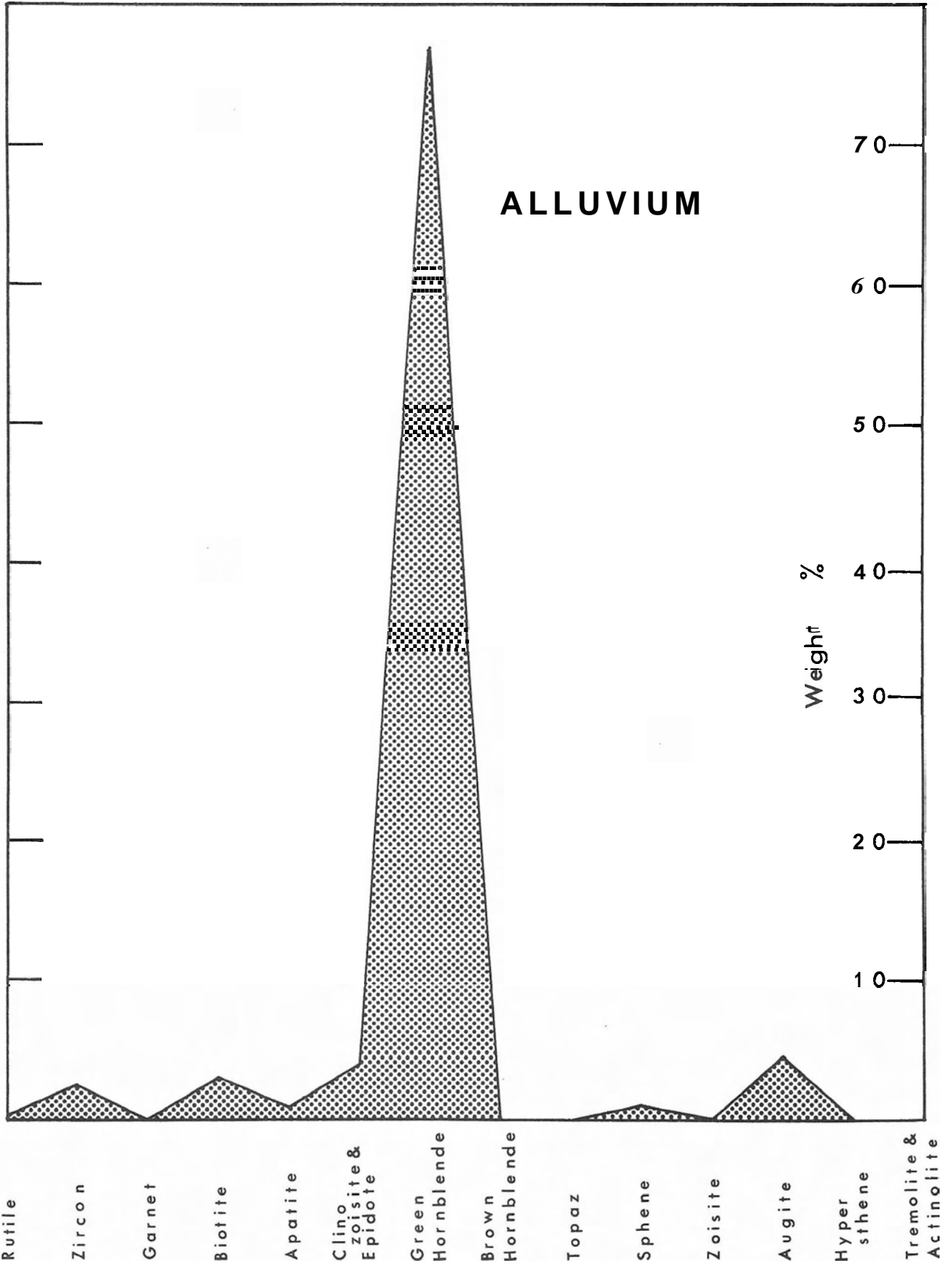


FIGURE 17

HEAVY MINERAL DISTRIBUTION

Pacific Beaches - Half-Moon

Bay to Pacific Grove

Source: Hutton, 1959

BEACH

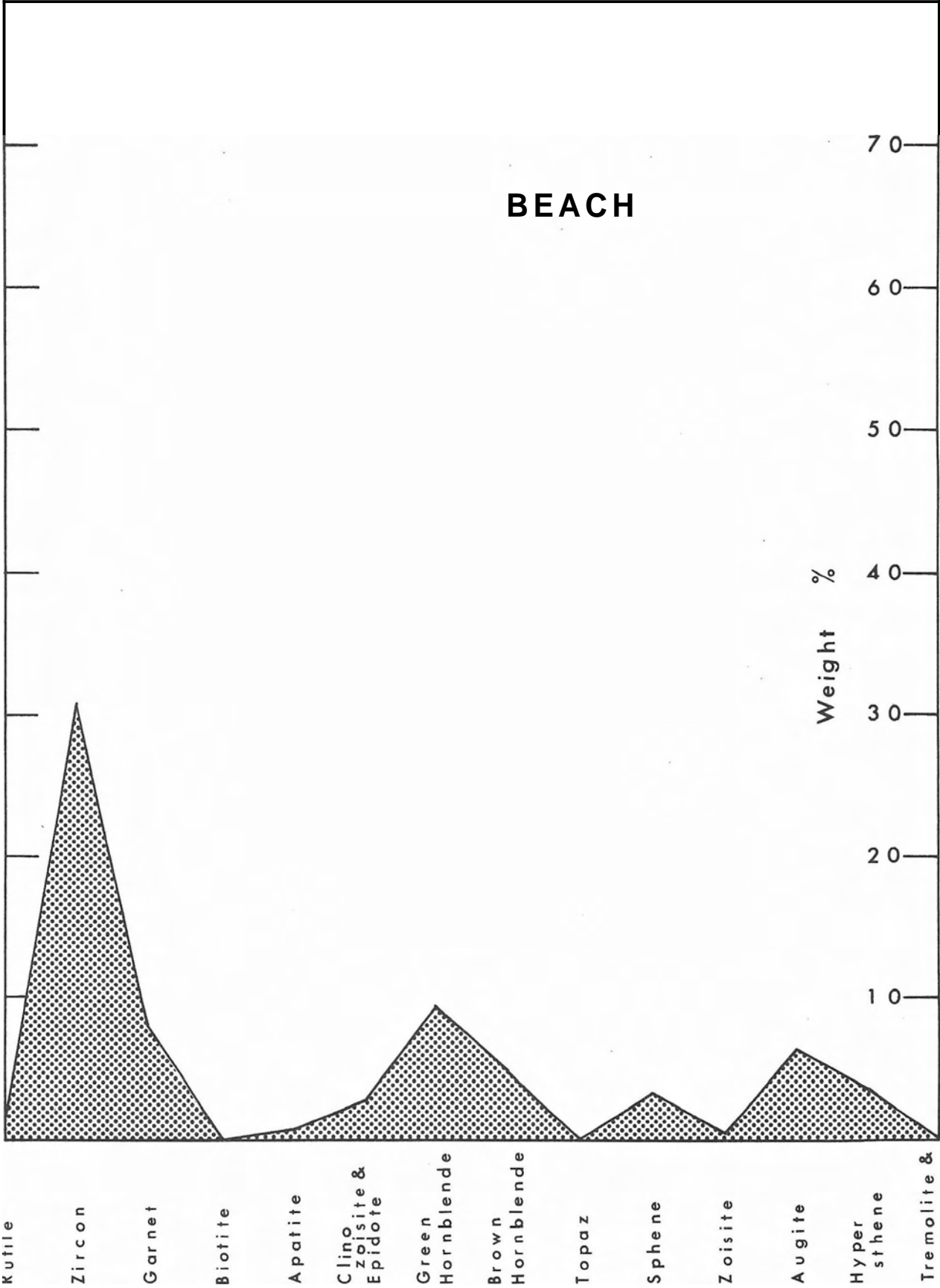


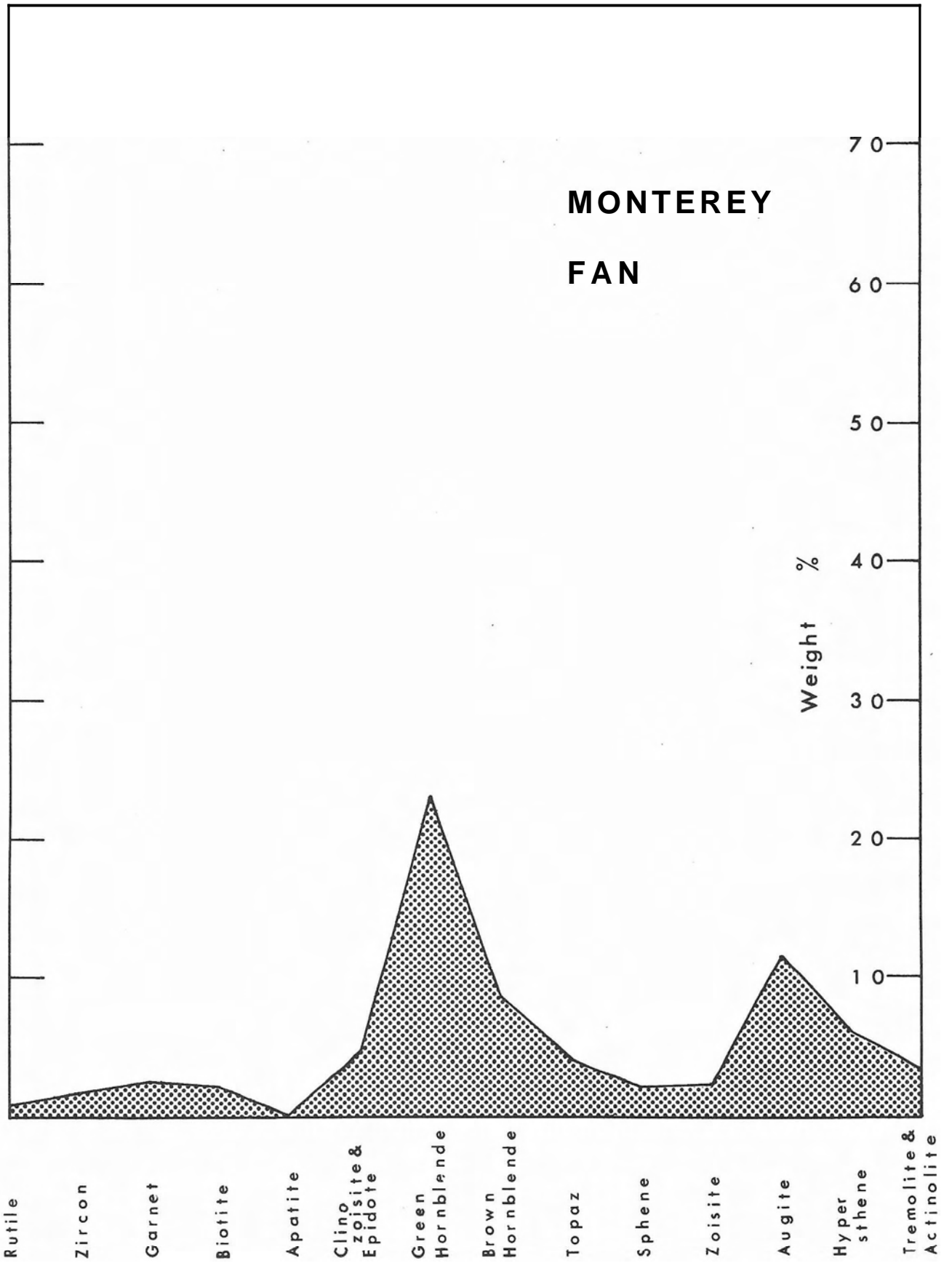
FIGURE 18

HEAVY MINERAL DISTRIBUTION

Monterey Fan Sands

Data from Table 11

MONTEREY FAN



composed of quartz diorite similar to the quartz diorite plutons of the Salinian geologic province on land. .

Table 17 lists discharge and drainage area information for the major streams in this region. The streams are essentially in two major drainage basins, (1) the Great Valley of central California, and (2) the Salinas Valley. The streams of the Great Valley drain (A) the northern Franciscan metamorphic belt, (B) the Sierra Nevadan felsic igneous and metamorphic province, and (C) the Great Valley sedimentary region. The Salinas River drains the Salinian quartz diorite province. The submarine canyons that drain onto the Monterey fan north of Point Sur head in Salinia. South of Point Sur the submarine canyons are cut in rocks of the central Franciscan metamorphic belt. The drainage area and discharge of the Great Valley and San Francisco Bay are respectively 10 and 30 times greater than those of the streams of Salinia and the central Franciscan province that drain directly into the various submarine canyons that feed the Monterey fan.

Coarser than .062 mm.:

Table 18 gives the comparison of the percentage of quartz and feldspar for rocks from Salinia, the Great Valley drainage area, and the composite quartz and feldspar plus alterite percentages for the Monterey fan. The best correlation of the Monterey sediments is with the Ben Lomond quartz diorite, which is exposed near the head of the Ascension and Soquel canyons. The sedimentary rocks from other possible source areas are, in general, too rich in quartz to be primary sources of the Monterey fan sediment.

Figures 14, 15, 16, 17, and 18 show a graphic representation of the heavy mineral composition respectively of (1) a typical sedimentary rock in Salinia, (2) quartz diorite pluton, (3) alluvium adjacent to a

TABLE 19

SAN FRANCISCO BAY AND BAR SEDIMENTATION*

Past 101 years (1855-1956)

into San Francisco Bay: 5,900,000 cubic meters per year

lost from San Francisco Bar (outside the bay):

650,000 cubic meters per year

or 11% of material has passed through the Golden Gate

Present

shoaling of bay plus bar: 6,000,000 cubic meters per year

shoaling of bar: 480,000 cubic meters per year

or 8% of material has passed through the Golden Gate

* Data from Homan and **Schultz** (1963) converted to metric units

quartz diorite pluton, (4) the Pacific beaches in the vicinity of Monterey bay, and (5) the sediments of the Monterey fan; all calculated for the very fine sand fraction. These graphs also indicate a quartz diorite source for the heavy minerals. The lack of pyroxene in the pure quartz diorite plot (Fig. 15) is no problem as mafic intrusions with pyroxene are associated with the quartz diorite intrusions (Spotts, 1958, p. 53-55). The Monterey fan assemblage is skewed towards the less persistent or more easily weathered suite of minerals (Fig. 18), which indicates a primary igneous source rather than a multicycled sedimentary source. This demonstrates that in the environment of the coastal and off shore regions of central California, one cycle, which includes short stream transport, resident on the high energy Pacific beaches, and marine bottom current transport, does not significantly alter the maturity of the source heavy minerals.

Finer than .062 mm. :

The bulk of material sampled on the Monterey fan is finer than sand size (Table 6). Holman and Schultz (1963, p. 3) found that the sediment now deposited in San Francisco Bay:

"is made up chiefly of fine particles in a colloidal or semi-colloidal suspension. Much of this material is precipitated by flocculation on contact with salt water and deposited in the bay. Sediment originally deposited in shallow areas may be resuspended by wind and wave action and a portion of material thus resuspended may be deposited in navigation channels or carried to sea through the Golden Gate".

Thus one possible source of fine sediment is the material from the Great Valley that is swept into the Pacific through the Golden Gate, or about 500,000 cubic meters per year (Table 19).

Unfortunately, there is no data on the amount of sediment contributed by the streams of Salinia and the Coast Ranges. The empirical relationship between discharge and suspended sediment load, according to Leopold and others (1964, p. 220) is:

$$(10) \dots\dots\dots G = pQ^j$$

where G = suspended load in tons per day,

Q = discharge in cubic feet per second,

p and j are numerical constants,

with j values between 2.0 and 3.0.

The suspended load, calculated from equation (10), of the Salinas River plus local streams is about 500,000 cubic meters per year. Therefore, the two major drainage areas, the Great Valley and Salinia, supply about equal amounts of suspended sediment to the Pacific, mostly silt plus clay size fractions.

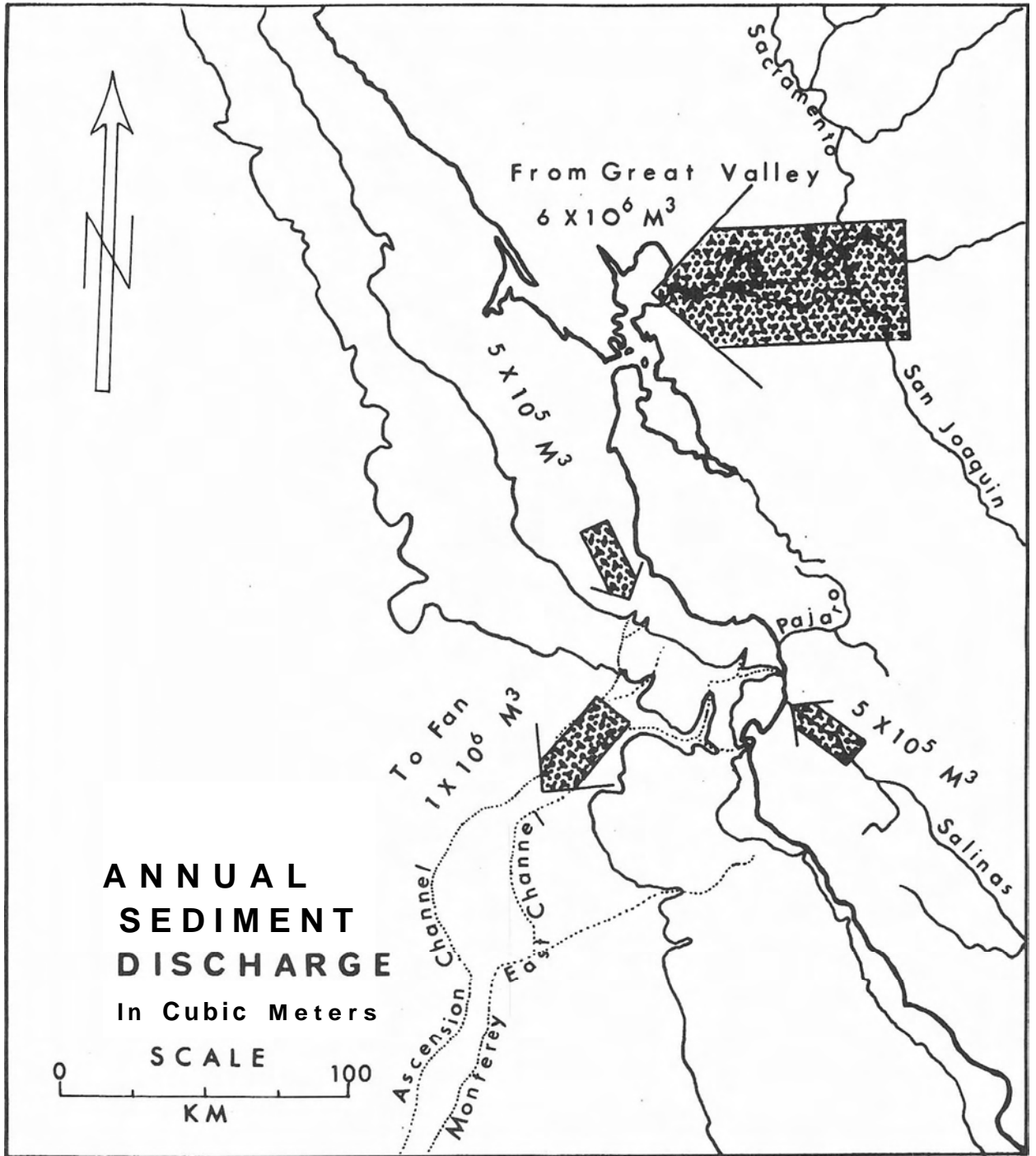
Summary:-

The mineralogy of both the light and heavy fractions of the sands of the Monterey fan indicate that the major sources for the sand and coarser fragments are the quartz diorite plutons in Salinia. The heavy fraction probably is derived directly from fresh quartz diorite, as the heavy mineral assemblage is unstable. The sedimentary rocks of Salinia, although essentially devoid of unstable heavy minerals (Beveridge, 1958) due to weathering, probably contributes some of the light fraction such as quartz, mica and weathered feldspar or alterite. Erosion of fresh quartz diorite produces the rest of the light fraction. The presence of glaucophane in some samples (Table 11) show that the central Franciscan metamorphic province is also a source of sediment.

FIGURE 19

SEDIMENT SOURCE AND DISTRIBUTION DIAGRAM

Data from Tables 19 and 20



The Great Valley contributes little or no sand because any sand in the bed load is trapped in San Francisco Bay and thus is prevented from reaching the Pacific and the fan. The streams of Salinia and part of the central Franciscan belt drain directly into or near the heads of the Monterey canyons. Thus the sand in the bed load of these streams can reach the Monterey fan via the various submarine canyons that discharge onto the fan.

Salinia, including local drainage basins that drain directly into the Pacific, and the Great Valley contribute about equal volumes of their suspended sediment load, chiefly silt and finer material, into the Pacific. This amount represents essentially all of the suspended load of the Salinian and local Coast Range streams, but only about 10 per cent of the suspended load of the Great Valley streams, that amount of fines swept out through the Golden Gate. Figure 19 depicts the postulated annual sediment contribution to the Monterey fan from the major sources.

Thus the sands on the fan are from local sources near the heads of the canyons, whereas the finer sediments, or bulk of the fan material, is partly locally derived and partly derived from the Great Valley.

Chapter Seven

AGE OF THE MONTEREY FAN

At the present state of knowledge, only three methods (1) fossil, (2) radioactive, and (3) sedimentary can give clues to the age of the Monterey fan. These three methods only give hints of the true age of the fan, as the older layers of the fan have not been sampled. Essentially these methods are used to compute rates of deposition of the surface layers. The volume of fan sediments divided by the various rates of deposition yields estimations of the age of the fan.

Fossil Method:

Ideally the simplest way to date the fan is by dating the fossils in the oldest and lowermost layers of the fan. Unfortunately only the upper few meters of the fan can be sampled. These samples do contain datable fossils. The chance of finding reworked fossils is high because turbidity currents often incorporate sediments from the upper fan into the flow, as shown in Chapter Five, before depositing its load downslope. Radiolaria, which are abundant in the open ocean, are the best fossils to use because most fall only on the fan and few fall in the canyons or on the shelf. Turbidity currents displace the radiolarian fauna only downslope and very little in time. As the radiolaria are pelagic, the downslope displacement does not effect their correlative value. William Riedel (oral communication, 1962) reports that all the radiolaria from samples from the Monterey fan have a time range from Pleistocene to Recent. No pre-Pleistocene forms have been found in the upper

TABLE 20

POTASSIUM ARGON AGES*

SALINIA

<u>Pluton</u>	<u>Age</u>
Santa Lucia granodiorite.	81.6 million years
Gabilan Mesa quartz diorite.....	83.8 million years
Point Reyes granodiorite....	83.9 million years
Santa Margarita granodiorite.....	84.1 million years
Farallon Island quartz diorite.....	89.5 million years
Montara quartz diorite.....	91.6 million years

*From Curtis, Evernden, and Lipson (1958, p. 9-10)

five meters of sediment sampled to date from the Monterey fan.

Radioactive Methods:

Radioactive techniques can give (1) dates of emplacement of probable igneous source rocks, and (2) age of recent sediment containing carbonaceous material.

The quartz diorite complexes of Salinia appear to be the primary sources for the sand sized sediment of the fan. Curtis, and others (1958), using potassium-argon dating methods, estimated the time of emplacement for several Salinian quartz diorites (Table 20) as Upper Cretaceous or about 80 to 90 million years ago. This figure is a maximum age for the deposition of the upper layers of sediment on the fan as some time must elapse between the time of emplacement and the unroofing of the plutons. Beveridge (1958, p. 77) showed that the Ben Lomond quartz diorite was unroofed in the early Cenozoic as this pluton has contributed heavy minerals to the Oligocene and Miocene rocks in the Santa Cruz Mountains, just north of Monterey Bay.

Emery and Bray (1962) dated sediments in cores from the basins and adjacent regions of the continental borderland, southeast of the Monterey fan, by carbon 14. The basins in this area are filled with turbidity current deposits (Emery, 1960) so they can give some information on the rates of deposition by turbidity currents off the California coast; Emery and Bray (1962, p. 1846) list 53 rates of deposition that range from 5 to 180 centimeters per thousand years. The higher rates are generally from basins near shore. The average value of 36 centimeters per thousand years is probably a

TABLE 21

AGE OF UPPER FIVE METERS OF THE
MONTEREY DEEP SEA FAN

Area of fan: 100,000 square kilometers

Depth of three core meters = 5.1 actual meters*

Volume of sediments: $(1 \times 10^{11}$ square meters) $(5.1 \times 10^0$ meters) =
 5.1×10^{11} cubic meters

Time to deposit, if source is material passed through the Golden Gate
plus local contributions

(A) at rate (1855-1956):

$$\frac{5.1 \times 10^{11} \text{ cubic meters}}{6.5 \times 10^{5\#} + 5.0 \times 10^5 \text{ cubic meters per year}} = 4.4 \times 10^5 \text{ years}$$

(B) at present rate:

$$\frac{5.1 \times 10^{11} \text{ cubic meters}}{4.8 \times 10^{5\#} + 5.0 \times 10^5 \text{ cubic meters per year}} = 5.2 \times 10^5 \text{ years}$$

Rate of sedimentation:

(A) at rate (1955-1956):

$$\frac{11.5 \times 10^8 \text{ cubic meters per } 10^3 \text{ years}}{1.0 \times 10^{11} \text{ square meters}} = 1.15 \times 10^{-2} \text{ meters per } 10^3 \text{ yrs.}$$

1.15 centimeters per 10^3 yrs.

(B) at present rate:

$$\frac{9.8 \times 10^8 \text{ cubic meters per } 10^3 \text{ years}}{1.0 \times 10^{11} \text{ square meters}} = .98 \times 10^{-2} \text{ meters per } 10^3 \text{ years} = .98 \text{ centi- meters per } 10^3 \text{ years}$$

* Core length = 59.4% of penetration (Pratje, 1935, p. 25)

#Rates based on data from Woman and Schultz (1963)
for material passed through the Golden Gate

good estimate for small turbidity current deposition in small closed basins, where appreciable thicknesses of sediment can accumulate in a short time. The average rate for the Monterey fan is probably much lower, as suggested by the rate of 8 centimeters per thousand years determined on sample from the deep-sea floor west of the continental borderland by carbon 14 techniques (Emery and Bray, 1962, p. 1846), than for the basins off southern California because the turbidity flows of the Monterey fan are not restricted to closed basins and can distribute sediment over a much larger area.

Sedimentary Method:

This classic geological method depends on knowledge of rates of erosion in the source area. San Francisco Bay acts as the basin for all the drainage of the Great Valley, which contributes about half of the silt and finer sediment for the Monterey fan. Fortunately the amount of sediment coming into and through San Francisco Bay has been intensely studied by the Corps of Engineers for many years. Table 19 gives a summary of this sediment information for San Francisco Bay. Most important for this study is the amount of sediment that passes through the Golden Gate into the Pacific. The assumption is made that all material that passes through the Golden Gate eventually will be transported across the shelf to a submarine canyon and onto the Monterey fan, as there are no basins on the narrow shelf to trap the sediment.

Table 21 shows the calculation of ages for the top five meters of sediment on the Monterey fan, based on the amount of sediment supplied annually to the Pacific from the Great Valley and from

Salinian and local coast range streams, which was derived in Chapter Six. The two values, 4.4×10^5 and 5.2×10^5 years indicate a Middle Pleistocene age and thus agree with the radiolarian age of Pleistocene to Recent for the sampled interval. Even if all the material that is now trapped in San Francisco Bay, gets onto the Monterey fan, the minimum age for deposition of five meters is 7.8×10^4 years. Louderback (1951) demonstrated that (1) the bay has been a trap for sediments from the Great Valley since the lower Pleistocene; and (2) other traps existed in the region before the appearance of the San Francisco graben. So it is unlikely that the Great Valley has contributed much more to the Pacific and to the fan than is now passing through the Golden Gate. As noted above, the carbon 14 derived rates of deposition for the southern California offshore basins probably are too high to be used as a check here, as these rates represent sedimentation in basins of limited areal extent, which is not the situation on the open Monterey fan. The rates of deposition derived by the sedimentary method for the entire Monterey fan are 1.1 and .98 centimeters per thousand years, which is somewhat lower than the rate of 8 centimeters per thousand years derived by carbon 14 methods for the near deep-sea off southern California.

Age of the Entire Fan:

Seismic data given by Raitt (in Menard, 1960, p. 1274) indicate that the total volume of sediment on the Delgada and Monterey fans is about 9×10^{13} cubic meters. The volume of the Monterey fan is about 3.7×10^{13} cubic meters. Thus, the Monterey fan has been in existence about 30 to 40 million years, or since the Early Oligocene,

TABLE 22

AGE OF MONTEREY FANVolume = 3.7×10^{13} cubic meters*

<u>Source</u>	<u>Rate</u>	<u>Age</u>
Material through Golden Gate (1855-1956)# plus Salinian and Coast Range Streams	11.5×10^5 cubic meters/year	3.2×10^d years
Material through Golden Gate (present)# plus Salinian and Coast Range Streams	9.8×10^5 cubic meters/year	3.8×10^d years
Entire Great Valley# plus Salinian and Coast Range Streams	6.5×10^6 cubic meters/year	5.0×10^6 years
<u>Comparison</u>		
Mohole Test Hole Guadalupe Site (Riedel, 1961)	1×10^6 cubic meters/year	3.7×10^7 years
C^{14} Dates of Southern California Closed Submarine Basins (Emery and Bray, 1962)	3.6×10^7 cubic meters/year	1.0×10^6 years
Pelagic Deposition (Arrhenius, 1963)	1×10^5 cubic meters/year	3.7×10^8 years

*Modified from Raitt in Menard (1960, p. 1274)

#From Homan and Schultz (1963)

according to the Holmes (1959) time scale, if the rates calculated in Table 21 are realistic, Table 22 lists ages for the fan calculated for various rates. It is interesting to note that the rate of about 1.0 centimeter per thousand years is the same as that for the Mohole test hole off Baja California (Riedel, and others, 1961), which is also on the continental rise.

The Oligocene age for the fan is a maximum age, as sediment from (1) pelagic sources, and (2) possible increased sediment discharge into the Monterey canyons created by a shift of the Great Valley drainage to Monterey bay (Howard,,1951) are ignored in the calculation of the average rate of deposition for the Monterey fan. Menard (1960, p. 1276) computed the ages of both the Delgada and Monterey fan to be about 4 to 20 million years, assuming essentially an equal distribution of sediment from the Great Valley to each fan. In summary, the Monterey fan is pre-Pleistocene to post-Mesozoic in age and probably began to form in the Oligocene or Miocene.

Chapter Eight

GEOLOGIC SIGNIFICANCE OF DEEP-SEA FANS

Both the Delgada and Monterey deep-sea fans are large scale features on the Earth's surface. The similarity of these California deep-sea fans with the submarine cones at the mouths of the Mississippi, Hudson, and Nile rivers is marked and suggests a common origin. Large scale deep-sea fans such as the Monterey are important in unraveling the history of the ocean basins, but the significance of the study of deep-sea fans with respect to the geologic history of terrestrial features is not so obvious. Indeed, most geologists separate phenomena from the true ocean and the continents as being essentially mutually exclusive. Kuenen (1950, p. 145) summed up this reasoning by noting "the important fact that nowhere has true oceanic sea floor been incorporated in the continents, because no extensive pelagic deep-sea deposits are found in geosynclinal or other sedimentary prisms". Whether or not Kuenen's statement will remain completely valid, it is true that nowhere on land are there extensive areas of unquestioned deep-sea deposits.

Does the absence of extensive deep-sea deposits in the geologic record on land mean that once terrestrially derived material is deposited on a deep sea fan or on abyssal plains, this material is lost to the continents? Menard (1961, p. 159) calculated that the average world-wide loss of material from the

continents, including the continental margins, to the abyssal plains is about 18 per cent^{1/}. As Menard (1961, p. 1961) stated, this loss continued throughout geologic time "would displace a large part of the continent into the ocean basins." This has not been the case, so either (1) the rate of loss is too high; (2) the rate of loss is variable and at present is at a high value; or (3) the rate indicates only temporary loss as the material adjacent to the continents returns to the land mass by (A) continental accretion (Wilson, 1951), (B) subcrustal convection (Gilluly, 1955), or (C) uplift. The rate of loss probably is high, because Menard makes no allowance for pelagic deposition in the abyssal plains. Whether the rate is highly variable can not be determined from such speculative data; however Gilluly's (1949) conclusion that the rate of mountain building throughout geologic time is relatively constant suggests that the world-wide average loss to the abyssal plains also would be relatively constant. Finally, the last reason (3) negates the idea that all material deposited in truly deep-sea basins does not return eventually to the continents.

The Monterey deep-sea fan, as demonstrated above, is composed of terrestrially derived material, not pelagic sediments, now at oceanic depths. If such material were exposed on land after lithification, it is unlikely that much of it could be differentiated on lithologic grounds alone from shallow marine shales with sandy partings. Possible distinguishing features of terrestrially derived

^{1/} The loss to the Monterey fan, which is part of the continental margin that grades into the abyssal plains, is about 15 per cent of the terrestrial sediment transported to the coast.

sediments deposited on deep-sea fans are (1) current structures in the sands such as graded beds and flute and groove casts, not usually associated with the shallow water environment, (2) large-scale fan shape, and (3) mixtures of deep and shallow water contemporaneous faunas.

Possible Deep-Sea Fans in the Geologic Record:

Kuenen and Migliorin (1950) proposed that turbidity currents can produce graded bed sequences. As (1) graded bedding is a characteristic of graywacke or flysch facies of sedimentary rocks, and (2) turbidity currents are cited above as the most probable depositional and transporting agent on the Monterey fan, areas with flysch facies rocks would be the logical place to search for ancient deep-sea fans,

The rocks of the classic areas of flysch facies in the Harz Mountains and the Alps, although similar in lithology to the sediment of the Monterey fan (see Gribnitz, 1952; Helmbold, 1958), appear to have been deposited in basins much smaller than the area of the Monterey fan (Crowell, 1955; Hsu, 1960). In fact, Crowell (1955) proposed that the Alpine flysch basins were similar to those of the present continental borderland off southern California. Kuenen and Sanders' (1956, p. 669) studies of the Harz and neighboring flysch deposits indicate that these rocks "accumulate in basins of moderate size and in depths that do not exceed 1000 meters". Foraminifera and lithologic investigations by Sullwold (1960) on the Miocene Tarzana submarine fan now exposed in the Los Angeles basin also show that the depth of water during deposition was about

1000 meters (3000 feet). Thus the classic flysch areas of Europe and southern California do not appear to have been regions of true deep-sea deposition, which would be in depths in excess of 3000 meters as is the case with the sediments on the Monterey fan.

The Martinsburg flysch of the central Appalachians has lithologic and current direction features which suggest deposition by turbidity currents (Van Houten, 1954) on an open gently sloping deep-sea floor. McBride (1962, p. 48) described and depicted portions of the "Martinsburg flysch composed largely of clay shale with lesser amounts of thin fine grained graywacke and siltstone beds". This description is identical with that of proposed lithified equivalents of the cores with thin sand layers from the Monterey fan. The wide divergence of paleocurrent azimuths (8 of 13 subdivisions have spreads between 90 and 180 degrees and 3 of 13, have spreads greater than 180 degrees, McBride, 1962, p. 79-81) is indicative of deposition on a fan-like surface.

Eugeosynclinal areas, now highly metamorphosed, are other possible sites for deep-sea fans. The pelitic schists and slates of the Paleozoic in the Piedmont and in New England could be formed from the metamorphism of sediment like that now on the Monterey fan. For example, the Ordovician Partridge formation in New Hampshire (Billings, 1937, 1956) has a unit in which slate and thin quartzites alternate in 0.5 cm. (one-quarter inch) thick bands, which initially could have been a mud-sand layer sequence, allowing for compaction of the mud into shale, as core BG 12 shows (Appendix A). Most of the Partridge is schist: the metamorphic equivalent of mud, the most abundant sediment on the Monterey fan. The

FIGURE 20

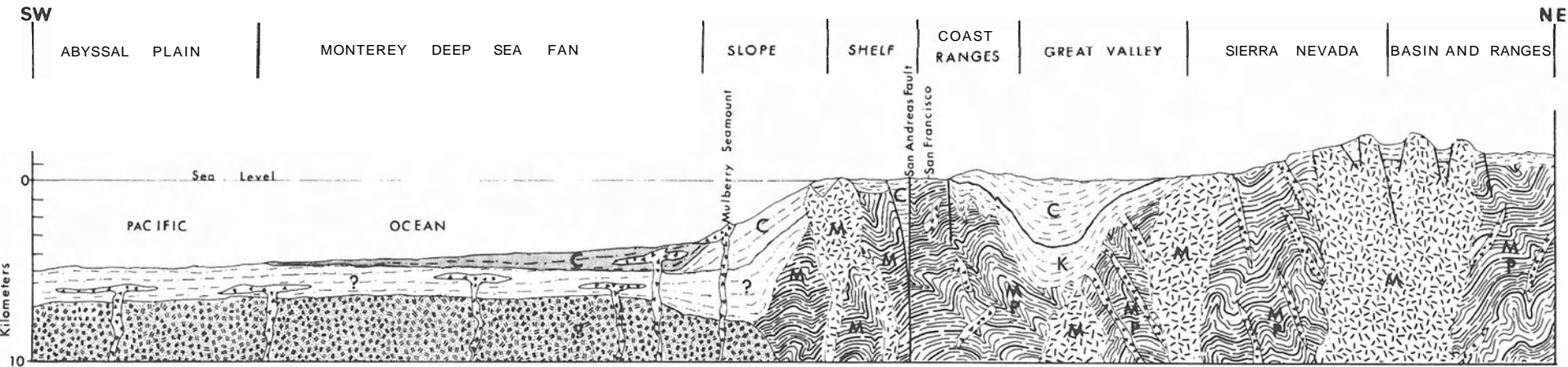
**SCHEMATIC COMPARISON OF GEOLOGIC
STRUCTURE BETWEEN RECENT OF CENTRAL
CALIFORNIA AND CAMBRO-ORDOVICIAN
OF WESTERN MAINE TO EASTERN NEW YORK**

Sources: Kay, 1951

Thompson and Talwani, 1964

SCHEMATIC CROSS-SECTIONS

CENTRAL CALIFORNIA AND OFFSHORE Recent

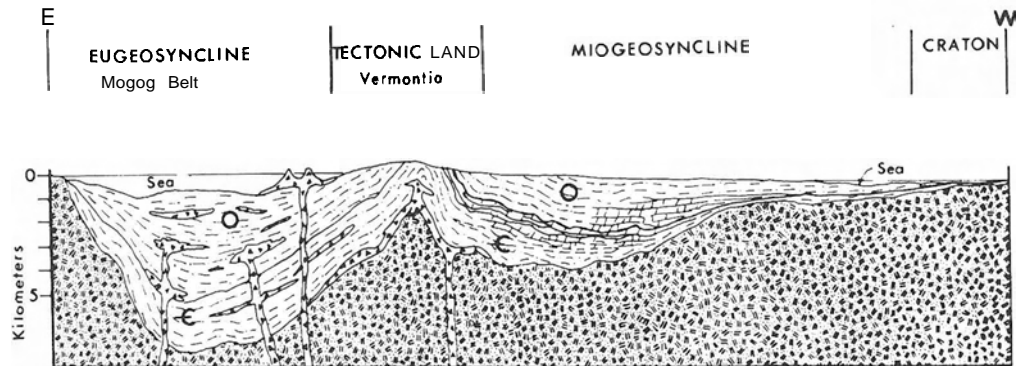


after Thompson and Talwani, 1964, p.1547

EXPLANATION

- | | | | |
|--|------------------------|---|------------|
| | Monterey Fan Sediments | C | Cenozoic |
| | Sedimentary Rocks | M | Mesozoic |
| | Basalts | K | Cretaceous |
| | Granitic Rocks | P | Paleozoic |
| | Metamorphic Rocks | O | Ordovician |
| | Basement Complex | ☉ | Cambrian |

MAINE TO NEW YORK Cambro-Ordovician



after Kay, 1951, p.26-27

Vertical Exaggeration 10X

Horizontal Scale

0 **KM** 100

APPENDIX A

LITHOLOGIC CORE DESCRIPTIONS

Cusp 1954 (Cusp)

Fanfare 1959

R/V Hugh M. Smith (HMS)

Fanfare 1959

R/V Spencer F. Baird (BG or BP)

Mendocino 1960 (MEN)

Marezine 1961 (MARE)

Leapfrog 1961

R/V Stranger (LFGS)

CUSP 4

Centimeters	0-120 cm
0-89	Light green mud speckled with black sandy blebs @ 27 and 34 gray bleb @ 70-77
89-98	Light green mud as 0-89, however scattered with blebs of black sandy material ca. 65 and weird shaped bleb @69-72
98-98.5	Black sandy layer in boudins
98.5-120	Light green mud as 0-89 rust colored bleb @113.5

CUSP 23

Centimeters	0-148
0-3.5	Brown mud streaked with darker brown near base
3.5-10.5	Olive green mud transitional colors
10.5-15	Gray green mud at top, towards base mixed with tongues of brown mud
15-21.5	Brown mud
21.5-23	Yellow brown mud
23-26	Brown mud
26-31	Light green mud flecked with brown and orange (Fe?)
31-34	Green mud (not as green as olive green)
34-40	Light gray mud
40-67.5	Yellow brown mud @67.5 one cm. break in core
69-74	Mixed zone, globs of light yellow brown mud and brown black mud at base transitional colors
74-83	Yellow brown mud
83-91.5	Brown mud speckled with yellow brown mud
91.5-96	Black brown (mixed?) sample taken out obscuring bedding
96-99	Yellow brown mud streaked with brown black mud
99-116.5	Olive green mud, not as green as 3.5-10.5, but has more brown transitional colors

Cusp 23 (continued)

116. 5-121	Light gray (wet cement colored) mud
121-131	Yellow brown at top mixed with light green
131-136	Chewed up, basal contact sharp
136-148	Light green mud with light brown mud

CUSP 24

Centimeters

0-145

0-12. 5	Brown mud streaked with darker brown mud and occasionally lighter brown mud, churned at the base
12. 5-30	Light yellow brown and light green mud transitional colors
30-40	Light gray (wet cement colored) mud
40-63	Light brown yellow mud, churned at base with black brown mud
63-79. 5	Churned black brown, yellow, and brown mud and light green mud light gray (wet cement colored) layer @74-76
79.5-93	Light brown yellow mud as 40-63, churned at the base
93-99	Churned mixed black brown, yellow brown mud as 63-79. 5
99-100	Light green and light brown mud
100-101	Olive green mud mixed with light green mud with sharp top and bottom contacts
101-102. 5	Light gray (wet cement colored) mud
102.5-103.5	Green mud, not as green as olive green see CUSP 23, 99-116.5 transitional colors
103. 5-106. 5	Light gray (wet cement colored) mud
106. 5-145	Light brown, occasional blebs of light gray and light green mud

HMS 6

Centimeters	0-104.5
0-2	Lost
2-3	Brown mud, black at the top
3-5.5/8	Yellow green mud, top has bits of brown mud
5.5-8	Dark gray sand layer inclined about 45°
8-41	Gray green mud, looks clayey sand glob @11-13
41-44	Gray sand layer
44-87.5	Gray green mud as 8-41, where samples taken mud has light green cast
87.5-91	Gray sand layer, inclined about 20°
91-104.5	Gray green mud as 8-41 Fe stained bleb @95 Sandy stringer, inclined about 30° @95.5-97

HMS 7

Centimeters	0-128
0-128	Brown green mud, tending towards olive drab black sandy lens @4.5-5 7-7.5 black sandy blebs @9 90-103.5 black sandy lens @103.5-104 109.5-111.5

HMS 8

Centimeters	0-131
0-131	Olive green mud possible sand @113.5-115

HMS 9

Centimeters	0-126
0-119.5	Light green (olive drab) mud
119.5-120	Gray sandy branch shaped layer
120-126	Light green mud as 0-119.5

HMS 10

Centimeters	0-109.5
0-63.5	Light green and light gray mud
63.5-64	Black sandy layer
64-66	Light gray green mud
66-68	Black sandy wedge
68-86	Light gray green mud
86-87	Black sand, not as distinct as 63.5-64
87-89	Light gray green mud
89-91	Black sandy U-shaped wedge, on its side, only one cm thick
91-109.5	Light gray green mud

HMS 11

Centimeters	0-148.5
0-4.5	Blue gray mud
4.5-12	Olive green mud
12-148.5	Blue gray mud, brown alteration
	black sandy lens @54.5
	black sandy gleb @63-66
	black sandy lens @67.5-68.5
	80-81
	81.5-83
	black sandy layer 87-94.5 good sharp bottom contact
	101.5-102
	103.5-107 mud layer @105
	111.5-113.5 layer canted
	119-122.5 mixed with matrix mud
	black sandy blebs 1-31-139
	black sandy lens 139-141
	black sandy blebs 141.5-142
	143-144

HMS 12

Centimeters	0-143
0-70	Light gray mud, tinge of green and brown
70-72/73	Gray mud in blebs
72/72-75	Brown and dark brown muddy sand

HMS 12 (continued)

Centimeters	0-143
75-139	Gray mud, brown on the side of the core
139-140	Black sandy layer
140-142.5	Black sandy layer, not continuous across the core
140-143	Brown mud

HMS 13

Centimeters	0-13
0-13	Green mud

HMS 17

Centimeters	1-120
0-12	Brown mud
12-18	Black brown mud transitional from above
18-31	Yellow brown mud (light brown)
31-32	Black brown mud, looks stained, transitional from above
32-47	Light brown gray mud
47-92	Green mud tending to olive drab, sharp boundaries above and below very fine sand lens at the base
92-96	Blue mud grading into blue green mud at base
96-98.5	Olive drab mud, more olive drab than 47-92
98.5-120	Blue mud grading into blue green mud as 92-96 blue mud until ca. 104

HMS 18

Centimeters	0-178
0-75.5	Dark brown and yellow brown mud mottled color, looks bored and filled
75.5-83.5	Light gray mud good sharp contacts at top and bottom
83.5-97.5	Light gray mud with blebs of brown and yellow brown mud
97.5-136	Dark brown to yellow brown mud, some light gray mud, looks like filled burrows, sharp basal contact

HMS 18 (continued)

136-166	Light gray mud transitional into dark brown and light brown mud, bottom looks like bottom of section from 97. 5-136
166-178	Light gray mud

BG 9

Centimeters 0-42
0-42 Blue gray mud interior, brown mud on sides of core
brown caused by alteration?

BP 10

Centimeters 0-273
0-183 Green brown sandy mud with rounded pebbles
about 5 cm (mudstone, quartz, feldspar, black rock?)
numerous brown white elongate pieces of shell or
bone, muscovite flakes common best name probably
pebbly sandy mud pebble 25 x 17 mm @49
yellow sand blob, medium to fine grained,
fairly clean (that is no mud) @52-54
mud globs @66-70
yellow sand, fine to medium grained, fairly clean,
in elongate fingers, probably dragged along the side
of the core, some dark minerals @102, about 2 cm
wide @ 99, yellow sand band from 73-126
mud bleb @100 - yellow sand band changes sides
from 85 and below matrix seems to lose sand, but
keeps the pebbles
mud glob (looks extruded) @125-136
sand appears to reappear @131
core bent from 149-162
mud glob @149-151
156-162, two glebs
sand mixed with fissile mud @162-169
iron strained pebble @180-181
indurated sandy mudstone ca. 20 mm
183-234.5 Gray green clay mud
fine sand lens stained blue with an outer rim of iron
staining @200
234.5-241 Dirty brown sand lens, top distinct and level,
base distinct but undulating, inclined 240-241
241-247 Mud as 183-234.5 not fissile, dirty sand dragged along
the sides
247-259 Dirty sand seems to have more pebbles than in 234-241
259-273 Core bent and twisted, mixture of mud and dirty sand,
bottom is mud

BG 12

Centimeters

0-77.5

0-12	Light green mud, tinge of brown and gray, 0-12 just about gone so top measurement not sure
12-12.5	Black sandy layer, badly curled in the liner
12.5-16.5	Light green mud as 0-12
16.5-17.5	Black sandy layer
17.5-44	Light green mud as 0-12
44-47	Sandy material in wisps in mud matrix
47-54	Light green mud as 0-12
54-54.5	Black sandy layer
54.5-65.5	Light green mud as 0-12
65.5-66	Black sandy layer
66-69.5	Light green mud as 0-12
69.5-70.5	Black sandy layer
70.5-75.5	Light green mud as 0-12
75.5-77.5	Gray sandy layer, wedge shaped in two parts

BG 13

Centimeters

0-42

0-42	Green mud black sandy material @11 14-15 27-28 black sandy layer @30.5-31.5, channel shaped black sandy blebs @36-37 white shell material @38-40
------	--

BG 15

Centimeters

0-171

0-115.5	Light green and light brown mud some fissility and very clayey from 0-45 has gaps and caverns (core separated and dried up while being stored?) milk white material scattered throughout. also tiny flakes of mica and pieces of glass (volcanic shards?)
---------	--

BG 15 (continued)

one cm lost from 85-86
115. 5-117 Black sand layer
117-158 Light green mud as 0-115. 5, sprinkled with white
flecks, several dark layers less than one cm. thick
which may be black sandy layers
158-161 Black sandy layer somewhat wedge shaped
161-165. 5 Light green mud as 0-115. 5
165. 5-167 Black sand layer with white flecks
167-171 Light green mud as 0-115. 5
black sand glob @169-170

BG 17

Centimeters 0-133. 5
0-13. 5 Light green mud
sand blob @10. 5
13. 5-15 Gray sandy layer, inclined 10-15°
about 0. 5 cm thick
15-133. 5 Light green mud as 0-13. 5

BP 17

Centimeters 0-713
0-10 Brown gray mud (top 2 cm missing)
10-15 Black sandy material in globs and stringers
biggest single glob @12-15
15-17 Brown gray mud
17-20. 5 Gray sandy layer, dirty very fine sand
20. 5-31. 5/33 Brown gray mud as 0-10
31. 5-34 Black sandy material
33-310 Brown gray mud, more cement colored than 0-10
may be alteration of core?
310-311 Black sandy layer
311-366 Brown mud (outside of core), blue gray mud as 33-310
366-371 Graded black sandy layer
sculptured base, some globs of sand below continuous
base
grades into mud above
371-483 Blue gray mud
black mud blebs @433 and 445-446

BP 17 (continued)

Centimeters

483-485 Black sandy layer
485-537 Blue gray mud as 33-310
537-545 Dark lens, may be filling of a boring (does not appear sandy)
545-570 Blue gray mud as 33-130
cone shaped fossils @549
570-577 Black sandy layer, appears graded, base jumbled up as core liner bent.
577-602 Blue gray mud as 33-310
black sandy material in bleb @581-582
602-606.5 Black sandy layer, arched upward
606.5-713 Blue gray mud as 33-310, from 650 and below everything sucked up by piston sand bleb @641.5-644
black sand lens 0666-675 dragged up into discontinuous stringers

BP 18

Centimeters

0-610

0-610 Light green mud (olive drab) becomes gray brown on sides of core (alteration of core?)
black bleb @100
bits of fossils @ca. 125
black chunks (MnO_2 ?) @134-134.5
583-586 core separated

BG 18

Centimeters

0-127

0-127 Green mud
black sand lens @72-72.5, crescent shaped
83.5-84.5, crescent shaped
black sandy material @94-95

BG 27

Centimeters	0-121
0-19	Brown mud, blebs, globs, and stringers of gray mud, black brown zone @9.5-10.5 18-19
19-103.5	Transitional colors brown mud to ca. 50 light brown grading into blue gray 50-73 light blue mud 73-103 green mud layer @77-80 green and gray mud layer @85-89
103.5-121	Light brown gray mud, tinge of green

MEN 3

Centimeters	0-177
0-177	Green gray mud as the matrix distinct bands: black mud @7 green mud @10-11 28-28.5 67 71.5-73 75 81-83 96-97 103 113-113.5 150-152 162-162.5 164 166

MEN 4

Centimeters	0-157
0-8	Brown mud
8-20	Mottled brown and black mud
20-23	Gray mud
23-26	Brown muddy sand, sharp basal contact
26-34	Brown mud
34-36	Green gray mud
39-42	Gray sand, layer canted
42-45	Light brown mud
45-50	Mottled brown and light brown mud
50-53	Gray mud grading into-
53-56	Brown sand, looks graded, sharp basal contact
56-63	Light brown mud
63-65	Blue green mud
65-68/69	Sand stringers mixed with light blue green mud very sharp basal contact
69-77	Mottled blue gray and gray mud
77-79	Brown mud
79-85	Mottled brown and light brown mud

MEN 4 (continued)

Centimeters

85-87	Brown gray mud
87-91	Brown sand
91	Light brown mud, separating the two sand layers
91-94	Blue sand
94-102	Mottled blue mud as 69-77
102-107. 5	Mottled brown mud as 79-85 or 45-50
107. 5-112. 5	Brown sand as 87-91 or 52-55
112. 5-114	Light brown mud
114-117	Blue sand as 91-94
117-118	Light gray mud
118-119. 5	Mottled blue gray and gray mud
119. 5-121. 5	Brown mud (some sand?)
121. 5-122	Light brown mud
122-124/124. 5	Gray green mud
124/124. 5-126. 5	Blue gray mud, blue band @126
126, 5-132	Green gray mud
132-149	Mixed brown and gray mud, more brown at base
149-157	Mottled yellow brown, dark brown mud, and light green mud

MEN 5

Centimeters

0-162

0-2	Brown mud
2-162	Green gray mud
	green mud layers @12-13
	blue mud layers @17
	green mud layers @28-29
	44-45
	53
	56
	57
	69-69. 5
	76-77
	82
	102-103
	120-121
	162

MEN 6

Centimeters	0-176
0-2.5	Olive green mud
2/2.5-4	Blue gray mud
4-17	Gray mud
17	Dark gray band
17-21/22	Gray mud transitional into
21/22-41	Olive green mud, blebs of gray mud
41-ca. 55	Gray mud. transitional into
ca. 55-86	Olive green mud, blebs and bands of gray mud sandy mud? @79.5-85
86-101.5	Gray mud
101.5-106	Olive green mud speckled with gray mud
106-108	Gray mud
108-116	Olive green mud with blebs of gray mud
116-119	Blue gray mud
119-144.5	Olive green mud with blebs of gray mud, sharp base
144.5-174	Gray mud, blue green layer @150-151
174-176	Olive green mud

MEN 7

Centimeters	0-98
0-5	Brown mud
5-16	Green gray mud
16-18/19	Black sand
18/19-63/65	Green gray mud with green clay @22 33 35 39/49
63/65-66/67	Black sand, looks graded, base looks channeled
66/67-98	Gray to green gray mud sand @70/71-72/74 89-92 sand mixed with mud in. sampling for rads. sand found underneath mud from 94-96

MEN 13

Centimeters

0-134

0-38	Brown and light brown mud mottled
38-75	Gray mud becoming greener from 58 down
75-78	Black sand layer
78-94	Green mud and gray mud mixture black sand globs @78.5-81 85-87 88-90.5
94-96	Green mud
96-103	Gray mud
103-118/120	Gray to blue gray mud
118/120-134	Green gray mud

MARE 1*

Centimeters	0-73
0-1	Brown mud (oxidized?)
1-16.5	Gray green mud
16.5-18	Dark sand layer
18-22	Gray green mud
22-23	Dark Sand layer
23-37	Gray green mud
37-38	Dark sand bleb
38-73	Gray green mud

*Plastic liner cracked when core was opened.

MARE 2

Centimeters	0-87.5
0-2	Brown mud (oxidized?)
2-40	Blue black clay core separated @15/17-16/18
40-41	Brown mud (oxidized?) shaped like a conodont
40-87.5	Blue black clay, looks sandy towards the bottom, possibly sandy mud

MARE 5

Centimeters	0-132
0-132	Green mud split from 10-60 87-91 gap from 93.5-94.5 dark bands @11 63 71 75-77 one half core 100

MARE 6

Centimeters	0-131
0-13.5	Green mud
13.5-14	Dark sand layer, sharp basal contact
14-16	Green mud
16-17	Dark sand, streaked into dabs
17-51	Green mud gap @19-20
51-52	Dark sand glob
52-97	Green mud sand dab @72 gaps @72.5-73 73-78 sand dab @94 dand dabs @96
96/97-98	Dark sand layer
98-101	Irregular sand body
101-120	Green mud
120-122	Dark sand layer, distinct basal contact, top is wavey
122-131	Green mud

LFGS 3

Centimeters	0-144.5
0-144.5	Green mud sand blebs @100 104 oily patch @120.5-128 sand bleb @131-133

LFGS 4

Centimeters	0-12
0-12	Green mud (catcher sample)

LFGS 5

Centimeters	0-18.5
0-18.5	Green mud (catcher sample)

LFGS 50

Oxidized Rine

Centimeters	0-161
0-3.5	Brown oxidized mud
3.5-9	Yellow brown mud, stringers and blebs of brown mud as 0-3.5 @5-6, layer of brown mud @7, blebs @9
9-15	Mottled yellow brown and gray mud
15-19	Yellow brown mud, gradational into above
19-20	Gray mud
20-22	Green mud, lower part black-maybe sharp contact
22-27	Light gray mud (oxidized), circular glob of green-gray mud @24-24
27-31	Light green mud
31-40	Light gray mud as 22-27
40-41	Green mud as 20-22
41-61	Light gray mud as 22-27 black blebs @42 black streak @43

LFGS 50 (continued)

Centimeters

	black streak @47
	black blebs @49-51
	green mud as 20-22 @56-57 and 59
61-68.5	Light green (almost olive) as 27-31
68.5-69.5	Black sand layer
69.5-75	Light green mud as 61-68.5
75-77	Light gray mud as 22-27
77-80	Light green mud as 61-68.5
80-84	Light gray mud as 22-27
84-87	Black organic looking mud
87-92.5	Light gray mud as 22-27
	grading downward into light green mud as 22-27
92.5-96	Light gray mud as 22-27
	grading into light green mud
96-97	Black mud as 84-87 in two bands, separated by gray mud
97-119	Light gray mud as 22-27
	green stringer @112
119-124	Olive mud just a shade darker than 61-68.5
	mottled with light gray mud as 22-27
	in what looks like borings
124-126	Light gray mud, green at the base as 20-22
126-131	Like 119-124
131-137	Light gray mud with green mud at the base like 124-126
137-139	Green mud as 27-31
139-144	Light green gray mud as 22-27
144-146	Green mud as 20-22
146-150	Light green gray mud as 22-27
	black streak @148-149.5
150-153	Olive mud
153-161	Light green gray mud as 22-27
	green mud as 20-22 in stringers @156-158

LFGS 62

Centimeters	0-66
0-4/7	Brown mud, very fluid, appears as if some flowage had occurred
4/7-32	Green gray mud dark streaks @21.5 23
32-36	Olive green mud mottled with above green gray mud, grades into green gray mud with depth
36-43	Green gray mud
43-48	Olive green mud mottled as 32-36
48	Thin sand layer
48-66	Green gray mud

LFGS 68

Centimeters	0-1.53
0-2	Green mud. with black streaks brown mud lens @1.5
2-50.5	Green mud
50.5-51.5	Dark sand layer, distinct top and bottom
51.5-64	Green mud
64-70	Dark sand layer, distinct top and bottom
70-153	Green mud, sand filed worm boring? from 70-78 sand blebs @134-136

LFGS 70

Centimeters	0-150
0-150	Green mud, brown mud rine around side of core (oxidized?) sand @60-61 sand layer @75-76.5 sand blebs @128-130 131 149-50 crescent-shaped points up

LFGS 72

Centimeter s 0-112

0-112 Green mud
 sand layer @59-60
 sand blebs @66
 90

LFGS 74

Centimeters 0-149

0-88 Green mud, brown rine around core (oxidized?)
88-90 Dark sand lens, slanted
90-98 Green mud
98-100/101 Dark sand layer, sharp contacts top and bottom
 bottom contact concave downward
100/101-149 Green mud
 sand blebs @102
 113

LFGS 80

Centimeters 0-117

0-117 Green mud
 dark streaks @39
 50
 whirl 110-111

LFGS 82

Centimeters 0-125

0-125 Green mud

LFGS 84

Centimeters

0-109

0-109

Green mud

dark bands @1-2, whorl

42-43

86

87.5

shell

@88.5

Littleton formation, which extends from west central Maine through New Hampshire into Massachusetts is about 10,000 feet of chiefly pelitic rocks with volcanic and graywacke units (Billings, 1956). The graywackes in the low rank metamorphic part of the Littleton in Massachusetts have some graded beds (Peter Robinson, oral communication). The depositional environment of the Littleton formation in the Devonian may have been a large scale deep-sea fan or apron on the continental margin as (1) the Littleton can be traced for about 5000 kilometers, which indicates an area of sedimentation with essentially uniform condition that long, and (2) the graded beds in the graywackes suggest a turbidite formed in relatively deep water. Kay's (1951, p. 26-27) studies on the northern Appalachians intimates a further similarity between the geologic environment, for the Cambro-Ordovician of New York and New England and for the Cenozoic of central California and the near-by off shore regions. In both cases the landward trough (the miogeosyncline in New York and the Great Valley of California) is separated from the seaward depositional site (the eugeosynclinal Magog belt in New Hampshire and the central California deep-sea fans) by a tectonically active land mass (Vermontia in Vermont and the Coast Ranges in California). This relationship is shown in Figure 20.

Other possible examples of ancient deep-sea fan deposits are in the Ouachitas in the Mid-Continent of North America. The shale and graywacke sandstones of the Stanley and Jackfork formations and the shales and boulder beds in the Johns Valley

formations have flow and sole markings of turbidites and are associated with pelagic and nektonic fossil faunas (Cline and Shelburne, 1959). The sands in these formations generally are much coarser than those of the Monterey fan. So the Ouachita sequence has more in common with the Alpine and Harz wildflysch sediments.

These comparisons do not mean that all or even any eugeosynclinal deposits are formed on deep-sea fans. My intent is to demonstrate that for some eugeosynclinal deposits, such as the Littleton formation, (1) with large aerial extent, (2) essentially pelitic but with some turbidite sands, and (3) which faced open oceanic areas, that a depositional environment on a deep-sea fan is possible if not probable. If such deposits, now incorporated into the continental landmass, were formed as a large scale deep-sea fan such as the Monterey (allowing that Alpine type flysch forms in a similar manner but in restricted basins in regions not at true oceanic depths). Then erosion products from the continents deposited on deep-sea fans are not lost forever to the ocean basins.

A return of the sediments now on the Monterey fan to the continental block means an uplift of at least 3000 meters of a large part of oceanic crust. Woolard and Strange (1962, p. 64) found that the area of the fans off central California is one of significant negative free-air gravity anomalies, where the gravity-derived depths to the M-discontinuity average about 2 kilometers greater than the seismically determined values. They believed that the seismic value was calculated to be low because of subnormal crustal density and correspondingly lower mean seismic velocities in this region compared

with typical oceanic crustal values. Whether the fans are (1) the cause of the modification of the oceanic crust, (2) the effect of the modification, or (3) a fortuitous relationship is not known. Whatever the cause, the fact remains that in the region underlying the Monterey fan, the crust is not typically oceanic but is beginning to approach the lower density of continental crust. If this process of conversion of oceanic crust to continental crust continues throughout future geologic time and is accompanied by isostatic uplift to compensate for the lower density; the sediment now on the Monterey deep-sea fan would eventually return to the continental block from whence it originally came.

REFERENCES

- Arrhenius, G. , 1963, Pelagic sediments, in Hill (Ed.), The Seas, v. 3, The Earth beneath the Sea: New York, Wiley, p. 655-727.
- Bailey, E. B. , 1930, New light on sedimentation in relation to tectonics: Geol. Mag., v. 67, p. 86-88.
- Beveridge, A. J. , 1958, Heavy minerals in Lower Tertiary formations in the Santa Cruz Mountains, California: Stanford, Unpub. Ph. D. Thesis, 109 p.
- Billings, M. P. , 1937, Regional metamorphism of the Littleton-Moosilauke area, New Hampshire: Geol. Soc. America; Bull., v. 48, p. 463-566.
- _____, 1956, The Geology of New Hampshire, Part II - Bedrock Geology: Concord, New Hampshire, New Hampshire State Planning and Development Commission, 203 p.
- Briggs, L. I., McCulloch, D. S., and Moser, F., 1962, The hydraulic shape of sand particles: Jour. Sed. Petrology, v. 32, p. 645-656.
- Briggs, L. I. Jr., 1953, Upper Cretaceous sandstones of Diablo Range, California: Univ. Calif. Pub. in Geol. Sci., v. 29, p. 417-452.
- Bull, W. B. , 1964, Geomorphology of segmented alluvial fans in western Fresno County, California: U. S. Geol. Survey Prof. Paper 352-E, p. 89-129,
- Chesterman, C. W., 1952, Descriptive petrology of rocks dredged off the coast of Central California: Calif. Acad. Sci. Proceedings, v. 27, p. 359-374.

- Cline, L. M., and Shelburne, O. B., 1959, Late Mississippian-Early Pennsylvanian stratigraphy of the Ouachita Mountains, Oklahoma, in *The Geology of the Ouachita Mountains - A Symposium*: Dallas, Dallas and Ardmore Geol. Societies, p. 175-208.
- Crowell, J. C., 1955, Directional current structures from the pre-Alpine flysch: *Geol. Soc. America Bull.*, v. 66, p. 1351-1384.
- Curtis, G. H., Evernden, J. F., and Lipson, J., 1958, Age determination of some granitic rocks in California by the potassium-argon method: *Calif. Div. Mines Special Report 54*, 16 p.
- Davies, S. N., 1946, Mineralogy of late Upper Cretaceous, Paleocene and Eocene sandstones of Los Banos district, west border of San Joaquin Valley, California: *Am. Assoc. Petroleum Geologists Bull.*, v. 30, p. 63-83.
- Dill, R. F., Dietz, R. S., and Stewart, H. B., 1954, Deep-sea channels and delta of the Monterey submarine canyon: *Geol. Soc. America Bull.*, v. 65, p. 191-194.
- Emery, K. O., 1960, *The sea off Southern California*: New York, Wiley, 366 pp.
- Emery, K. O., and Dietz, R. S., 1941, Gravity coring instrument and mechanics of sediment coring: *Geol. Soc. America Bull.*, v. 52, p. 1685-1714.
- Emery, K. O., and Tschudy, R. H., 1941, Transportation of rock by kelp: *Geol. Soc. America Bull.*, v. 52, p. 855-862.
- Emery, K. O., and Bray, E. E., 1962, Radiocarbon dating of California basin sediments: *Am. Assoc. Petroleum Geologists Bull.*, v. 46, p. 1839-1856.
- Fisk, H. M., 1944, *Geological investigation of the alluvial valley of the lower Mississippi River*: War. Dept., Corps Engineers (Miss. River Commission), 78 p.

- Flint, R. F. , 1957, *Glacial and Pleistocene Geology*: New York, John Wiley, 553 p.
- Gilluly, J., 1949, The distribution of mountain building in geologic time: *Geol. Soc. America Bull.* , v. 60, p. 561-590.
- _____ 1955, Geologic contrasts between continents and ocean basins, In Poldervaart (Ed.) *Crust of the Earth*: *Geol. Soc. America Special Paper* 62, p. 7-18.
- Goldberg, E. D., 1954, Marine geochemistry, 1: Chemical scavengers of the sea: *Jour. Geology*, v. 62, p. 249-265.
- Gorsline, D. S. , and Emery, K. O. , 1959, Turbidity-current deposits in San Pedro and Santa Monica basins off Southern California: *Geol. Soc. America Bull.*, v. 70, p. 279-290.
- Gould, H. R. , 1951, Some quantitative aspects of Lake Mead turbidity currents, in *Turbidity Currents*: *Soc. Econ. Min. and Paleont. Spec. Pub.* no. 2, p. 34-52.
- Gribnitz, K. H. , 1952, Petrographische Untersuchung an Nebengesteinen der Magerkohlschichten (Namur ob. C.) Westfalens, bei besonderer Berücksichtigung der Grauwacken: *Neues Jahrbuch für Min.* , Monatshefte A. , s. 174-190.
- Grim, R. E. , 1942, Modern (concepts of clay materials: *Jour. Geology*, v. 50, p. 225-275.
- Grim, R. E., Dietz, R. S., and Bradley, W. F., 1949, Clay mineral composition of some sediments from the Pacific Ocean off the California coast and the Gulf of California: *Geol. Soc. America Bull.*, v. 60, p. 1785-1808.
- Heezen, B. C. , Tharp, M. , and Ewing, M. , 1959, The floor of the oceans, I The North Atlantic: *Geol. Soc. America Special Paper*, 65, 122 p.

- Heezen, B. C., and Menard, H. W., 1963, Topography of the deep-sea floor; in Hill (Ed.), The Seas, v. 3, The Earth beneath the Sea: New York, Wiley, p. 233-280.
- Heezen, B. C., and Hollister, C., 1964, Deep-sea current evidence from abyssal sediments: Jour. Marine Geology, v. 1, p. 141-174.
- Helmbold, R., 1958, Contributions to the petrology of the Tanner graywacke: Geol. Soc. America Bull., v. 69, p. 301-314.
- Hdfmann, W., and Phillips, K. N., 1961, Surface water supply of the United States 1960 - Part II Pacific slope basins in California: U. S. Geol. Survey Water Supply Paper 1715, 751 p.
- Hollister, C. D., and Heezen, B. C., 1964, Modern graywacke-type sands: Science, v. 146, p. 1573-1574.
- Holmes, A., 1959, A revised geological time-scale: Edinburgh Geol. Soc., Trans., v. 17, p. 183-216,
- Homan, W. J., and Schultz, E. A., 1963, Model tests of shoaling and dredge disposal in San Francisco Bay: Jackson, Miss., Federal Interagency Sedimentation Conf., 30 p.
- Howard, A. D., 1951, Development of landscape, San Francisco Bay .counties: Calif. Div. of Mines Bull. 154, p. 95-106.
- Hsu, K. J., 1960, Paleocurrent structures and paleogeography of the Ultrahelvetic flysch basins, Switzerland: Geol. Soc. America Bull., v. 71, p. 577-610.
- Huey, A. S., 1948, Geology of the Tesla Quadrangle, California: Calif. Div. Mines Bull. 140, p. 95-106.
- Hurley, R. J., 1964, Analysis of flow in Cascadia deep-sea channel; in Papers in Marine Geology, Miller, R. L. Ed.: New York, Macmillan Co., p. 117-132, 531 p.

- Hutton, C. O. , 1959, Mineralogy of Beach sands, between Halfmoon and Monterey Bays, California: Calif. Div. Mines Special Report 59, 32 p.
- Jennings, F. D. , and Schwartzlose, R. A., 1960, Measurements of the California Current in March 1958: Deep-Sea Research, v. 7, p. 42-47.
- Johns, W. D., Grim, R. E. , and Bradley, W. F. , 1954, Quantitative estimations of clay minerals by diffraction methods: Jour. Sed. Petrology, v. 24, p. 242-251.
- Johnson, M. A. , 1962, Turbidity currents: Sci. Progress, v. 50, no. 198, p. 257-273.
- Kay, M. , 1951, North American Geosynclines: Geol. Soc. America Memoir, 48, 143 p.
- Kuenen, Ph. H. , 1950, Marine Geology : New York, Wiley, 568 p.
- _____ , 1951, Properties of turbidity currents of high density, in Turbidity Currents and transportation of coarse sediments to deep water: Soc. Econ. Paleont. and Mineralogists, Spec. Pub, no. 2, p. 14-33.
- Kuenen, Ph. H. , and Migliorini, C. I. , 1950, Turbidity currents as a cause of graded bedding: Jour. Geology, v. 58, p. 91-127.
- Kuenen, Ph. H., and Sanders, J. E., 1956, Sedimentation phenomena in Kulm and Flozleeres graywackes, Sauerland and Overharz, Germany: Am. Jour. Sci., v. 254, p. 649-671.
- Krause, D. C. , 1962, Interpretation of echo sounding profiles: Internat. Hydrographic Review, v. 39, p. 65-123.
- Krumbein, W. C. , 1937, Sediments and Exponential curves: Journal Geology, v. 45, p. 577-601.

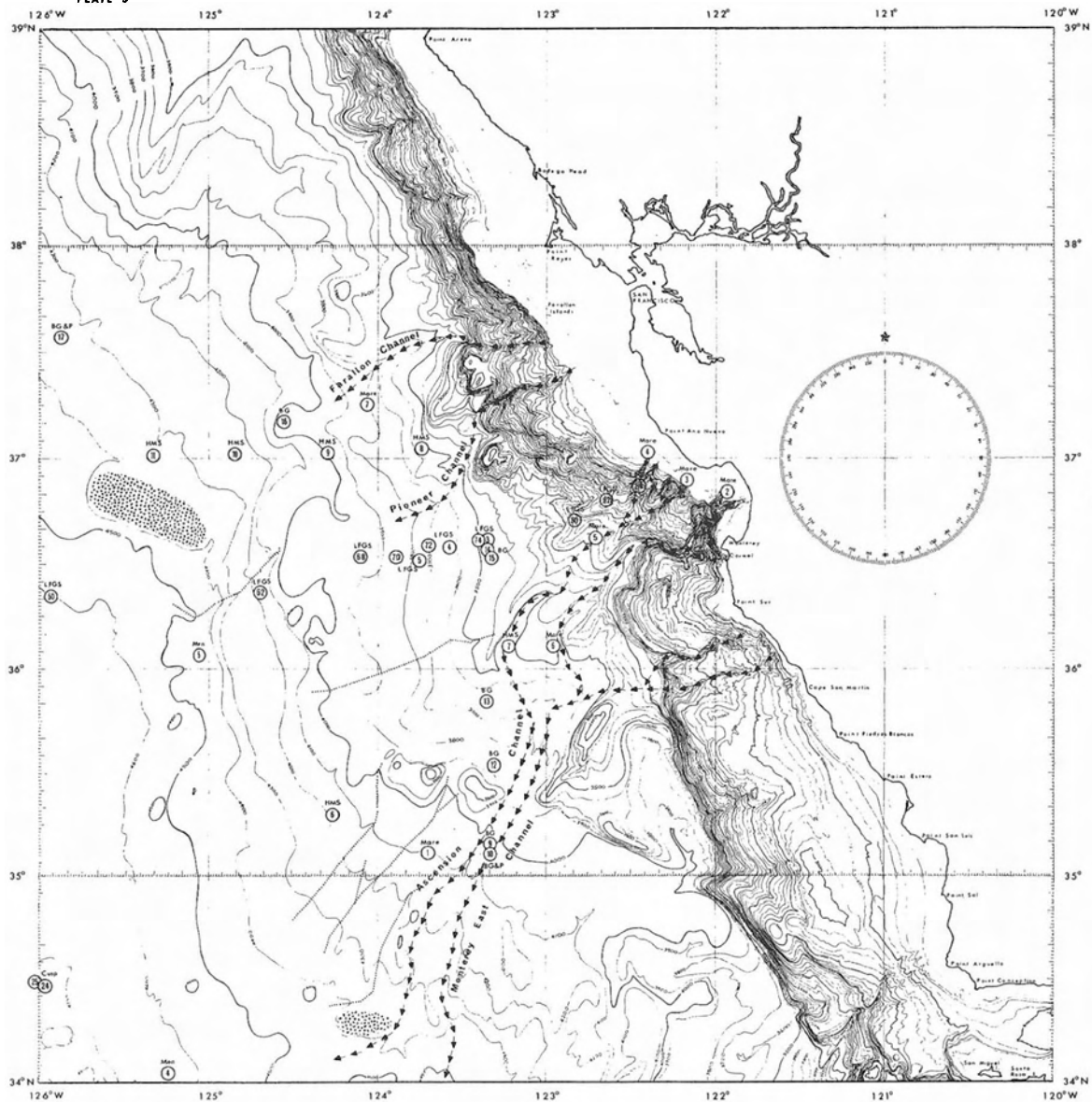
- Krumbein, W. C. and Pettijohn, F. J. , 1938, Manual of sedimentary petrography: New York, Appleton-Century-Crofts, Inc. , 549 p.
- Kullenberg, B. , 1954, Remarks on the Grand Bank turbidity current: Deep-Sea Research, v. 1, p. 203-210.
- _____, 1956, Deep-sea coring: Reports of the Swedish Deep-Sea Expedition, v. 4, Bottom Investigations, p. 37-96.
- Leo, G. W. , 1961, The plutonic and metamorphic rocks of Ben Lomond, Mountain, Santa Cruz County, California: Stanford, Unpub. Ph. D. Thesis, 169 p.
- Leopold, L. B. and Maddock, T. , 1953, The hydraulic geometry of stream channels and some physiographic implications: U. S. Geol. Survey Prof. Paper 252, 57 p.
- Louderback, G. D. , 1951, Geologic history of San Francisco Bay: Calif. Div. Mines Bull. 154, p. 75-94.
- Martin, B. D., 1964, Marine Geology of Monterey Submarine Canyon: Univ. of Southern California, Unpub. Ph. D. thesis.
- Mason, R. G. and Raff, A. D. , 1961, Magnetic survey off the west coast of North America, 32° N. latitude to 42° N. latitude: Geol. Soc. America Bull, v. 72, p. 1259-1266.
- McBride, E. F. , 1962, Flysch and associated beds of the Martinsburg formation (Ordovician), Central Appalachians: Jour. Sed. Petrology, v. 32, p. 39-91.
- Menard, H. W. , 1955, Deep-sea channels, topography and sedimentation: Am. Assoc. Petrol. Geol. Bull., v. 39, p. 236-255.
- _____, 1960, Possible pre-Pleistocene deep-sea fans off central California: Geol. Soc. America Bull. , v. 71, p. 1271-1278.

- _____, 1961, Some rates of regional erosion: Jour. Geology, v. 69, p. 154-161.
- Milner, H. B., 1962, Sedimentary Petrography, v. 2, Principles and Applications: London, George Allen and Unwin Ltd. , 715 p.
- Myrick, R. M. and Leopold, L. B., 1963, Hydraulic geometry of a small tidal estuary: U. S. Geol. Survey Prof. Paper 422-B, 18 p.
- Murray, H. H. , and Harrison, J. L. , 1956, Clay mineral composition of recent sediments from Sigsbee Deep: Jour. Sed. Petrology, v. 26, p. 363-368.
- Petelin, V. P. and Aleksina, I. A., 1961, The choice of an aqueous mechanical method in analysis of bottom sediments; (trans. in Deep-Sea Research, 1963, v. 10, p. 45-56): Okeanologiya, v. 1, p. 717-733.
- Pettijohn, F. J. , 1957, Sedimentary Rocks: Harper and Brothers, New York, 718 p.
- Piggot, C. S. , 1941, Factors involved in submarine core sampling: Geol. Soc. America Bull., v. 52, p. 1513-1524.
- Plapp, J. E. , and Mitchell, J. P. , 1960, A hydrodynamic theory of turbidity currents: Jour. Geophys. Res., v. 65, p. 983-992.
- Pratje, O. , 1935, Die Sedimente des Sudatlantischen Ozeans: Deutschen Atlantischen Expedition, Meteor Reports, B. 3, Teil 2, p. 1-56.
- Reed, R. D., 1933, Geology of California: Tulsa, Am. Assoc. Petroleum Geologists, 355.p.

- Reiche, P., 1937, Geology of the Lucia Quadrangle: Univ. Calif. Pub. in Geol. Sci., v. 24, p. 115-168.
- Revelle, R. R., 1944, Marine bottom samples collected in the Pacific Ocean by the Carnegie on its seventh cruise: Carnegie Inst. Washington Pub. 556, p. 1-133.
- Rex, R. W.**, and Goldberg, E. D., 1958, Quartz contents of pelagic sediments of the Pacific Ocean: *Tellus*, v. 10, p. 153-159.
- Richmond, W. , Wentworth, C. , Birkeland, P. , and Sides, P. , 1959, Investigation of Quaternary sediments, Montara Mountain and vicinity: Stanford, Unpub. Sedimentology Report, 24 p.
- Riedel, W. R., Ladd, H. S., Tracey, J. I. Jr., and Bramlette, M. N., 1961, Preliminary drilling phase of Mohole project, II Summary of coring operations: Am. Assoc. Petroleum Geologists Bull., v. 45, p. 1793-1798.
- Rouse, H., 1960, Elementary Mechanics of Fluids: New York, John Wiley, 376 p.
- Rubey, W. W. , 1933, Settling velocities of gravel, sand, and silt particles: Am. Jour. Sci., v. 225, p. 325-338.
- Shepard, F. P., 1963, Submarine Geology: New York, Harper and Row, 557 p.
- Shepard, F. P. and Emery, K. O., 1941, Submarine topography off the California coast: Geol. Soc. America Spec. Paper 31, 171 p.
- Spotts, J. H. , 1958, Heavy minerals of some granitic rocks of central California: Unpub. Ph. D. Thesis, Stanford, 80 p.
- Stoneley, R. , 1957, On turbidity currents: Verhandl., Ned. Geol. Mijnbouwk, Genoot., Geol. Ser. 18, p. 279-285.

- Sullwold, H. H. , 1960, Tarzana fan, deep submarine fan of Late Miocene age, Los Angeles County, California: Am. Assoc. Petroleum Geol. Bull., v. 44, p. 433-457.
- Swallow, J. C. , 1957, Some further deep current measurements using neutrally-buoyant floats: Deep-Sea Research, v. 4, p. 93-104.
- Taliferro, N. L. , 1943, Franciscan-Knoxville problem: Am. Assoc. Petroleum Geologists Bull., v. 27, p. 109-219.
- _____ , 1944, Cretaceous and Paleocene of Santa Lucia Range, California: Am. Assoc., Petroleum Geologists Bull. , v. 28, p. 449-521.
- Thompson, G. A. , and Talwani, M. , 1964, Geology of the crust and mantle, Western United States: Science, v. 146, p. 1539-1549.
- Trask, P. D., 1952, Source of beach sand at Santa Barbara, California as indicated by mineral grain studies: U. S. Beach Erosion Board Tech. Memo., no. 28, 24 p.
- Uchupi, E. and Emery, K. O. , 1963, The continental slope between San Francisco, California and Cedros Island, Mexico: Deep-Sea Research, v. 10, p. 397-447.
- U. S. Weather Bureau and U. S. Hydrographic Office, 1961, Climatological and Oceanographic Atlas for Mariners; V. 2, North Pacific Ocean: Washington, U. S. Govt. Print. Office, 159 charts.
- Van Andel, Tj. H. , 1958, A defense of the term alterite: Jour. Sed. Petrology, v. 28, p. 234-235.
- Van Houten, F. B. , 1954, Sedimentary features of Martinsburg slate, northwestern New Jersey: Geol. Soc. America Bull., v. 65, p. 813-818.

- Weaver, C. E. , 1956, The distribution and identification of mixed layer clays in sedimentary rocks: *Am. Mineralogist*, v. 41, p. 202-221.
- Wilde, P. , 1964, Deep-sea channels on the Cocos Ridge, east-central Pacific: *Trans. Am. Geophys. Union*, v. 45, p. 70.
- Wilson, J. T. , 1951, On the growth of continents: *Papers and Proc. Royal Soc. Tasmania*, p. 85-111.
- Woodford, A. O. , 1951, Stream gradients and Monterey sea valley: *Geol. Soc. America Bull.*, v. 62, p. 799-852.
- Woollard, G. P., and Strange, W. E., 1962, Gravity anomalies and the crust of the earth in the Pacific basin; in the *Crust of the Pacific Basin*, Macdonald and Kuno (Eds.): *Am. Geophys. Union Geophysical Mono.* 6, p. 60-80.
- Yoder, H. S. , and Eugster, H. P. , 1955, Synthetic and natural muscovites: *Geochim. et Cosmochim. Acta*, v. 8, p. 225-280.



EXPLANATION

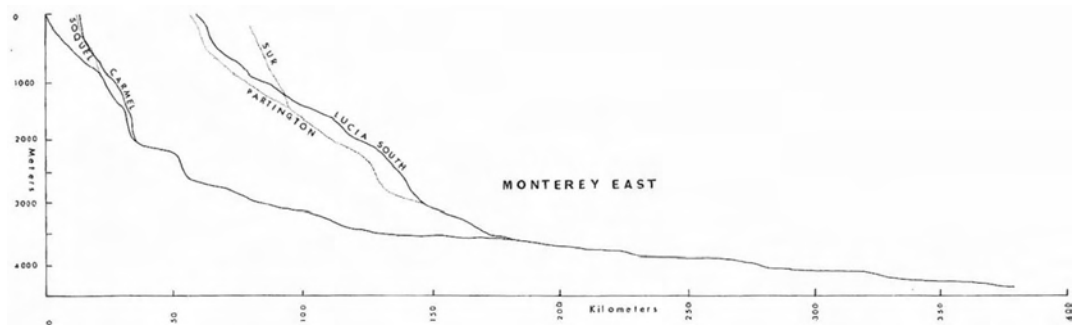
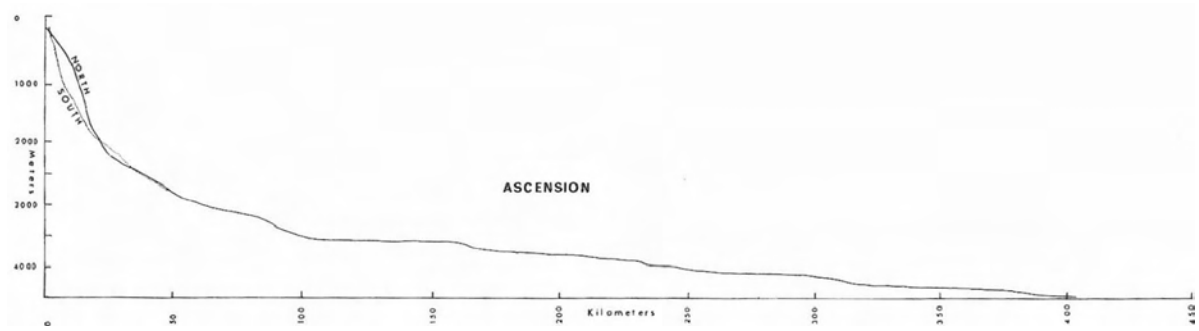
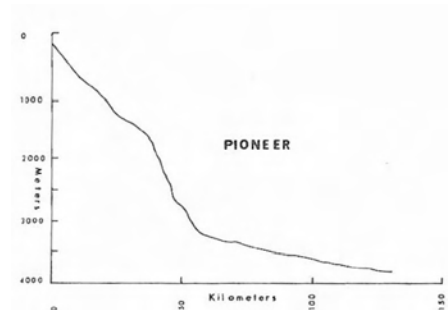
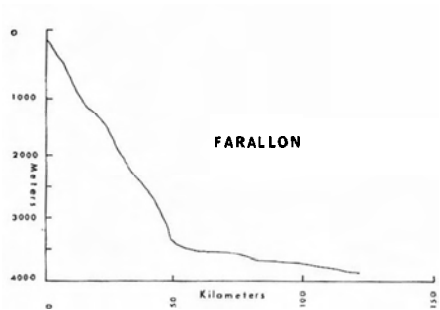
- SP (in a circle) Core location
- Present canyon channel system
- - - Possible abandoned channel
- Positive relief feature

Compiled and contoured by
 Pat Wilde
 Stanford University and
 Scripps Institution of
 Oceanography

Sources:
 Shallower than 3000M. Deeper than 3000M.
 BC 1306 N Menard 1960
 BC 1307 N Various SIO cruises
 Shepard and Emery 1941

Contour interval
 100 Meters
 Depths corrected from
 Matthews' Tables Area 44

THALWEG CANYON CHANNEL PROFILES



Vertical Exaggeration 25X